Supplementary Information for: Runtime Bias Correction of Regional Climate Model Driving Data. Part I: Continental Scale Impacts

J.F. Scinocca[1,*], V.V. Kharin[1], D. Matte[2], Y. Jiao[1], M. Labonté[2], M. Qian[1], D. Paquin[2], A. Akingunola[1], and M. Lazare[1]

[1]Canadian Centre for Climate Modelling and Analysis, Environment and Climate Change Canada, 2474 Arbutus Rd., Victoria, V8N 1V8, British Columbia, Canada
[2]Ouranos Consortium , Organization, 550 Rue Sherbrooke W., Montréal, H3A 1B9, Québec, Canada

[*]**Corresponding author:** J.F. Scinocca, john.scinocca@ec.gc.ca

S1 Sea-Surface Bias Correction

The actions of the diagnostic bias corrections on sea-ice concentration and sea surface temperature described in Section 2.3 are illustrated in Figs.S1.1 - S1.4.

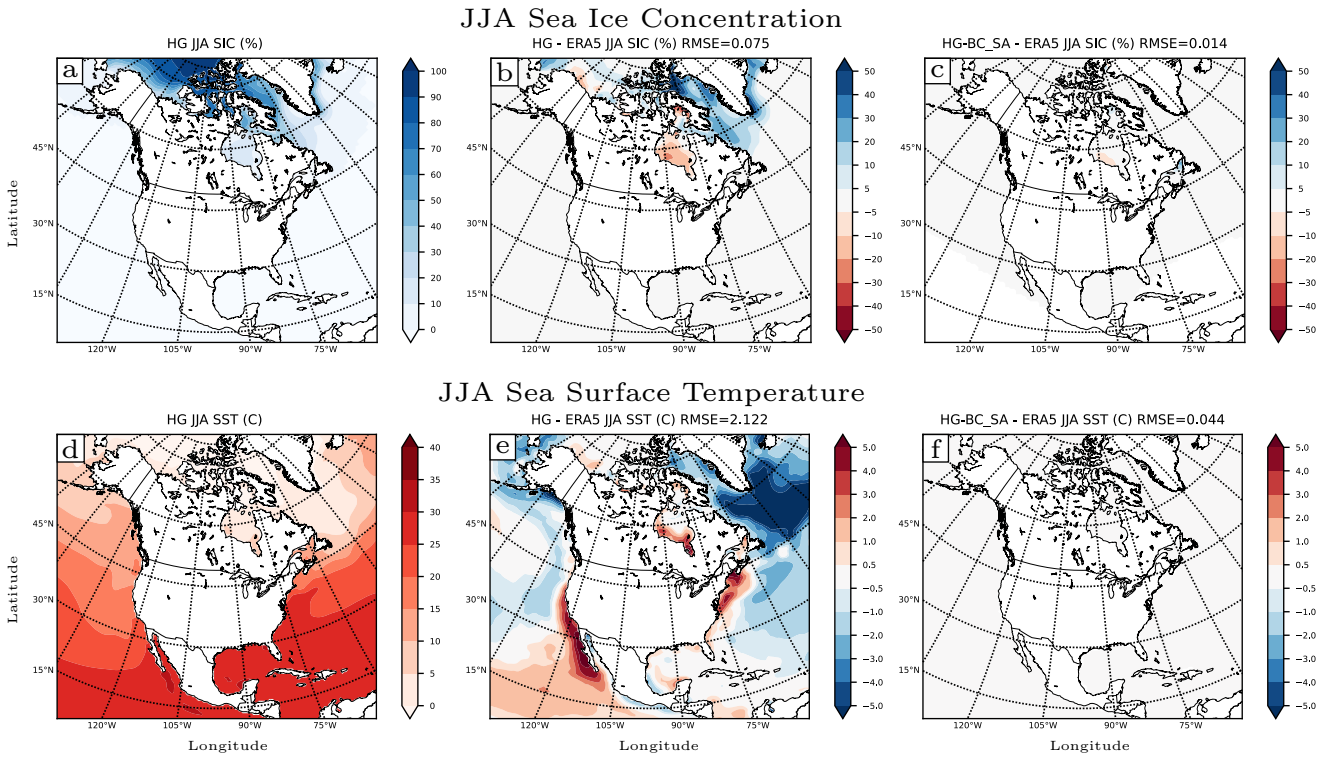


Figure S1.1: Diagnostic climatological bias correction of sea ice concentration in June-July-August (JJA), SIC (top row) and sea surface temperature, SST (bottom row). (a) climatological SIC in CanESM5 (1981-2010), (b) climatological SIC bias in CanESM5 relative ERA5, (c) climatological SIC bias of bias corrected SIC relative to ERA5. (d)-(e) identical to (a)-(c) except for SST. Root-mean-squared-errors of the bias fields, averaged over the domain, appear in the titles of the panels.

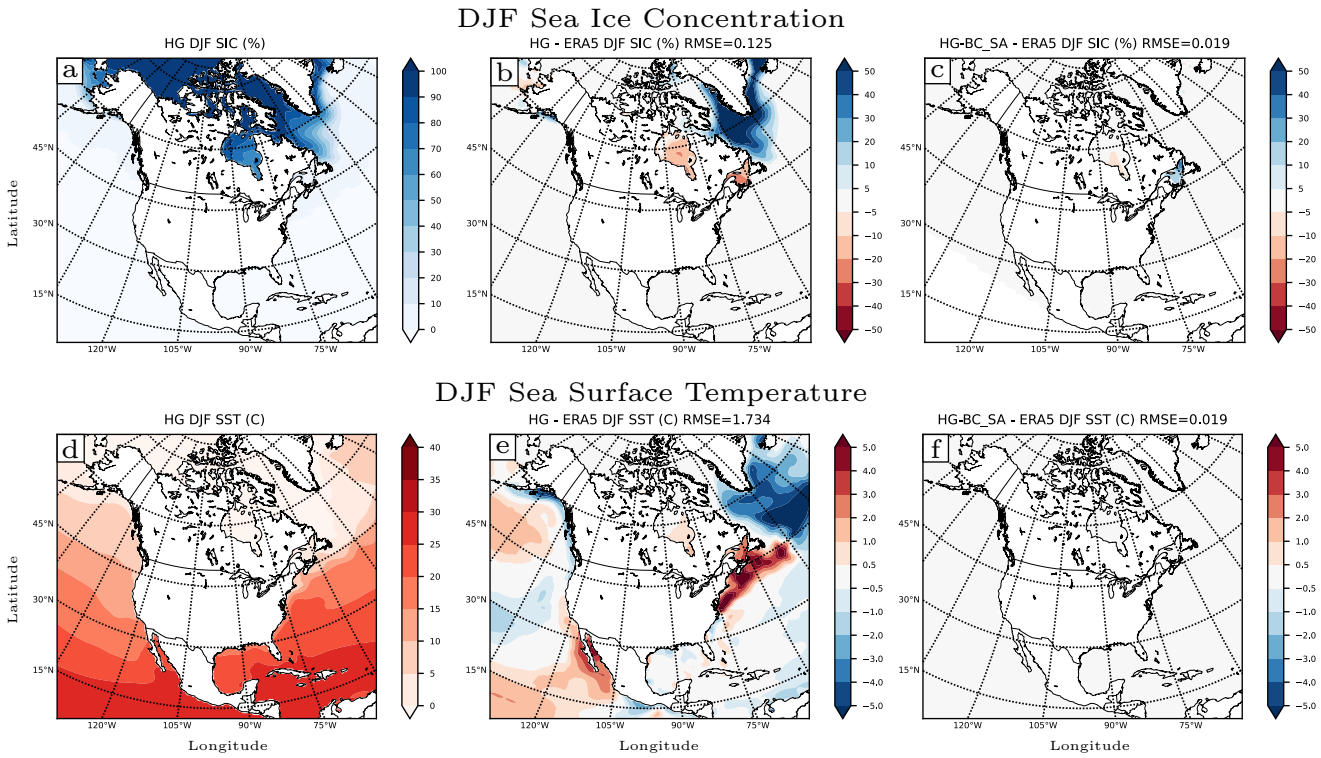


Figure S1.2: As in Fig.S1.1 except for DJF.

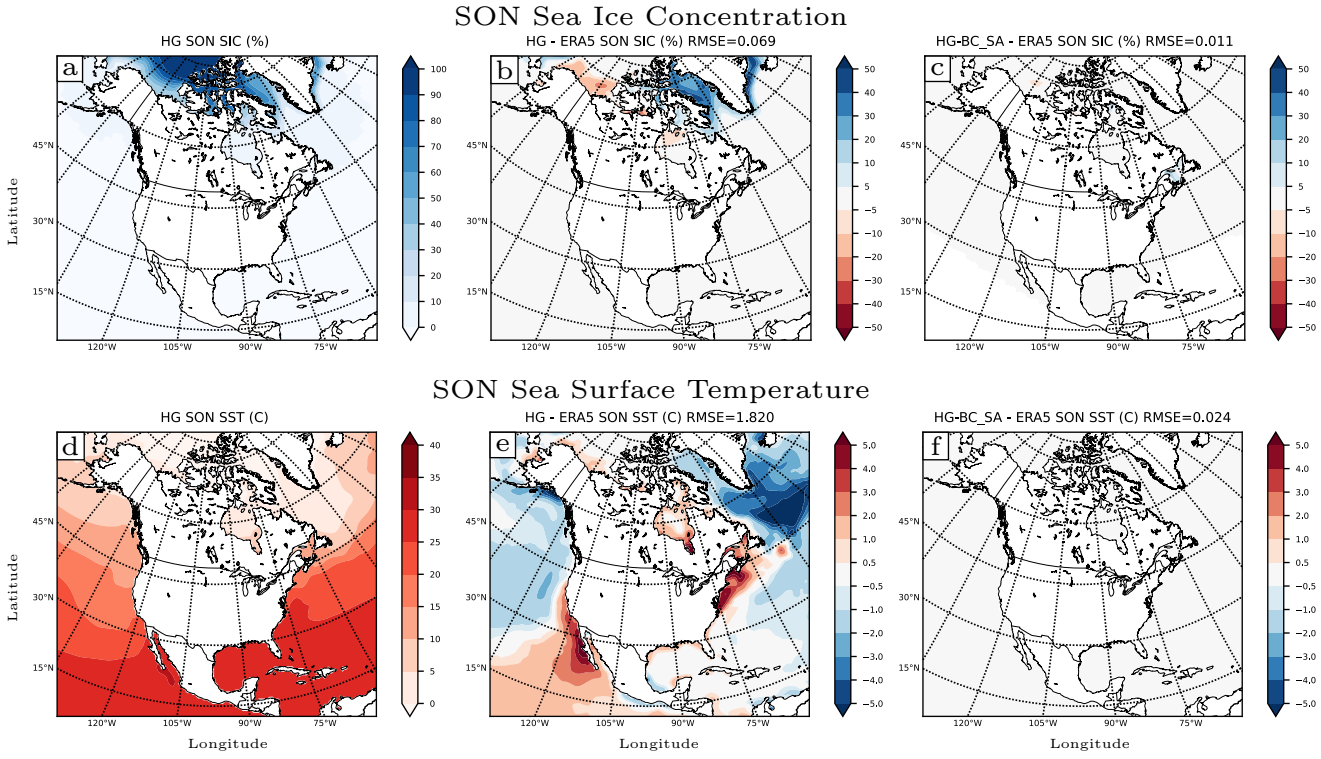


Figure S1.3: As in Fig.S1.1 except for SON.

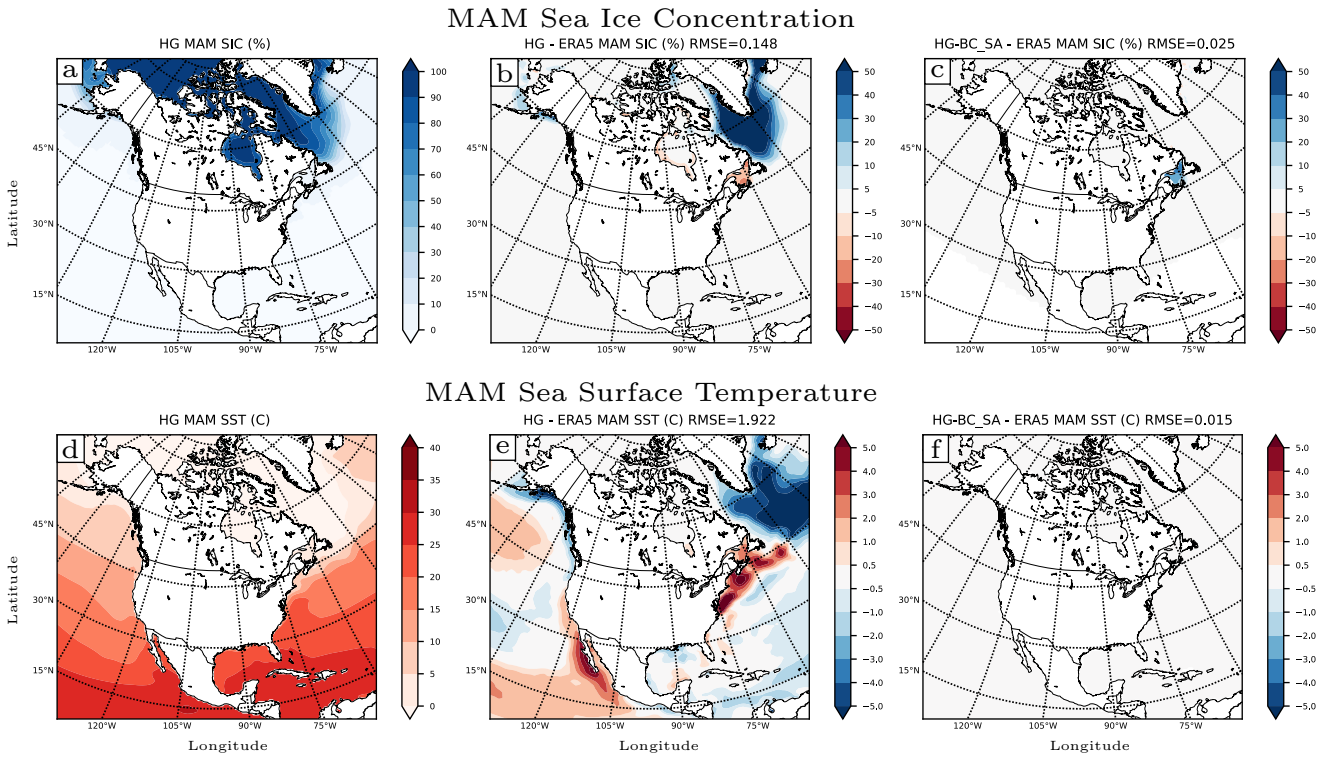


Figure S1.4: As in Fig.S1.1 except for MAM.

S2 Empirical Runtime Bias correction of Global ESM

Plots similar to Figs. 1-3 are presented here for each variable summarized in Table 1.

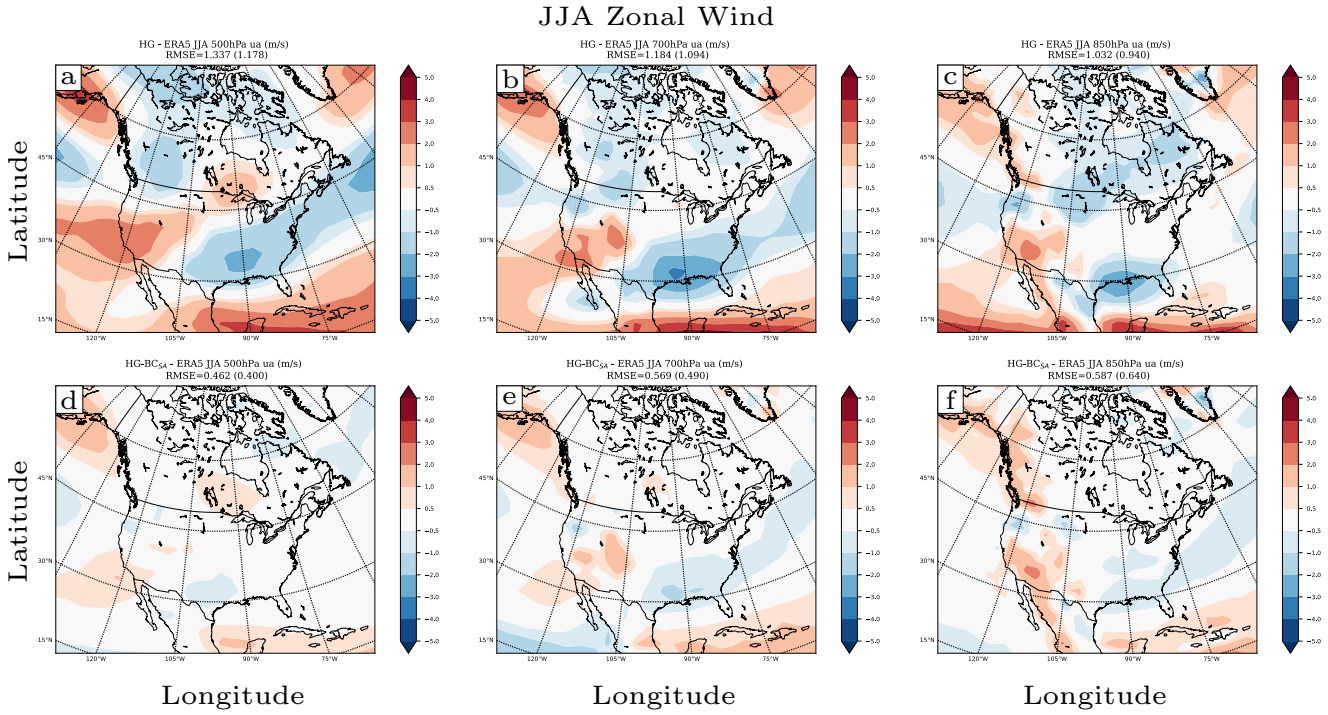


Figure S2.1: Climatological June-July-August (JJA) biases of zonal wind (ua) relative to ERA5 during the period 1981-2010. (top row) the CanESM5 HG ensemble, (bottom row) the ERBC HG-BC_{SA}. Results are displayed on the levels (a,d) 500hPa, (b,e) 700hPa, and (c,f) 850hPa. A root-mean-square-error (RMSE) measure of the bias, which is integrated over this domain, is displayed in the top right of each panel with the RMSE over land indicated in parentheses. The normalized RMSE values presented in Table. 1 are calculated as the ratio of the RMSE in HG-BC_{SA} to the corresponding RMSE in the HG ensemble.

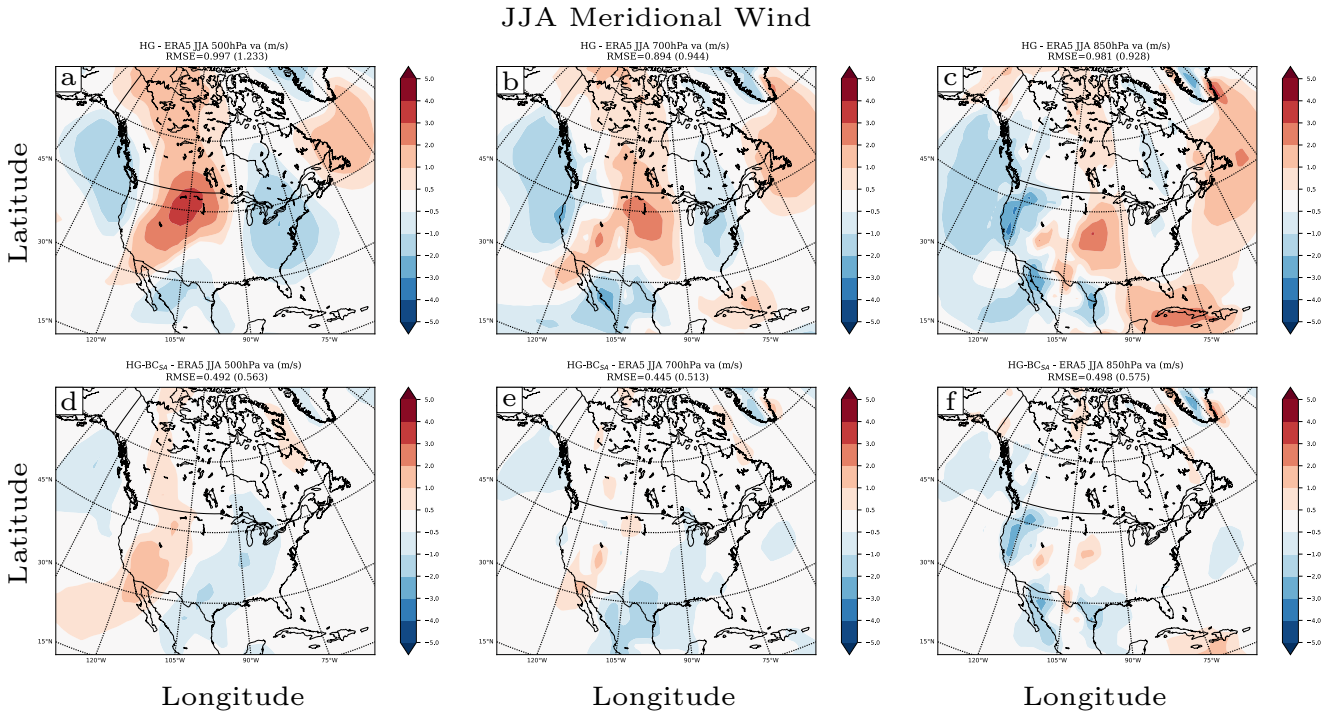


Figure S2.2: As in Fig.S2.1 except for meridional wind (va).

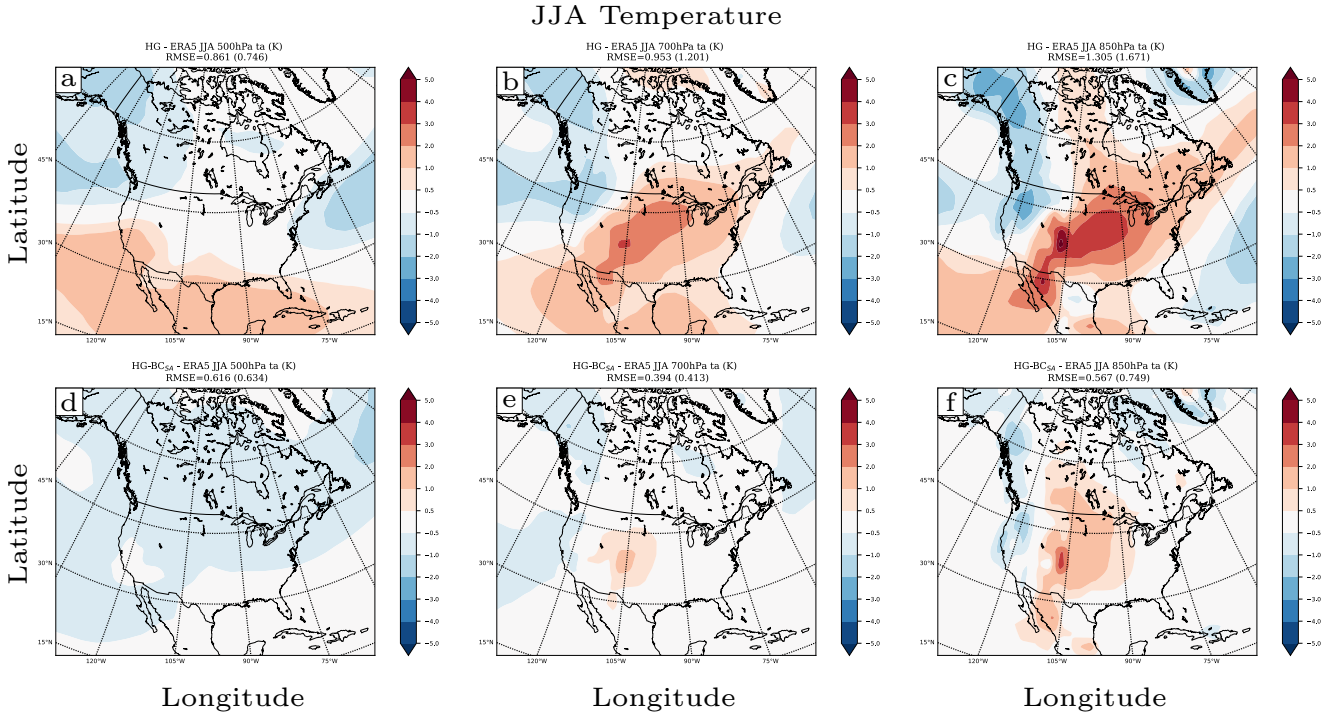


Figure S2.3: As in Fig.S2.1 except for air temperature (ta).

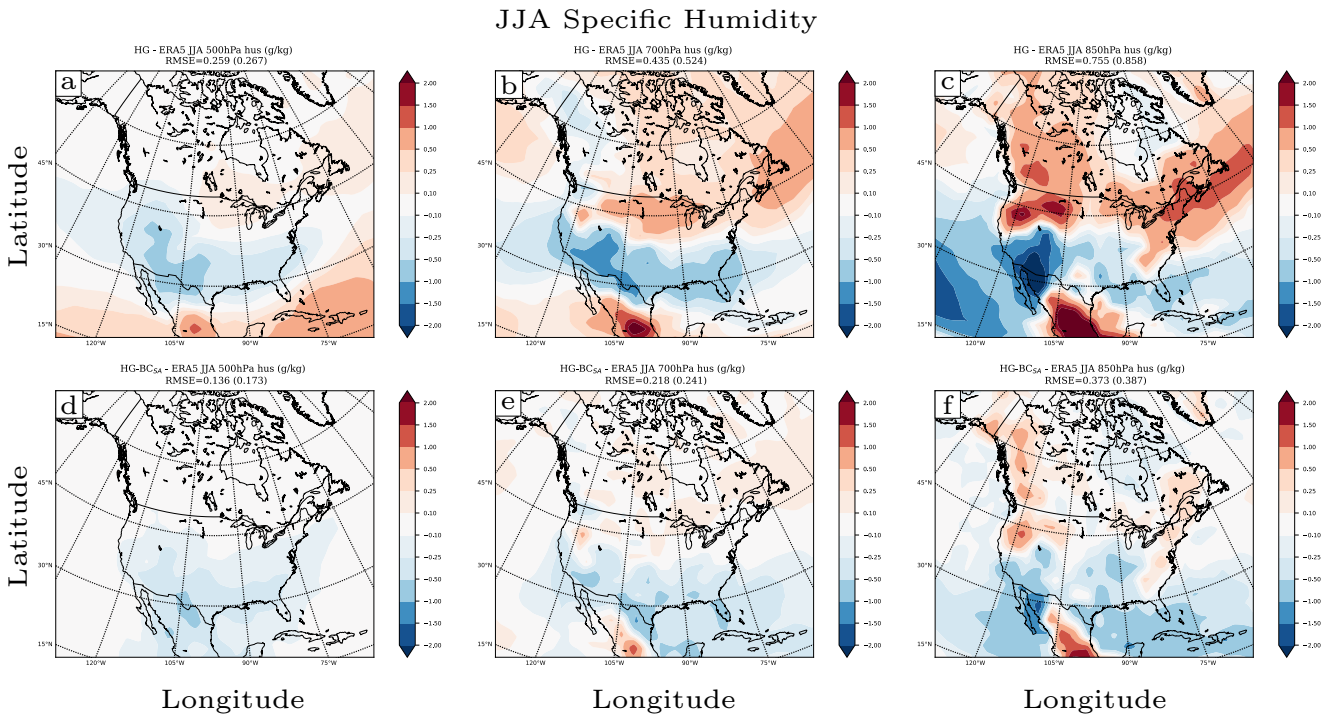


Figure S2.4: As in Fig.S2.1 except for specific humudity (hus).

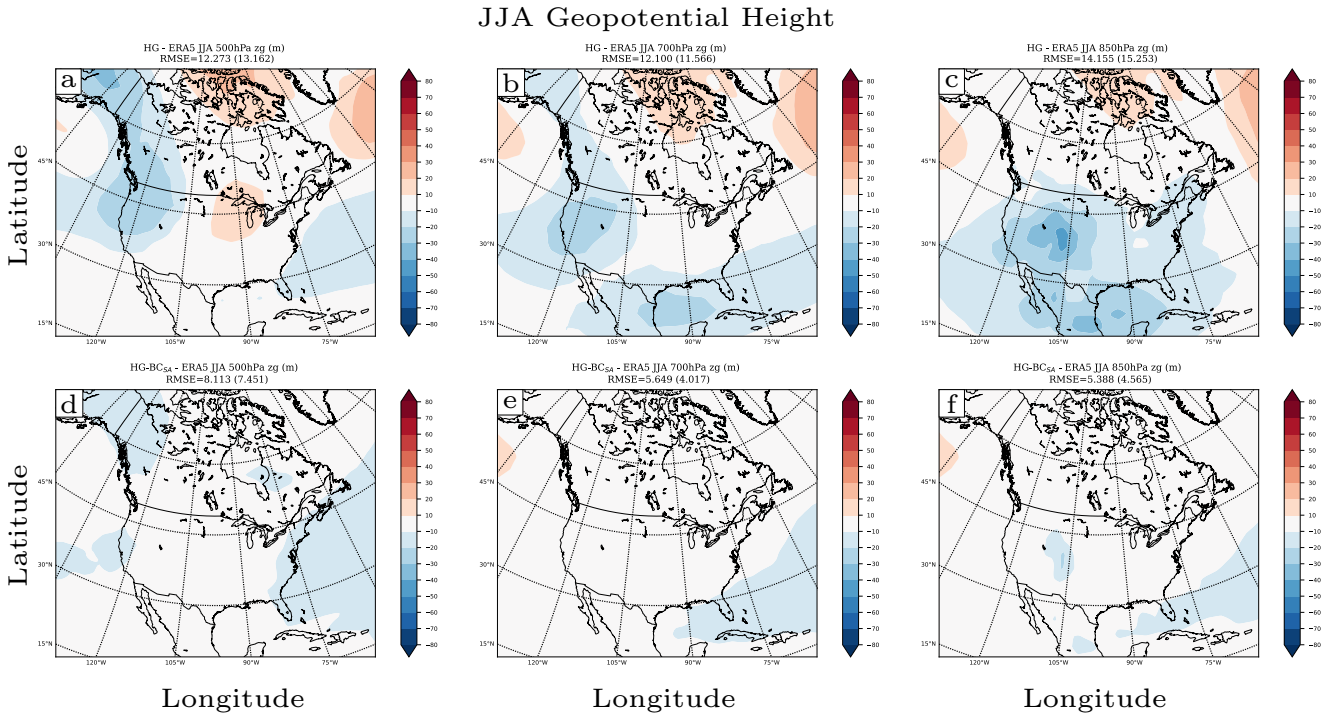


Figure S2.5: As in Fig.S2.1 except for geopotential height (zg).

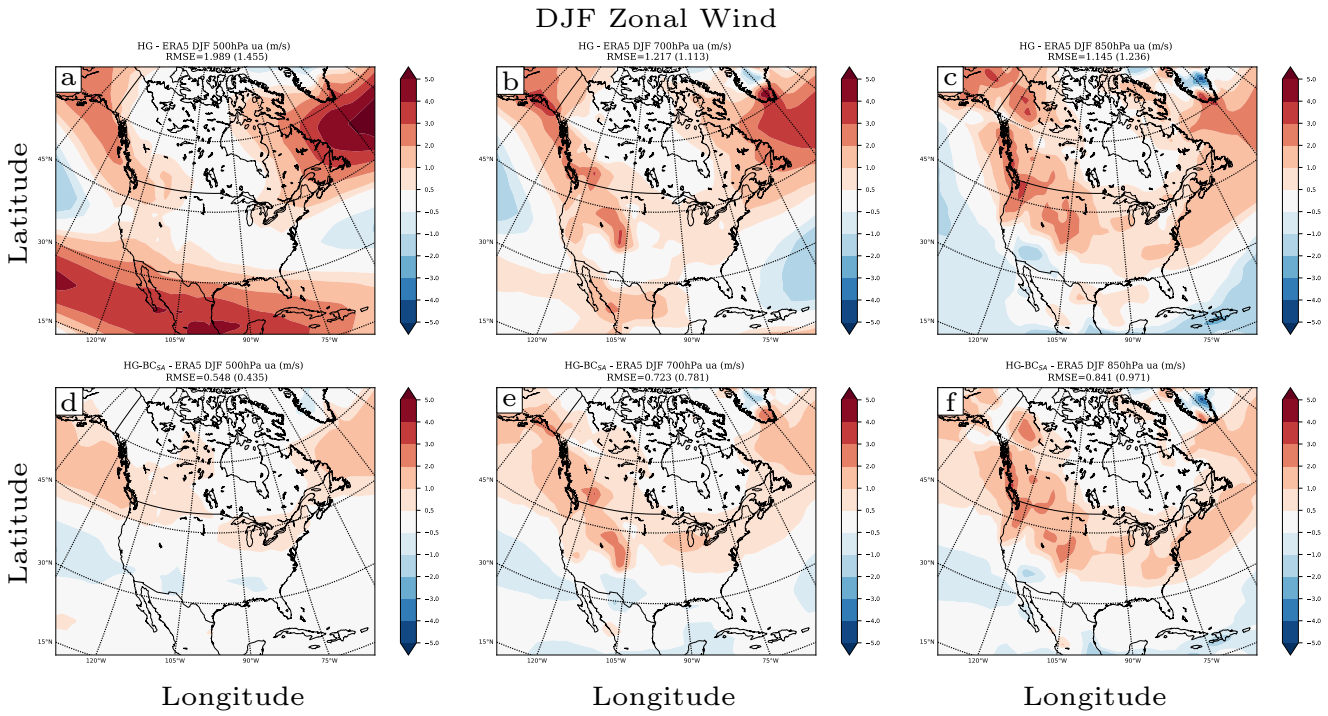


Figure S2.6: As in Fig.S2.1 except for December-January-February (DJF) Zonal Wind (ua).

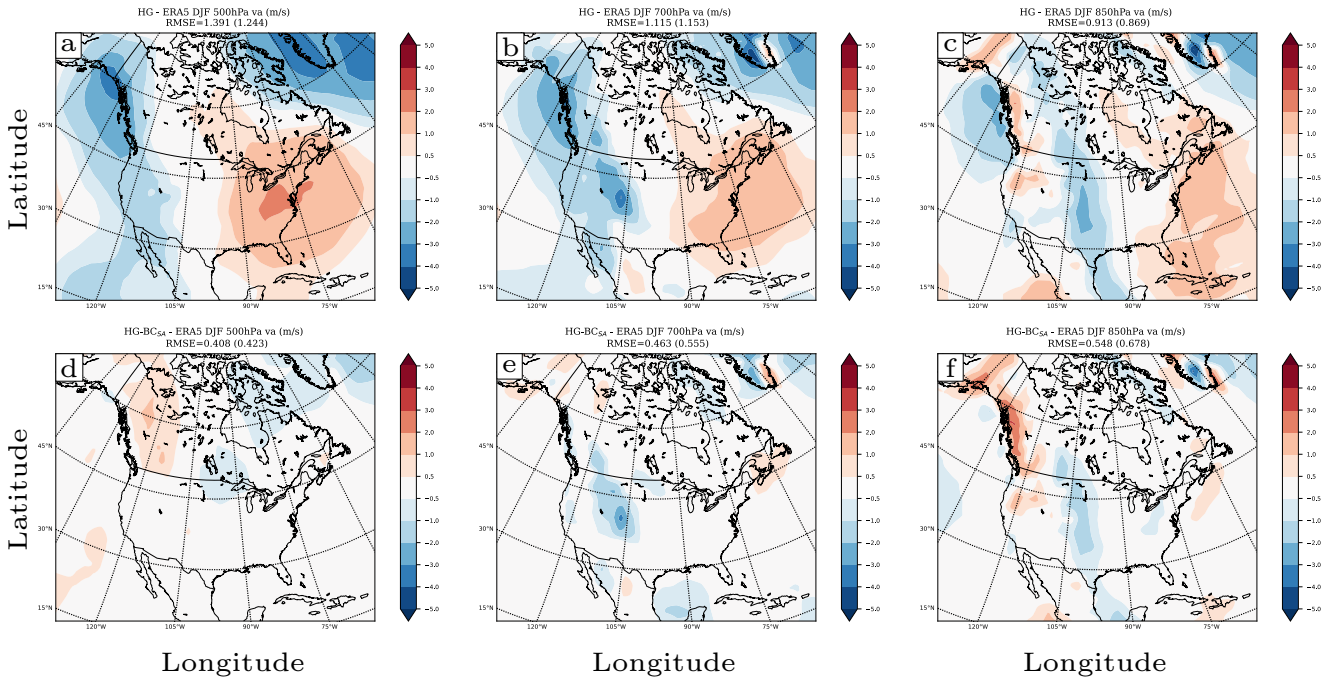


Figure S2.7: As in Fig.S2.1 except for DJF meridional wind (va).

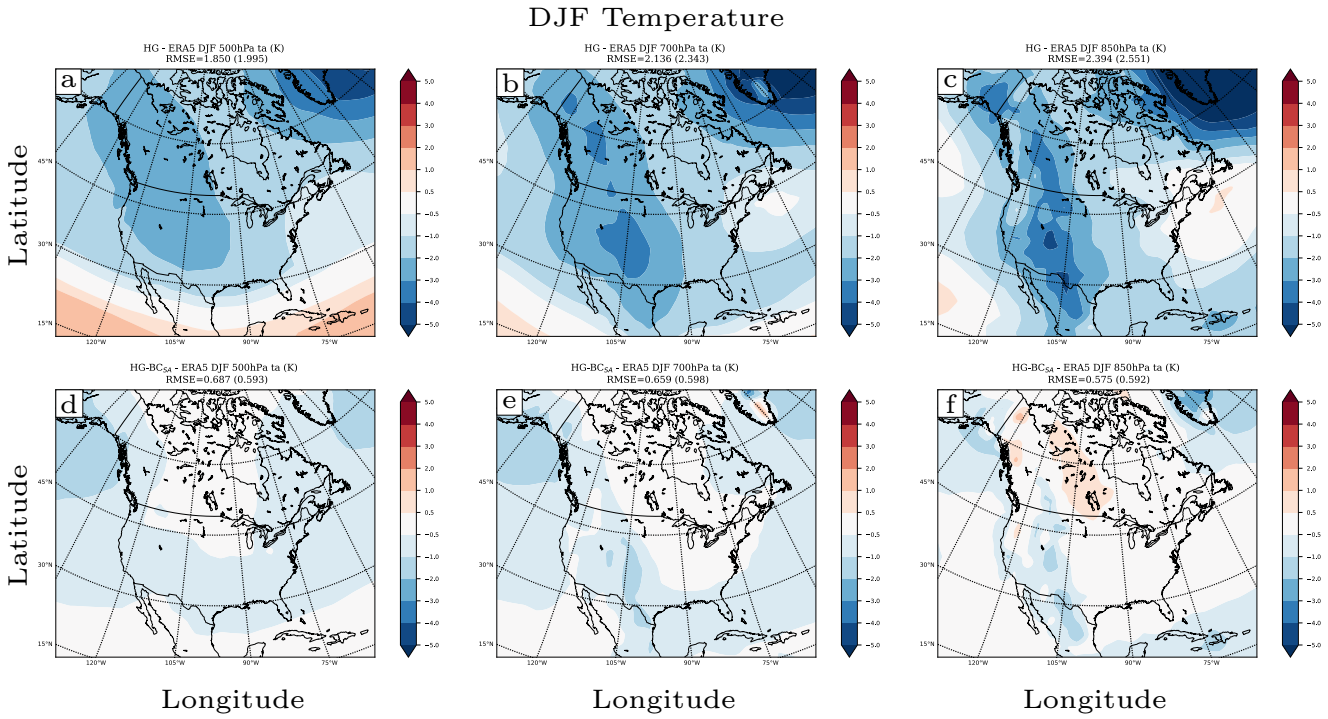


Figure S2.8: As in Fig.S2.1 except for DJF air temperature (ta).

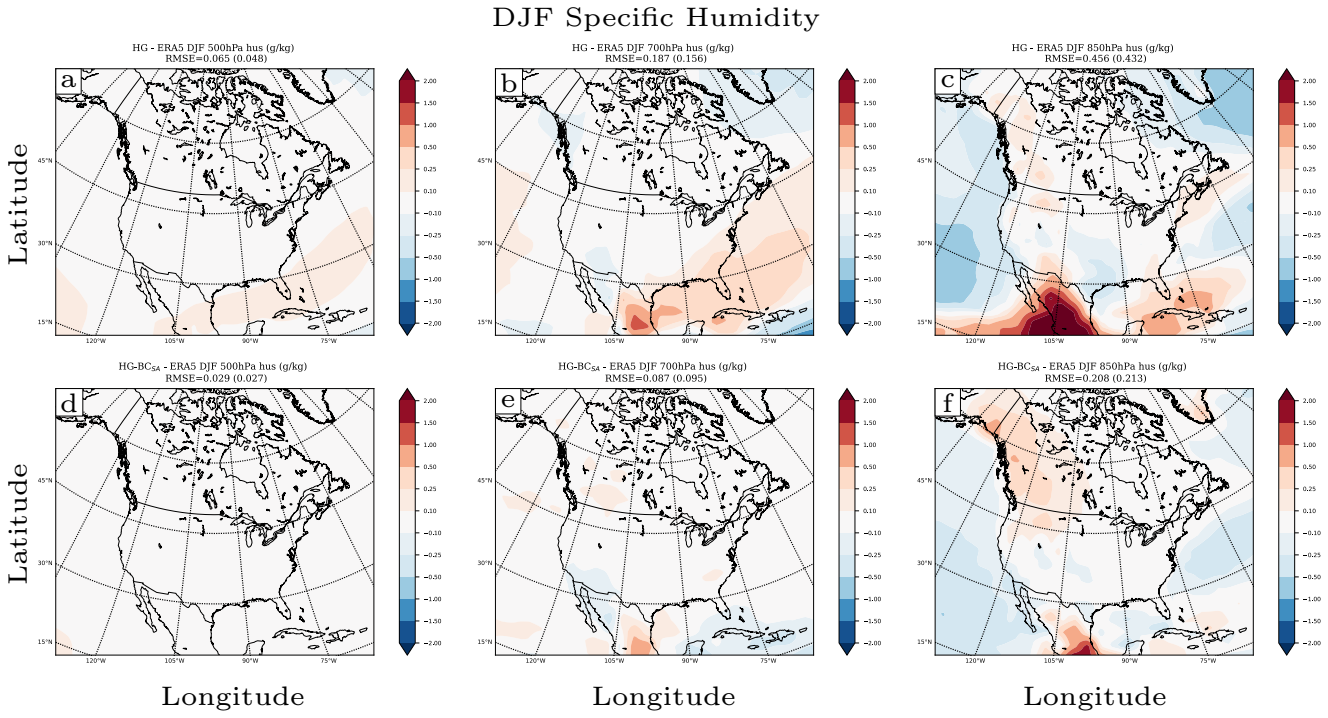


Figure S2.9: As in Fig.S2.1 except for DJF specific humudity (hus).

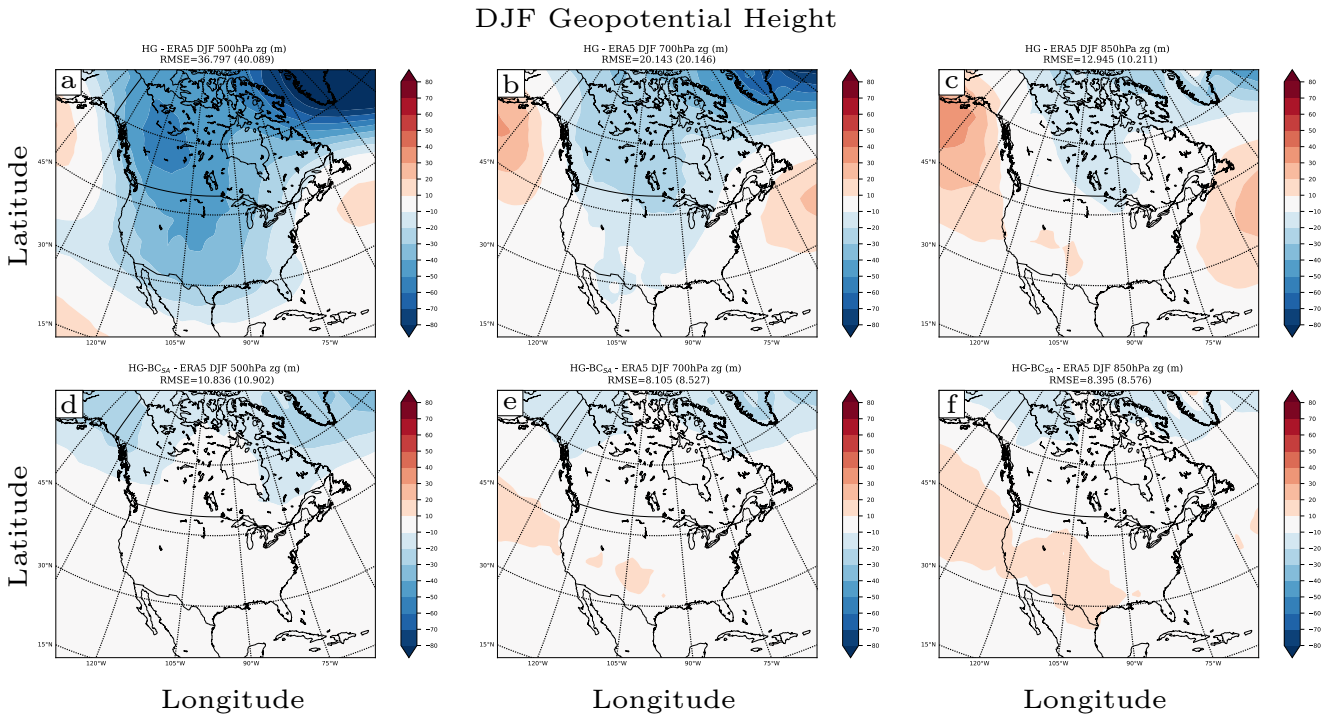


Figure S2.10: As in Fig.S2.1 except for DJF geopotential height (zg).

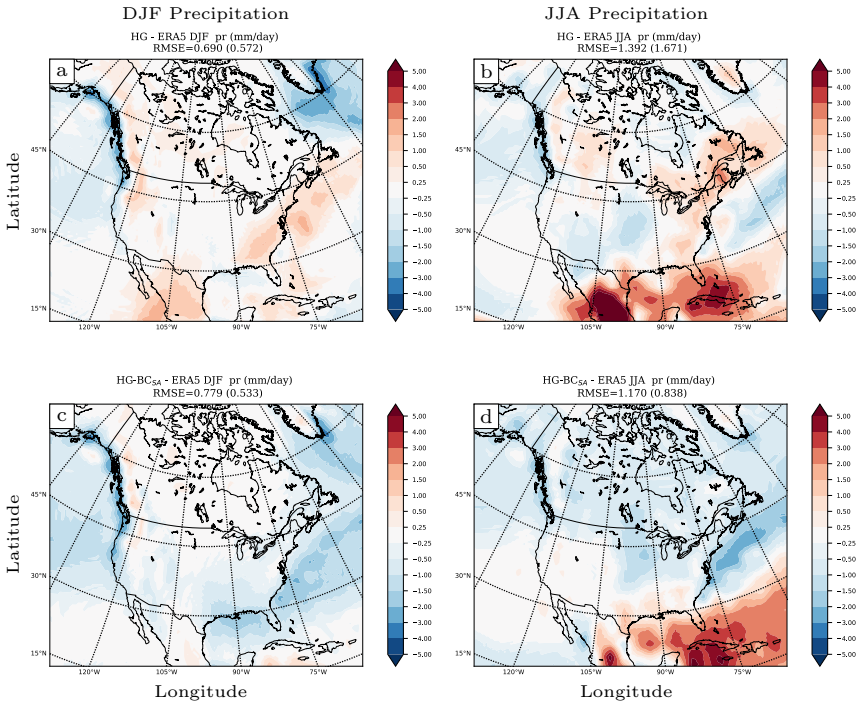


Figure S2.11: As in Fig.S2.1 except for DJF and JJA total precipitation.

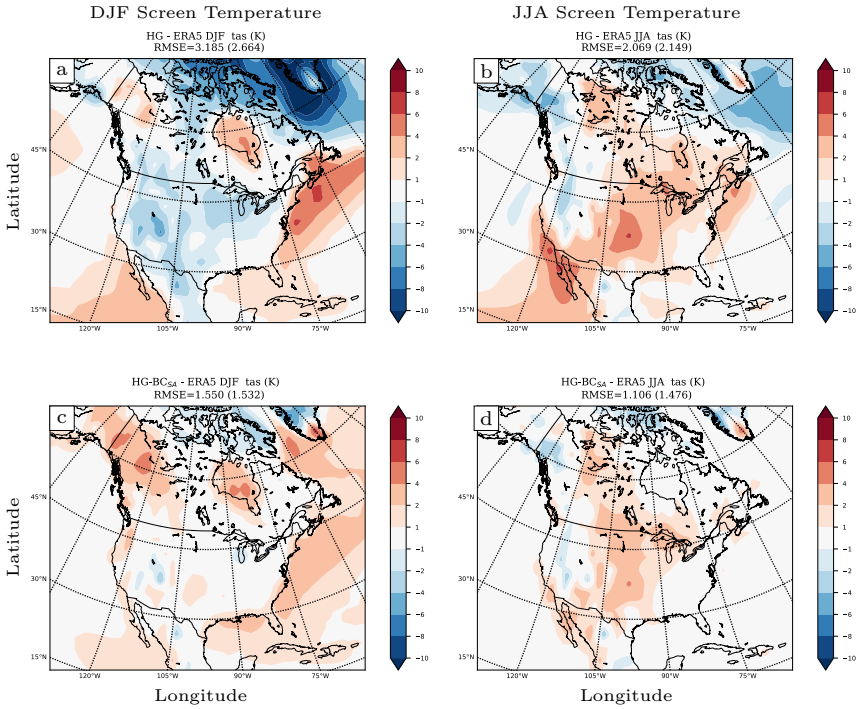


Figure S2.12: As in Fig.S2.1 except for DJF and JJA screen temperature (tas).

S3 Inherent Regional Model Biases and Combined ESM/Regional Model Biases

Plots of the inherent RCM biases (i.e. in evaluation simulations) and plots of combined RCM/ESM biases (i.e. in historical simulations) similar to Figs. 4 and 5 are presented here for additional variables.

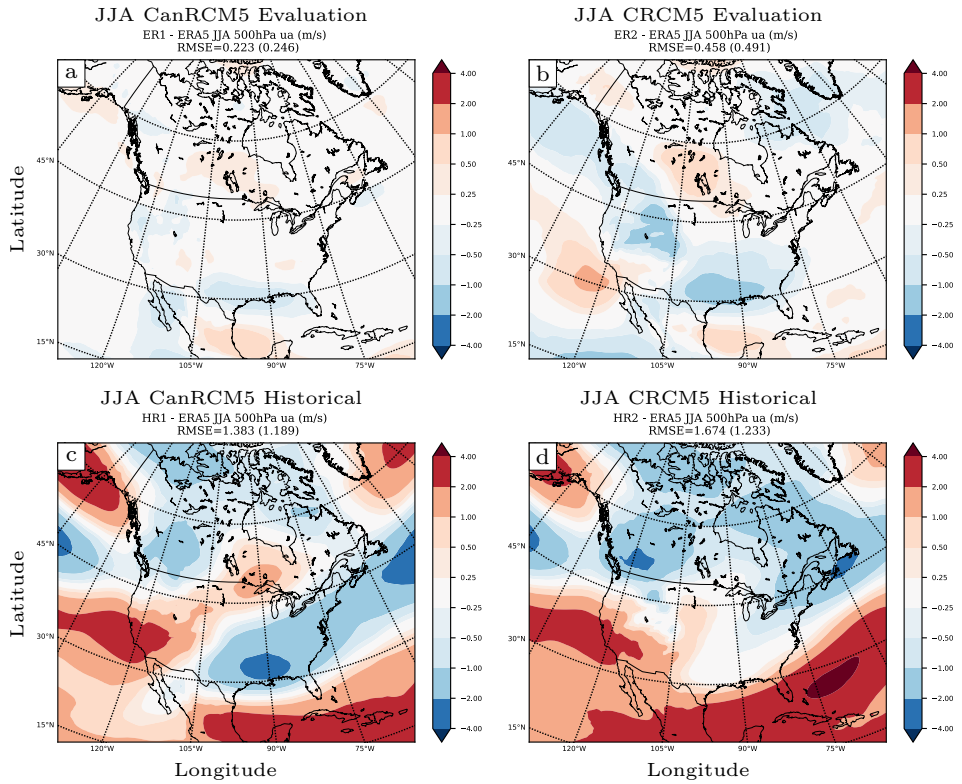


Figure S3.1: Regional model zonal wind (ua) biases relative to ERA5 in JJA over the period 1981-2010. Panels a/b, inherent CanRCM5/CRCM5 biases derived from their evaluation downscaling ensembles ER1/ER2; panels c/d, combined ESM/RCM downscaling biases derived from the CanRCM5/CRCM5 historical ensembles HR1/HR2. A root-mean-square-error (RMSE) measure of the bias, which is integrated over this domain, is displayed in the top right of each panel with the RMSE over land indicated in parentheses.

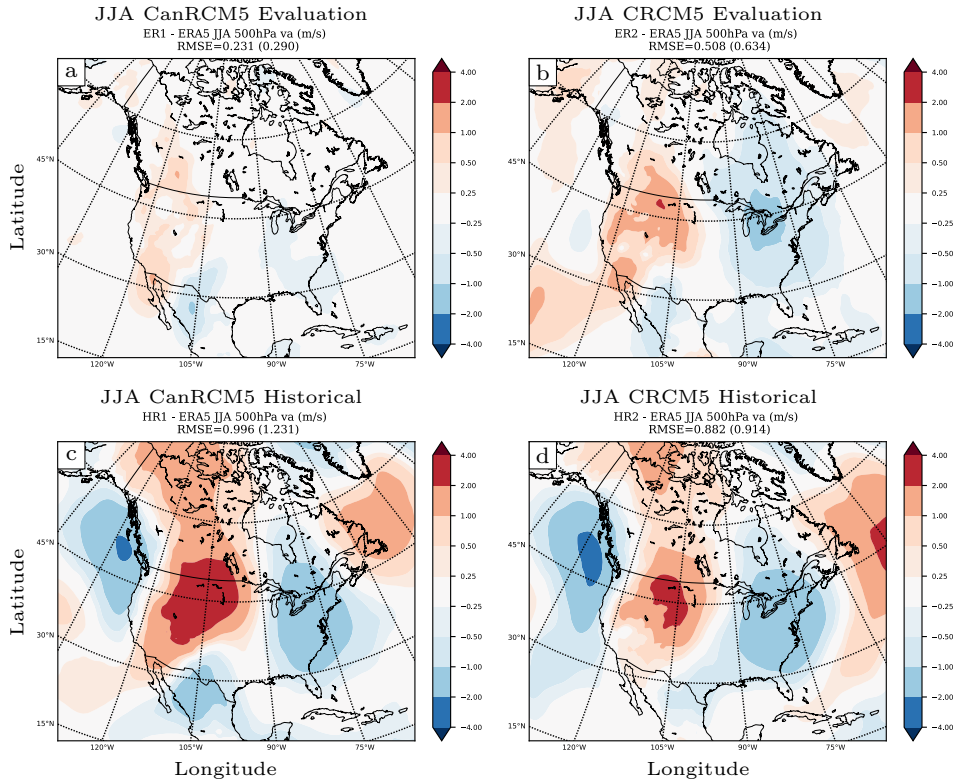


Figure S3.2: As in Fig.S3.1 except for meridional wind (va).

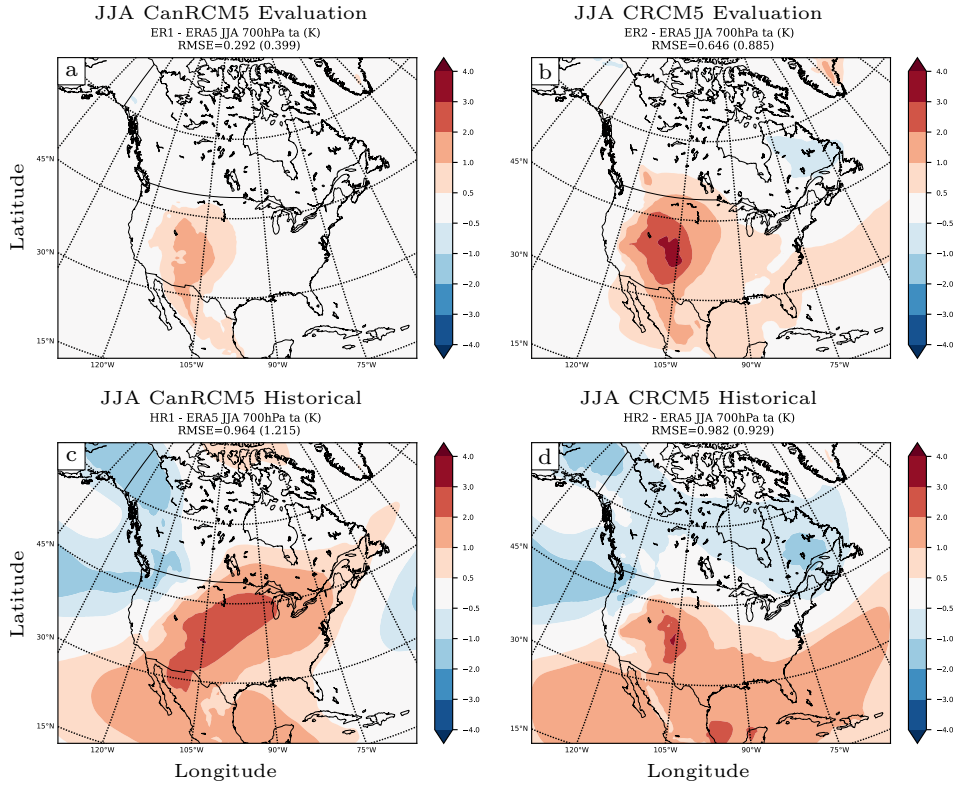


Figure S3.3: As in Fig.S3.1 except for air temperature (ta).

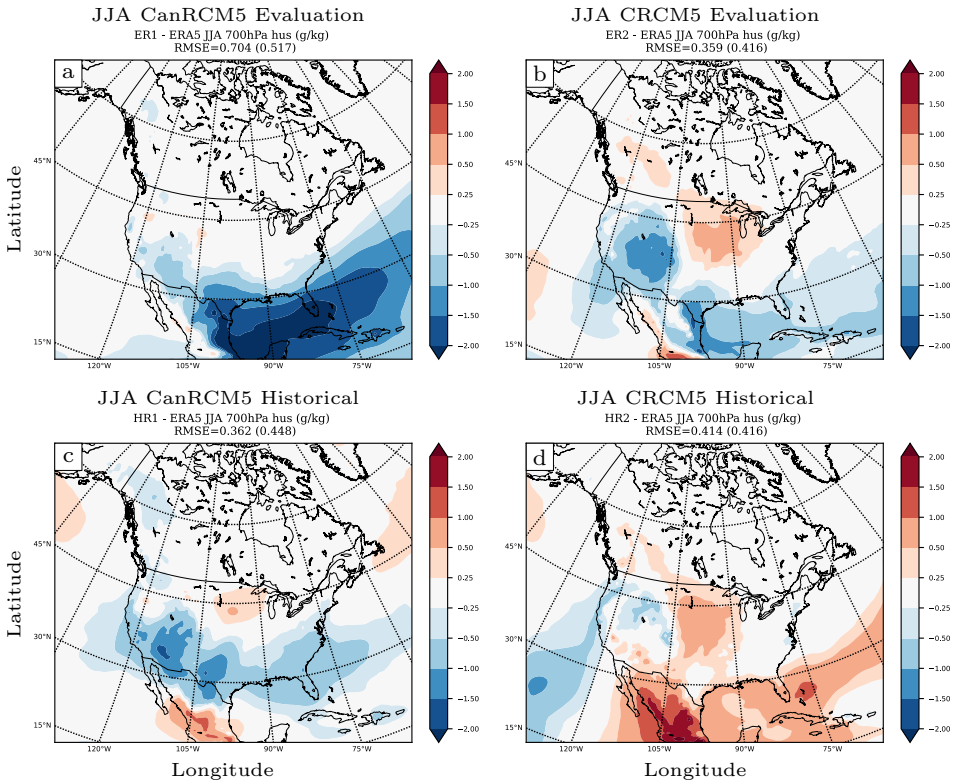


Figure S3.4: As in Fig.S3.1 except for specific humidity (hus).

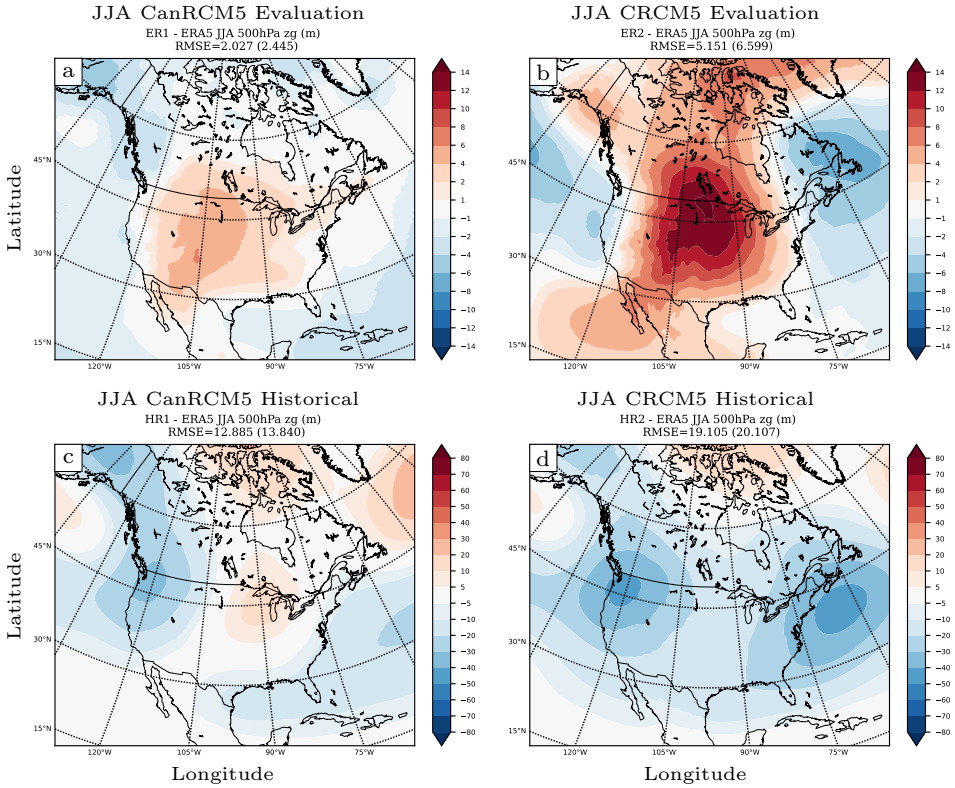


Figure S3.5: As in Fig.S3.1 except for geopotential height (zg).

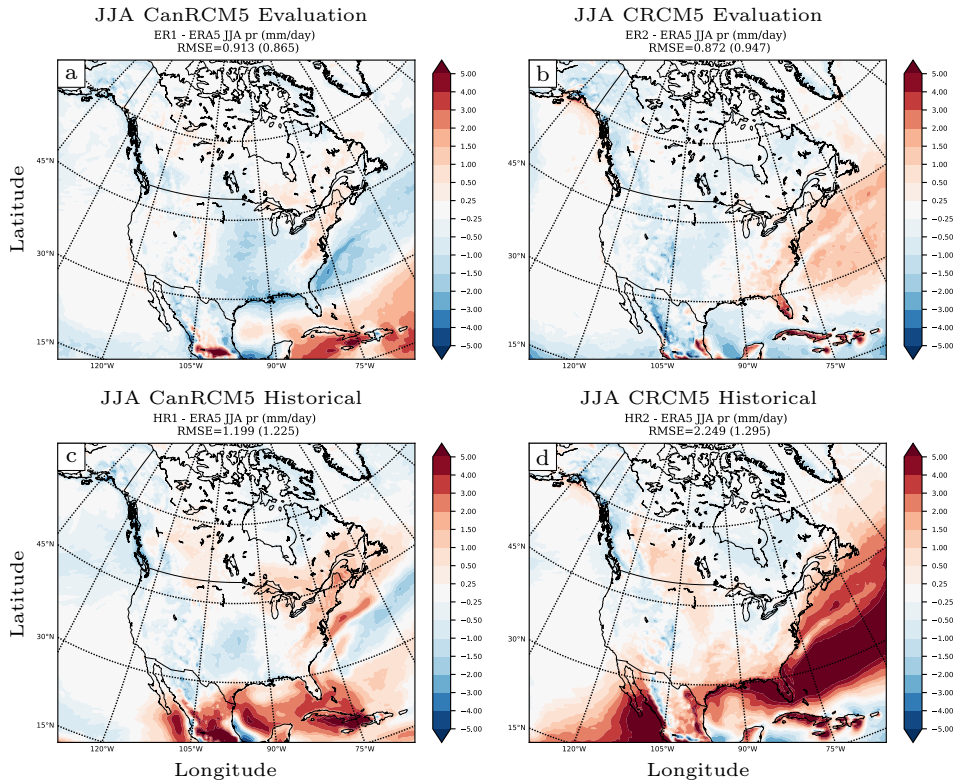


Figure S3.6: As in Fig.S3.1 except for total precipitation (pr).

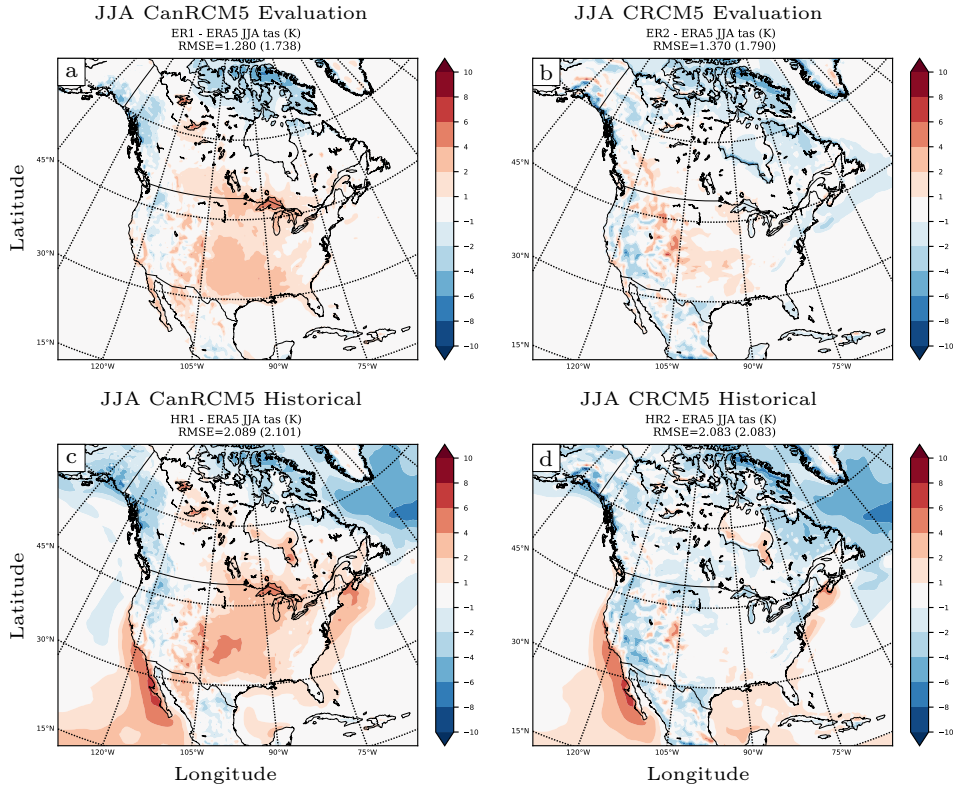


Figure S3.7: As in Fig.S3.1 except for screen tenperature (tas).

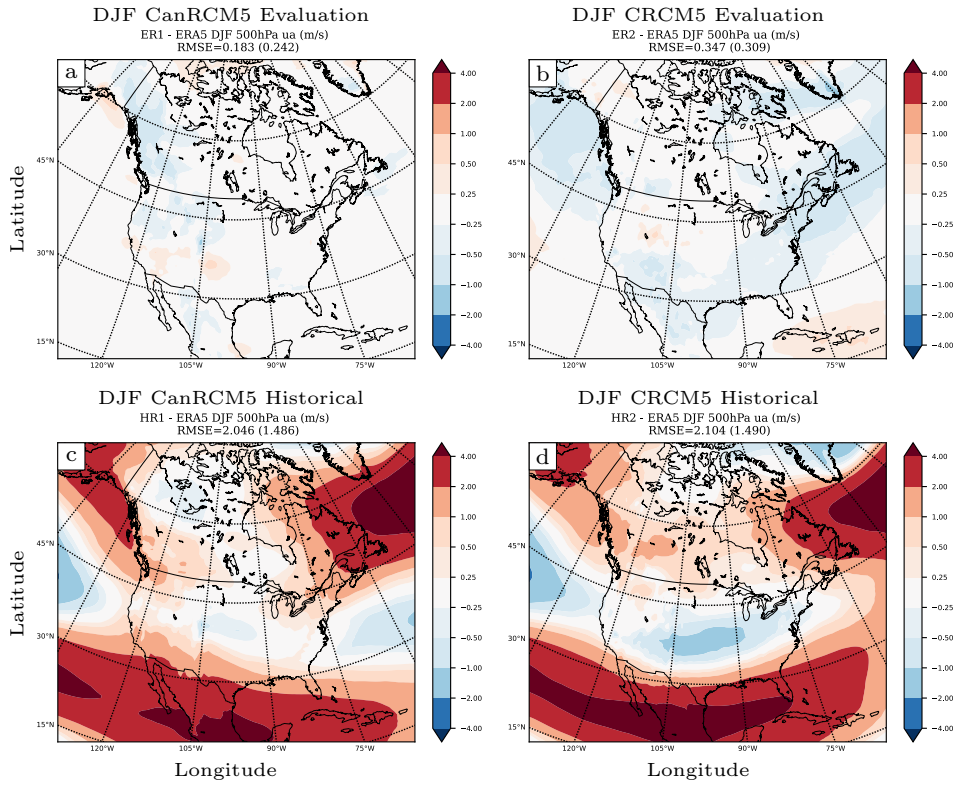


Figure S3.8: As in Fig.S3.1 except for DJF zonal wind (ua).

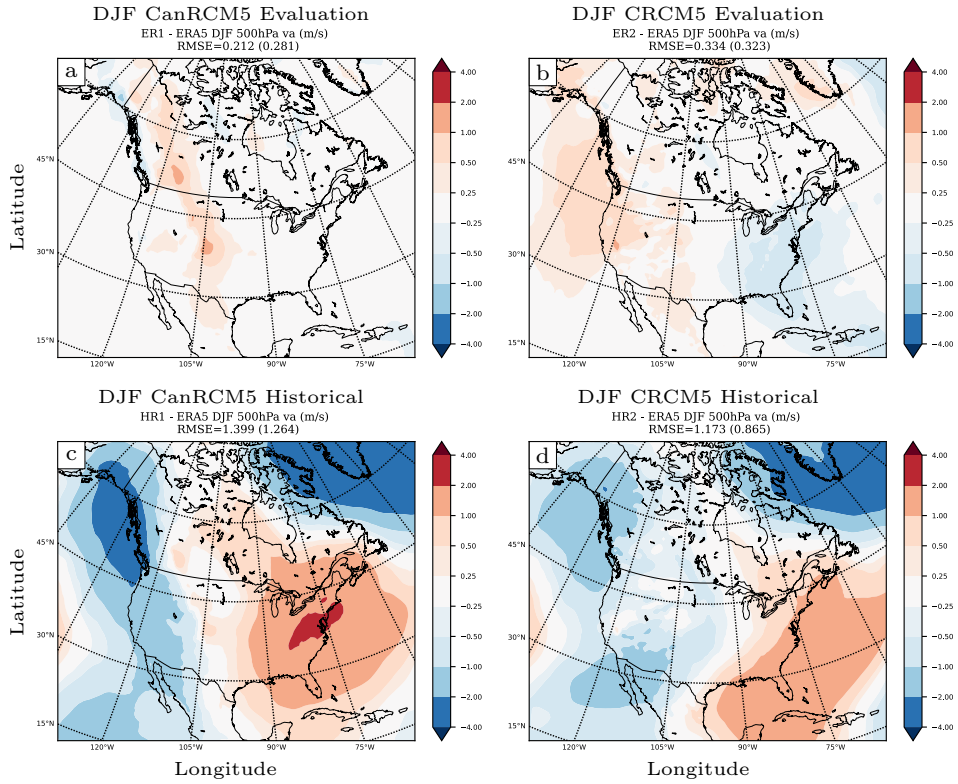


Figure S3.9: As in Fig.S3.1 except for DJF meridional wind (va).

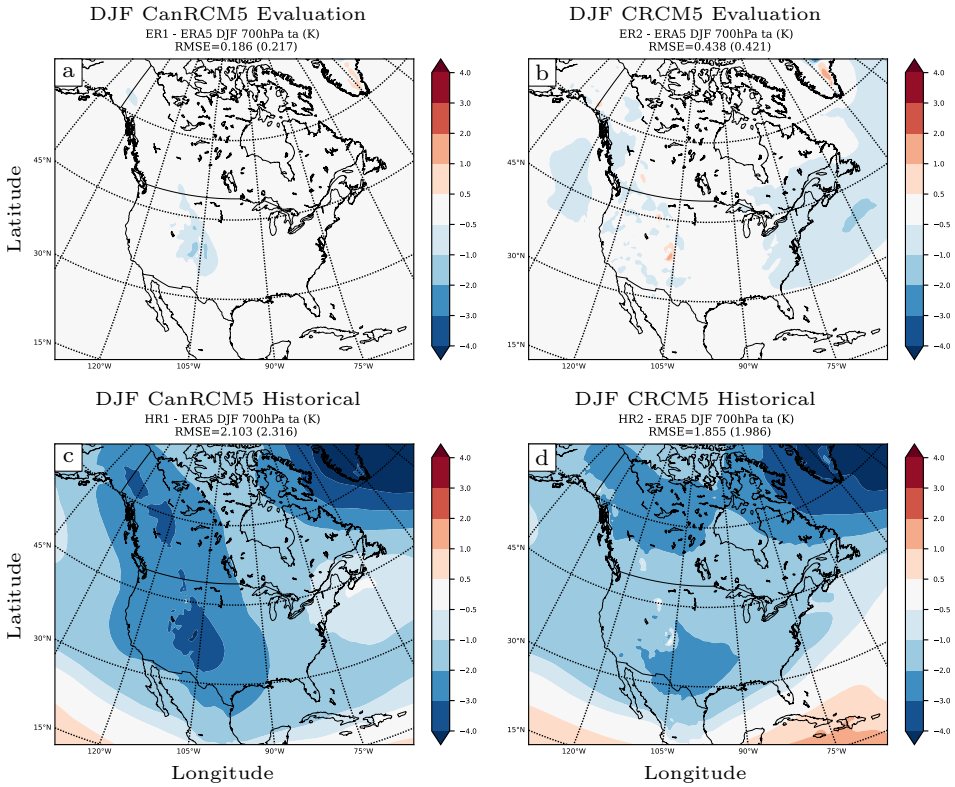


Figure S3.10: As in Fig.S3.1 except for DJF air temperature (ta).

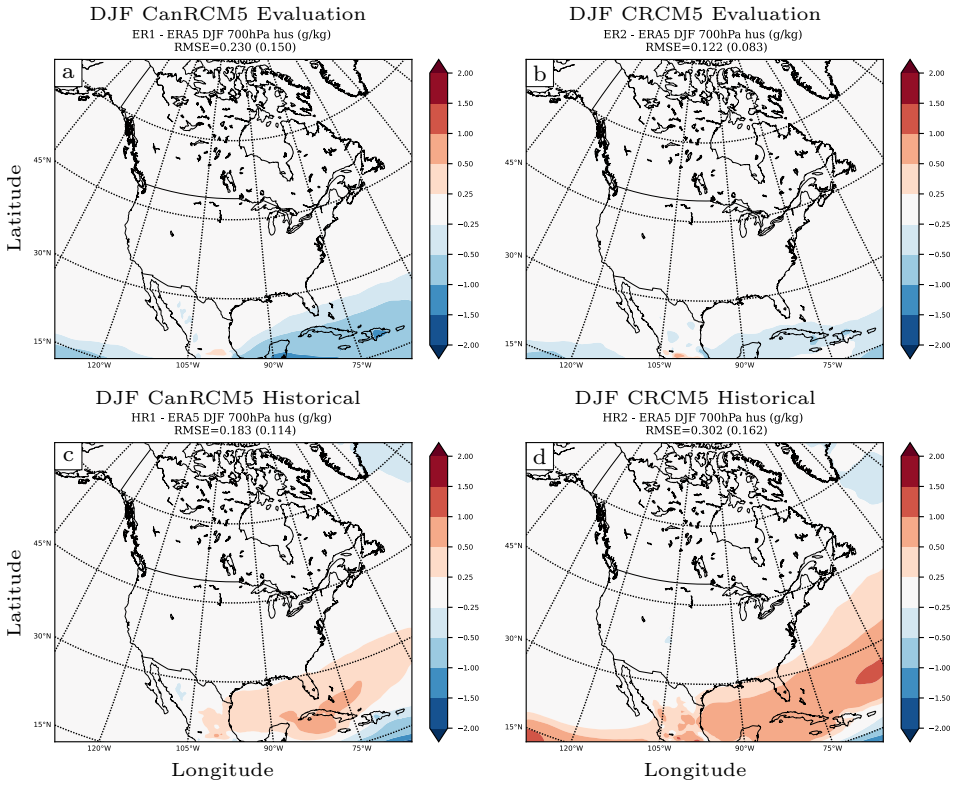


Figure S3.11: As in Fig.S3.1 except for DJF specific humidity (hus).

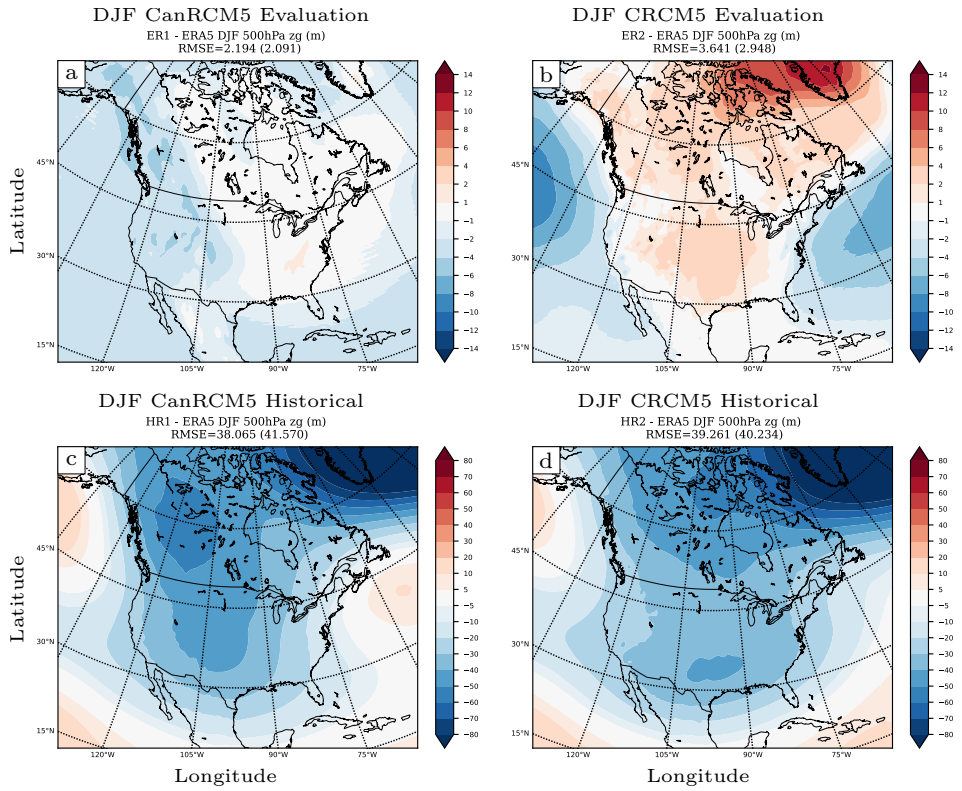


Figure S3.12: As in Fig.S3.1 except for DJF geopotential height (zg).

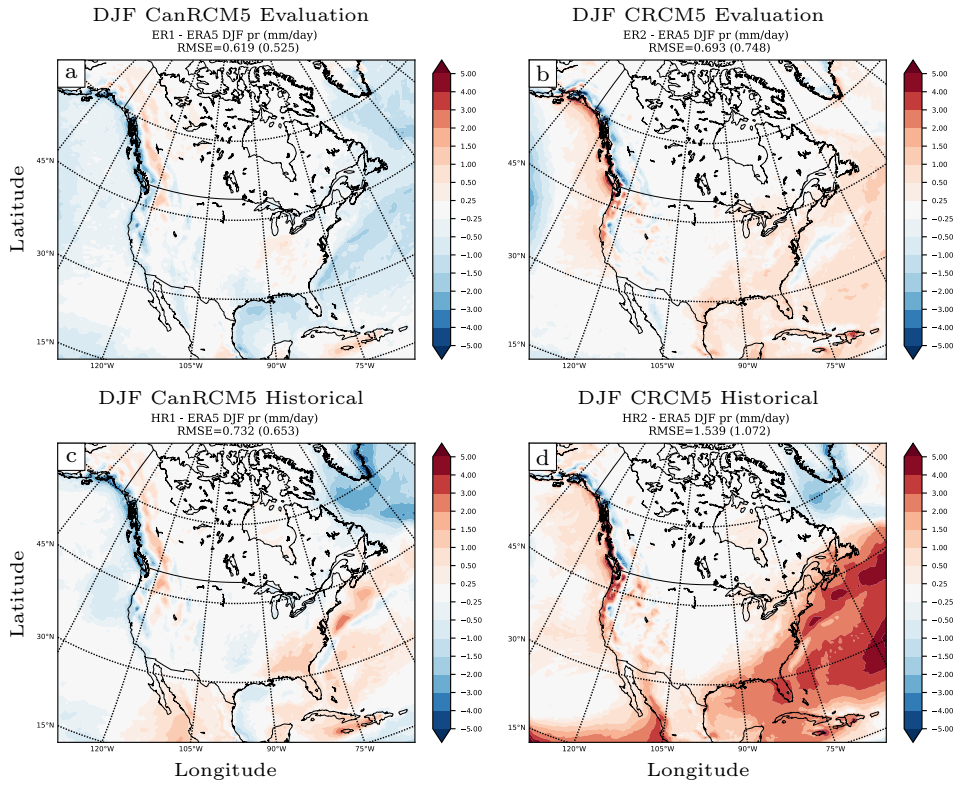


Figure S3.13: As in Fig.S3.1 except for DJF total precipitation (pr).

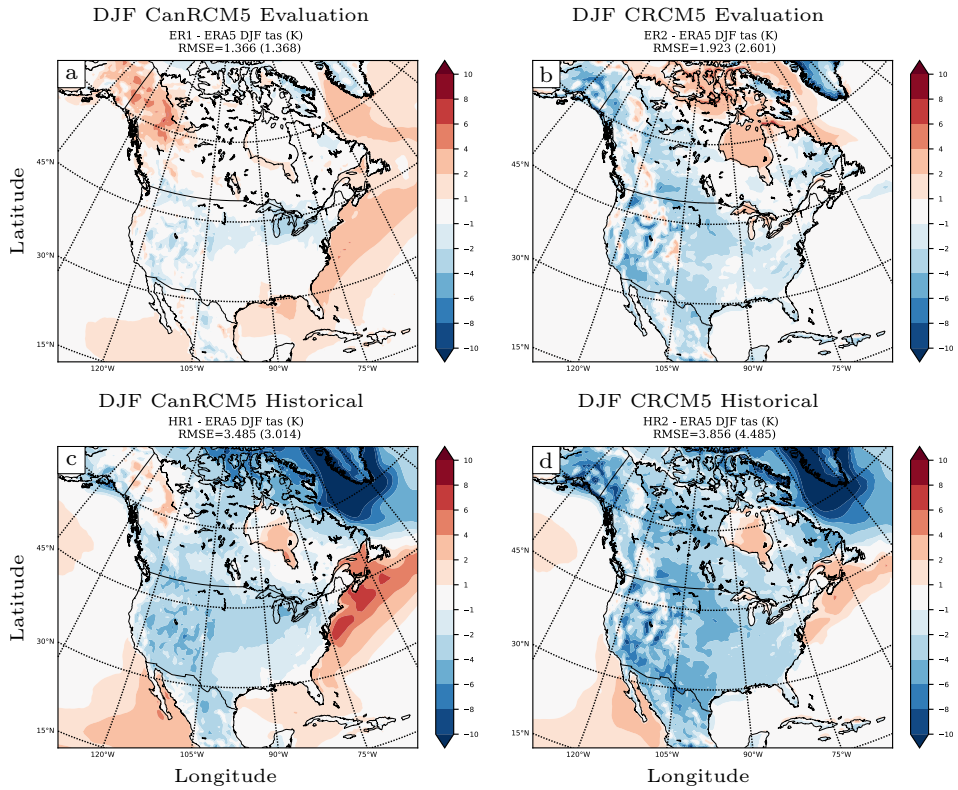


Figure S3.14: As in Fig.S3.1 except for DJF screen tenperature (tas).

S4 Driving Bias Influence During the Historical Period

Plots similar to Figs. 6 and 7 are presented here for each variable summarized in Table 4.

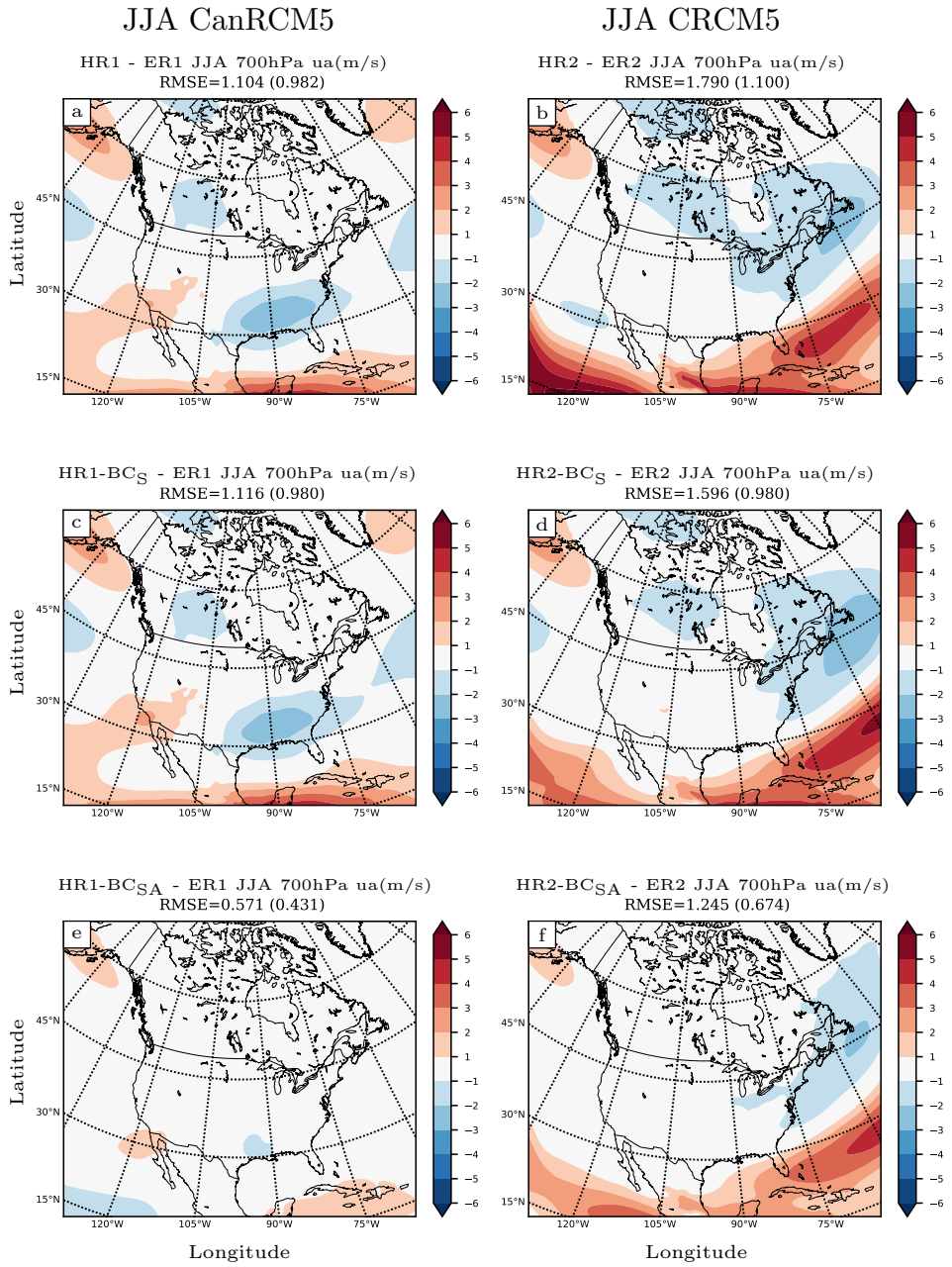


Figure S4.1: The Driving Bias Influence on the JJA 700hPa zonal wind (ua) field in ESM driven historical simulations of CanRCM5 (first column) and CRCM5 (second column). Panels (a,b): historical ensembles (HR1,HR2), driven by the uncorrected CanESM5 HG ensemble; panels (c,d): historical ensembles (HR1-BC_S,HR2-BC_S), driven by the CanESM5 HG ensemble but with bias corrected sea-surface forcing; panels (e,f): historical ensembles (HR1-BC_{SA},HR2-BC_{SA}), driven by the CanESM5 HG-BC_{SA}HG ensemble. A root-mean-square-error (RMSE) measure of the bias, which is integrated over this domain, is displayed at the top of each panel with the RMSE over land indicated in parentheses.

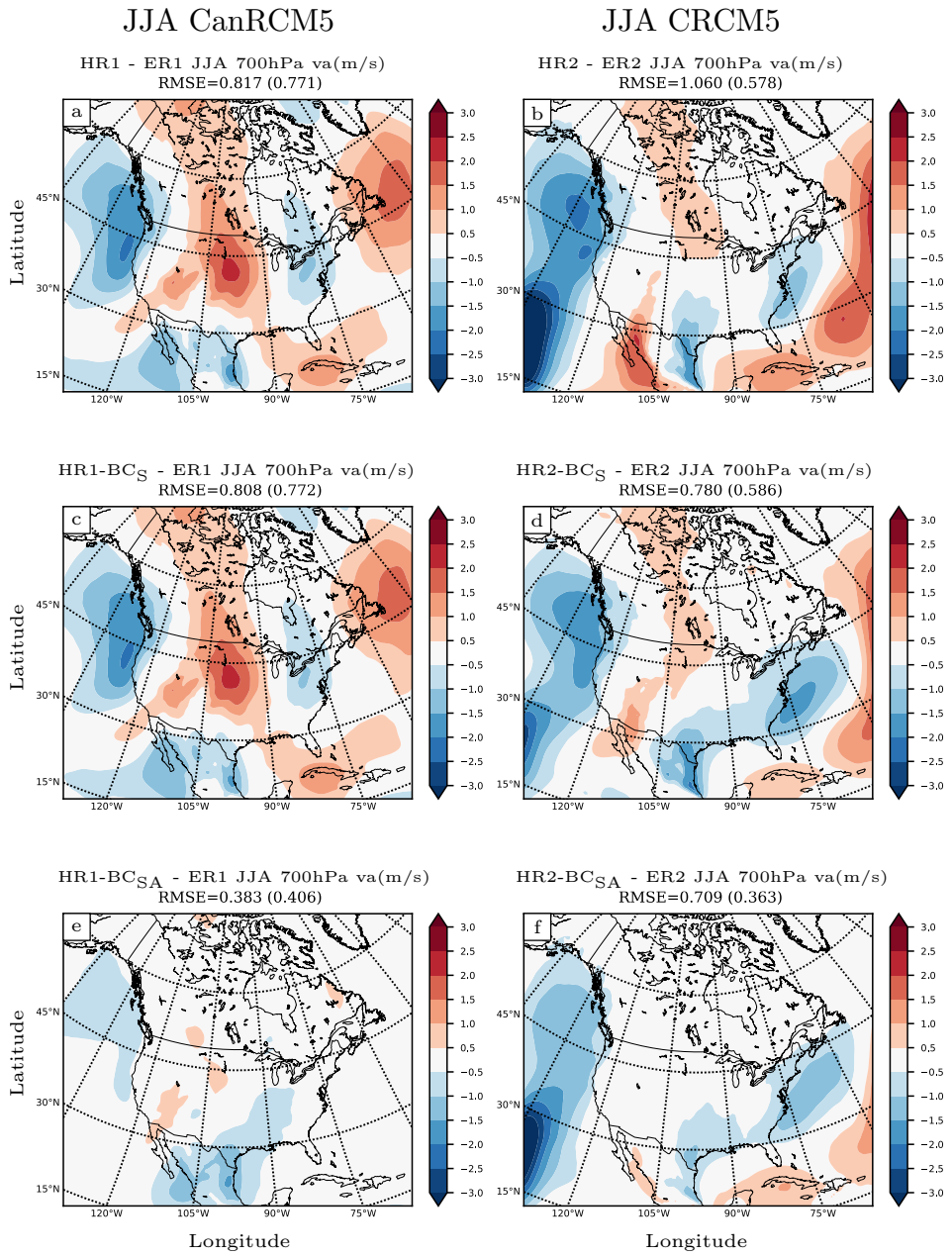


Figure S4.2: As in Fig.S4.1 except for meridional wind (va).

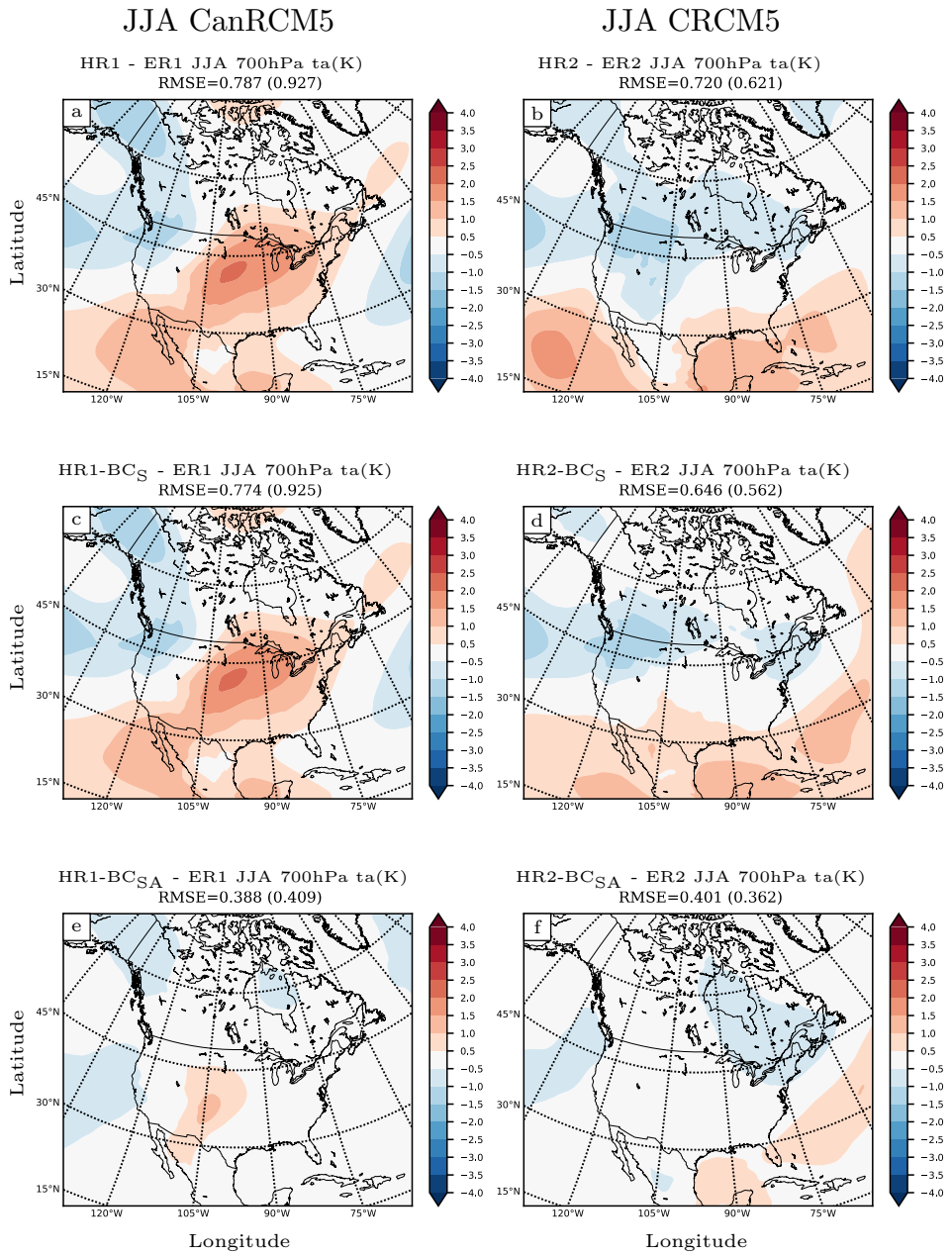


Figure S4.3: As in Fig.S4.1 except for DJF air temperature (ta).

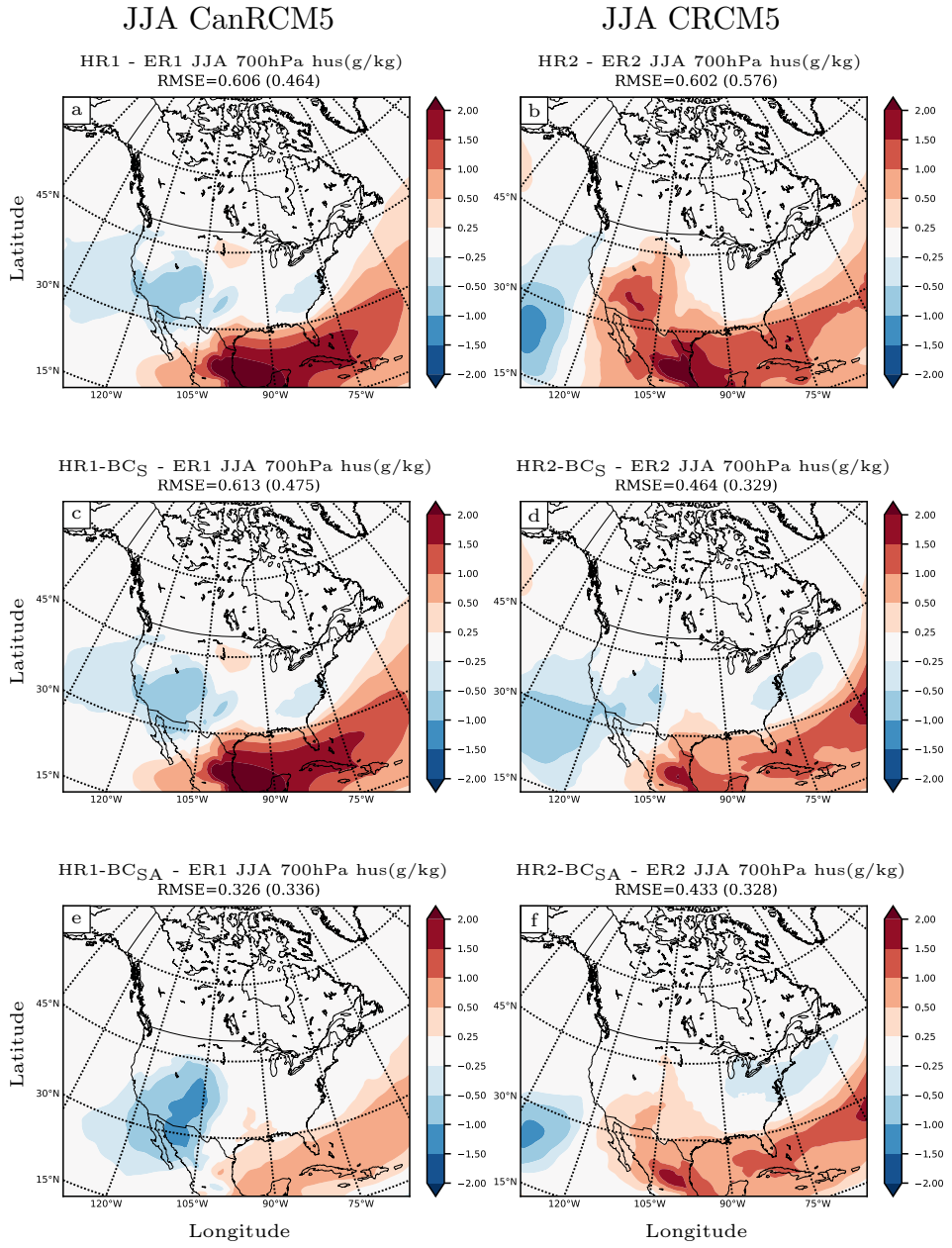


Figure S4.4: As in Fig.S4.1 except for specific humidity (hus).

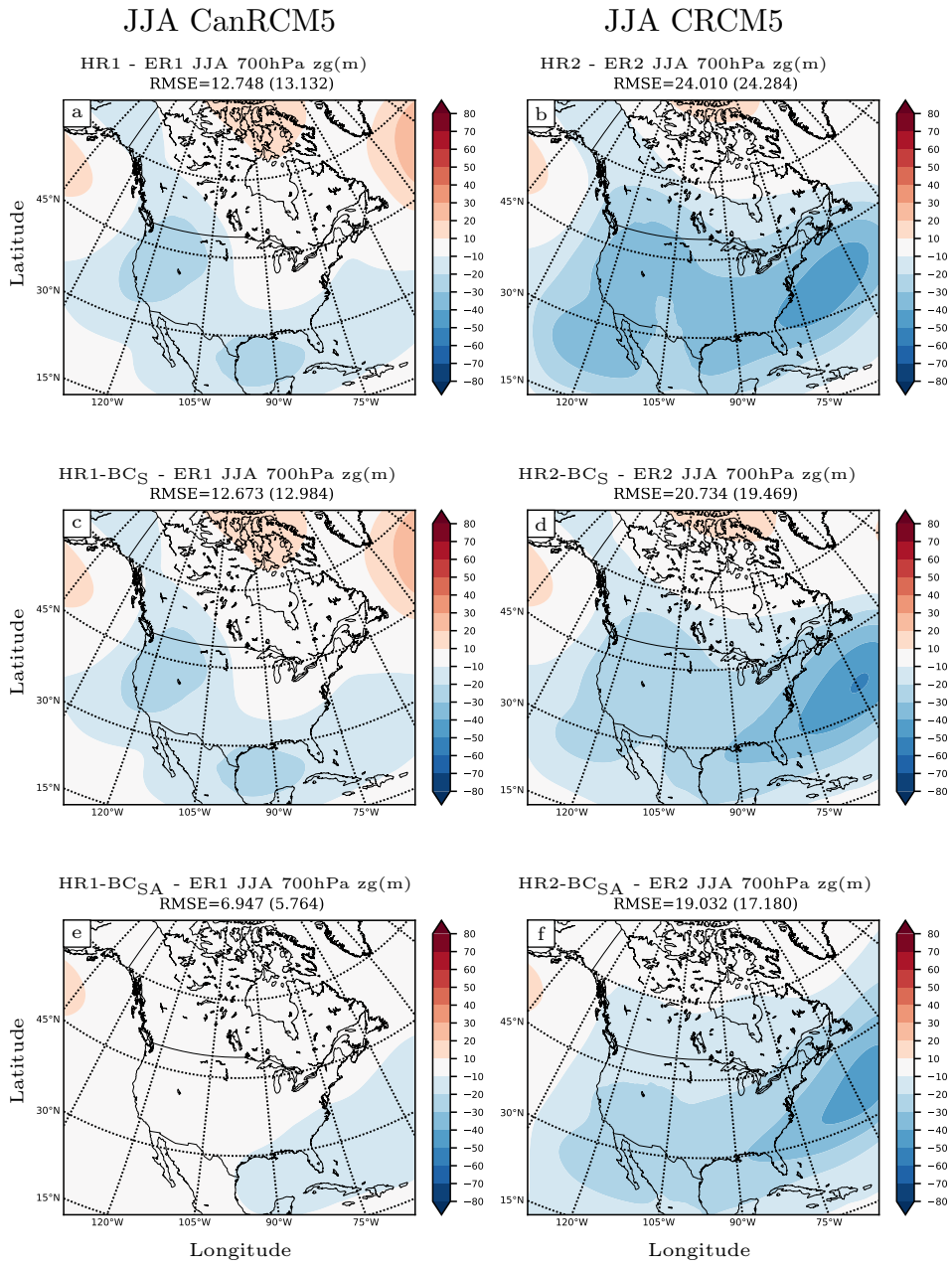


Figure S4.5: As in Fig.S4.1 except for geopotential height (zg).

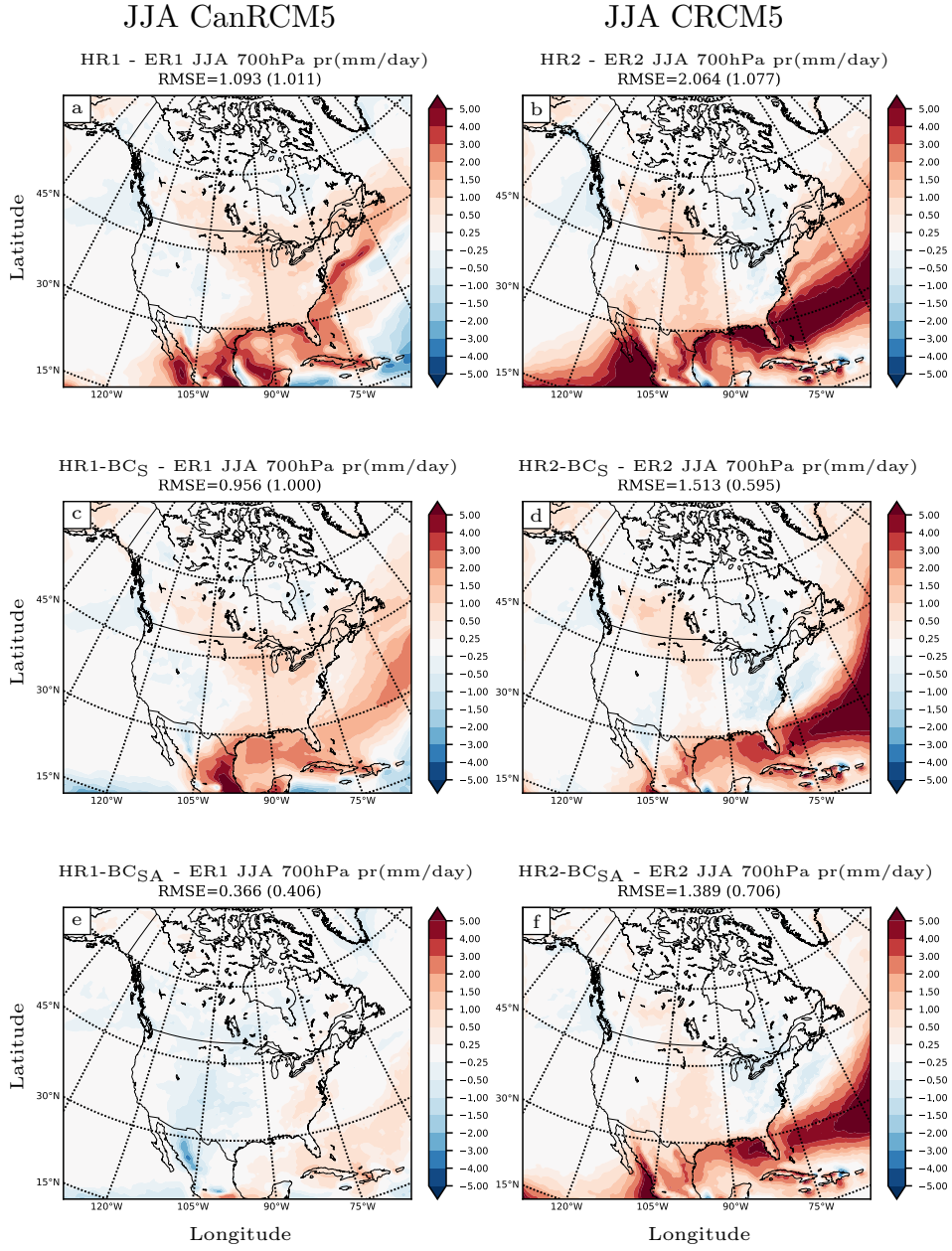


Figure S4.6: As in Fig.S4.1 except for total precipitation (pr).

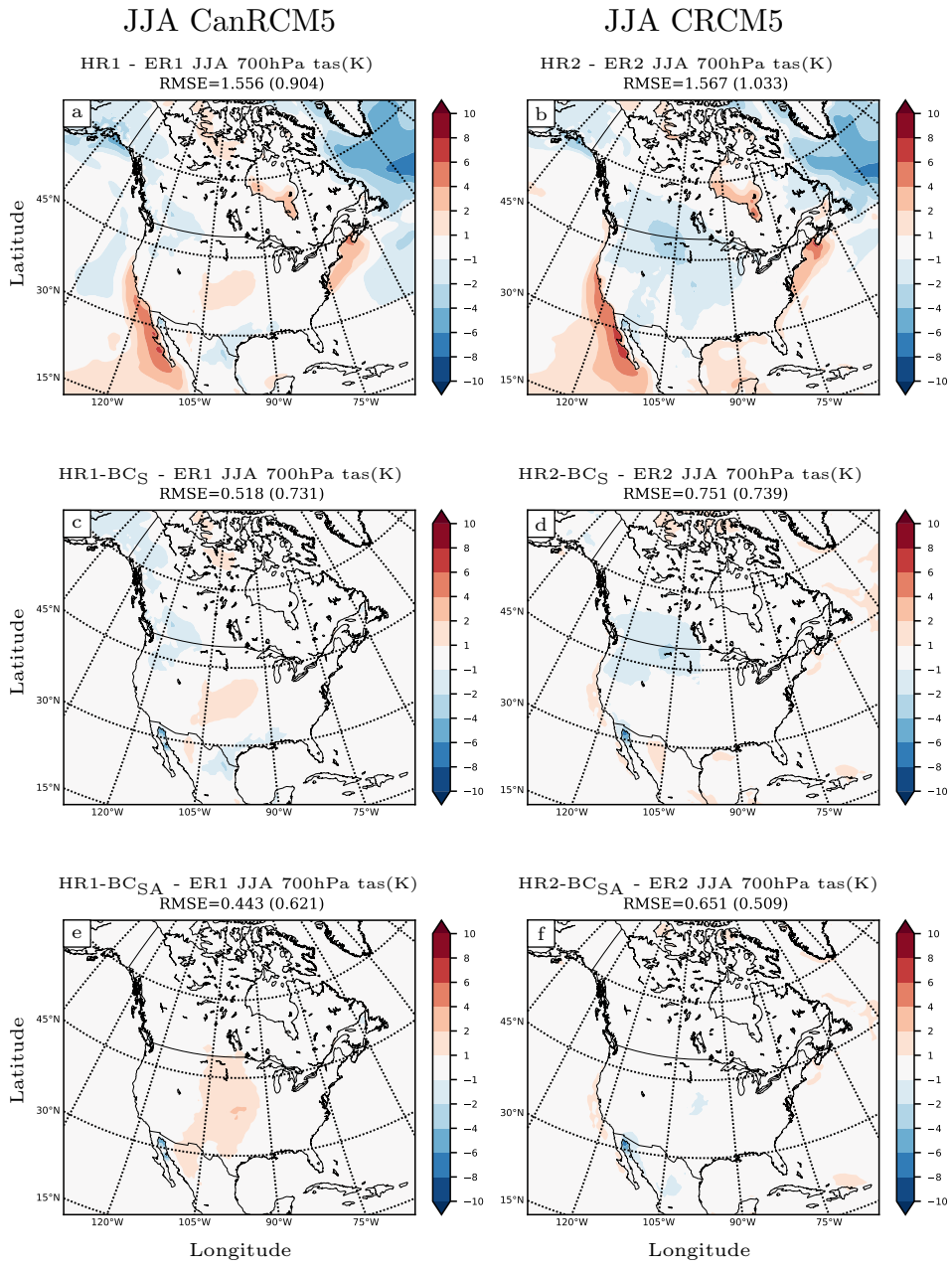


Figure S4.7: As in Fig.S4.1 except for screen tenperature (tas).

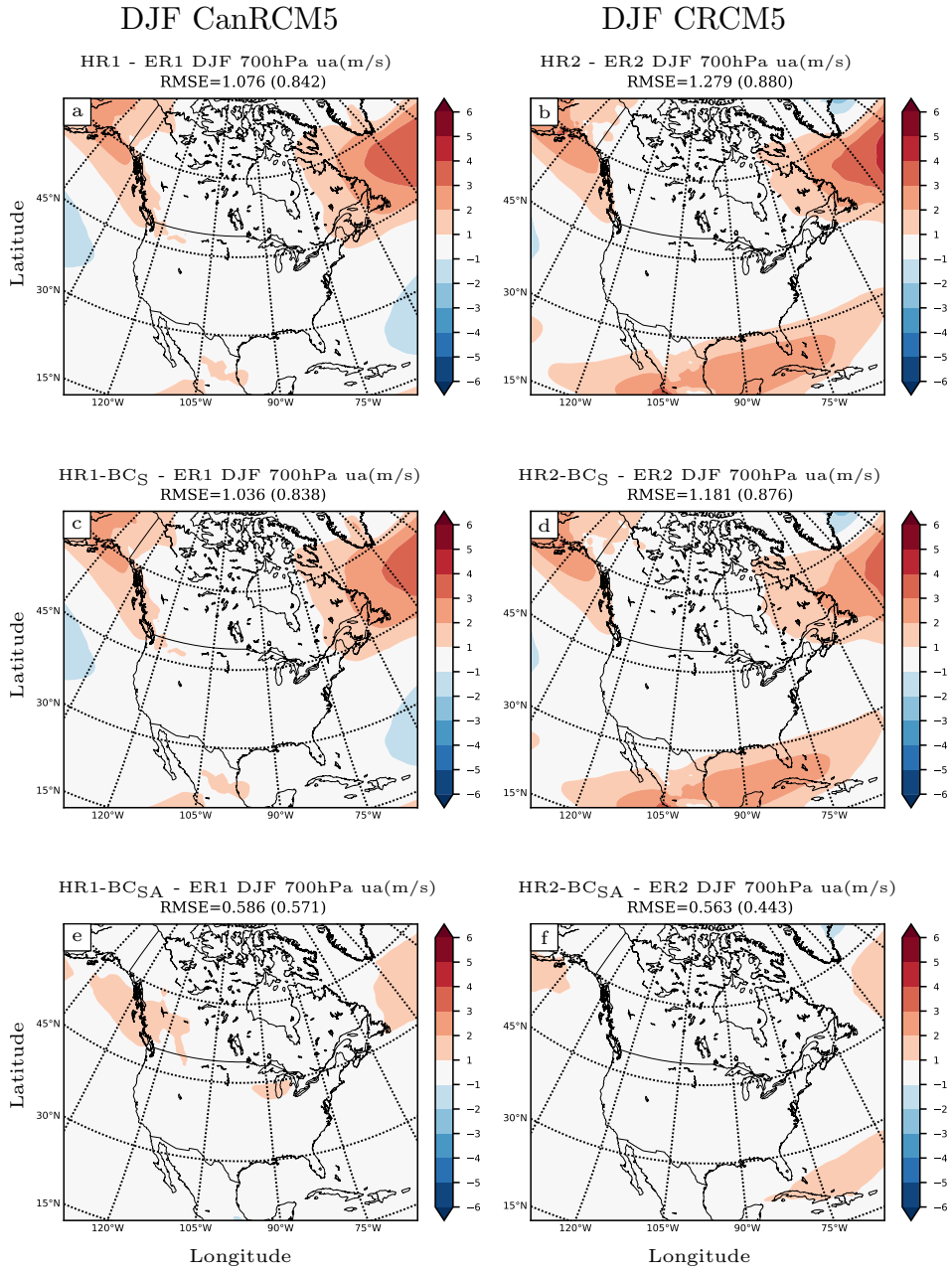


Figure S4.8: As in Fig.S4.1 except for DJF zonal wind (va).

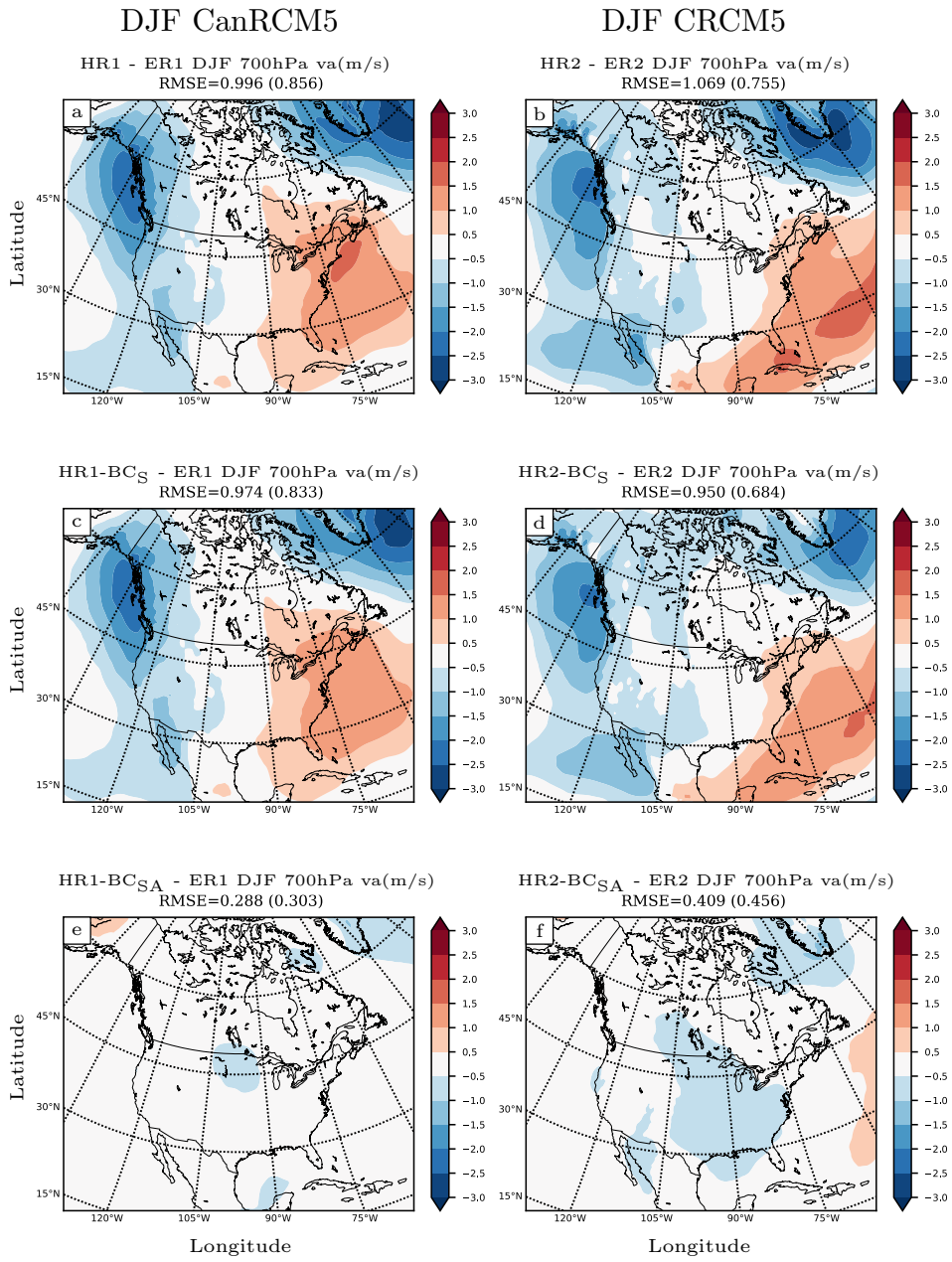


Figure S4.9: As in Fig.S4.1 except for DJF meridional wind (va).

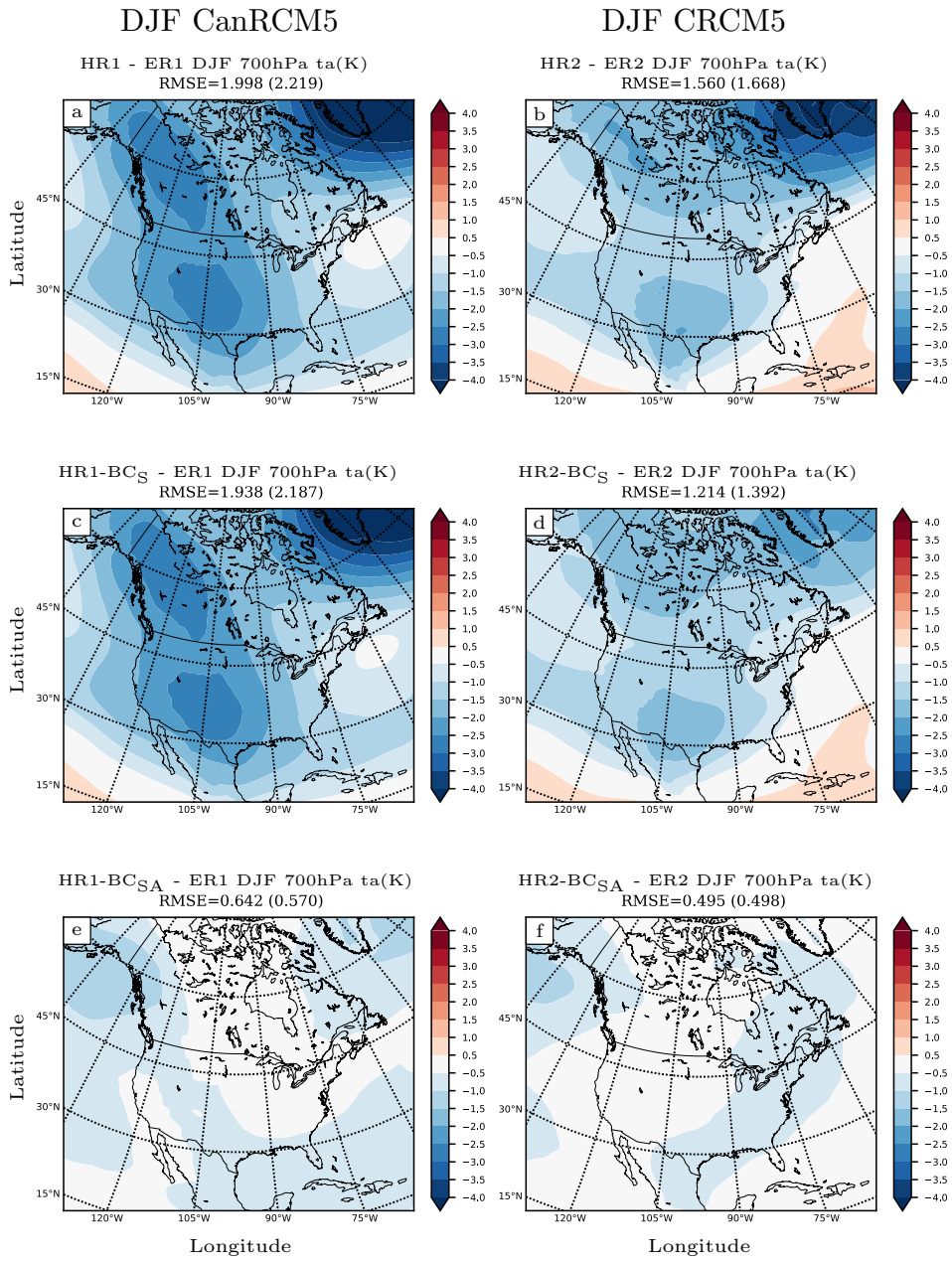


Figure S4.10: As in Fig.S4.1 except for DJF air temperature (ta).

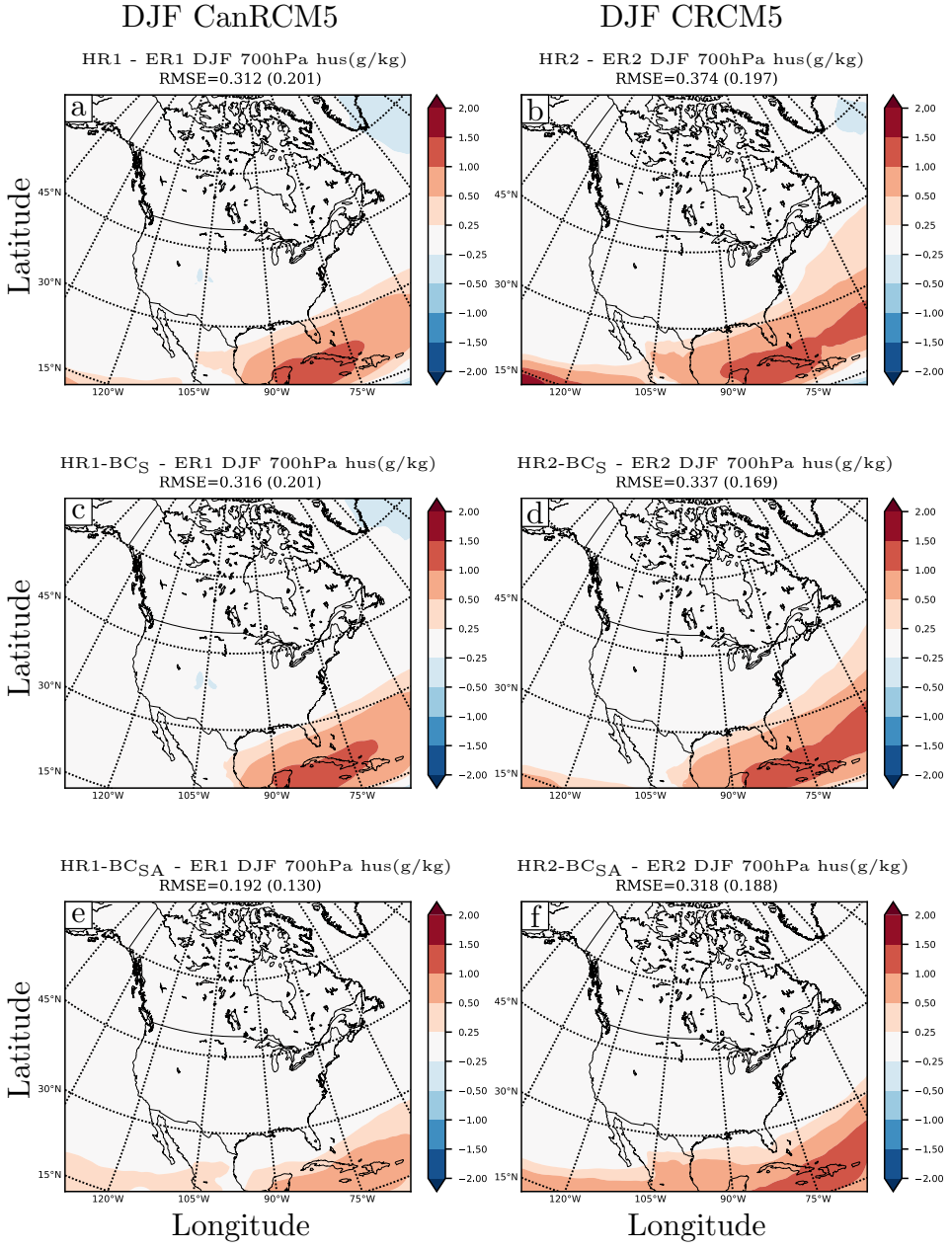


Figure S4.11: As in Fig.S4.1 except for DJF specific humidity (hus).

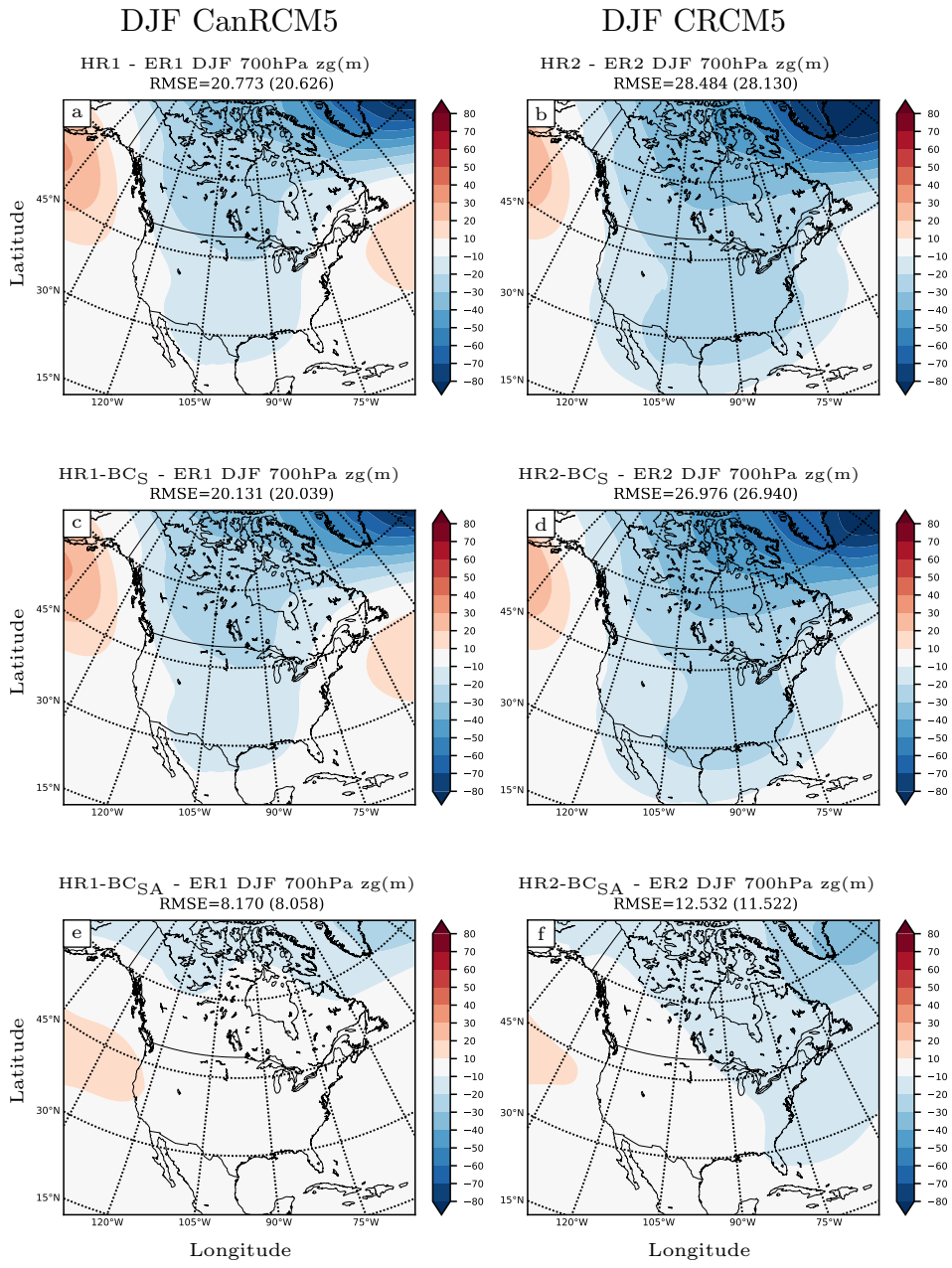


Figure S4.12: As in Fig.S4.1 except for DJF geopotential height (zg).

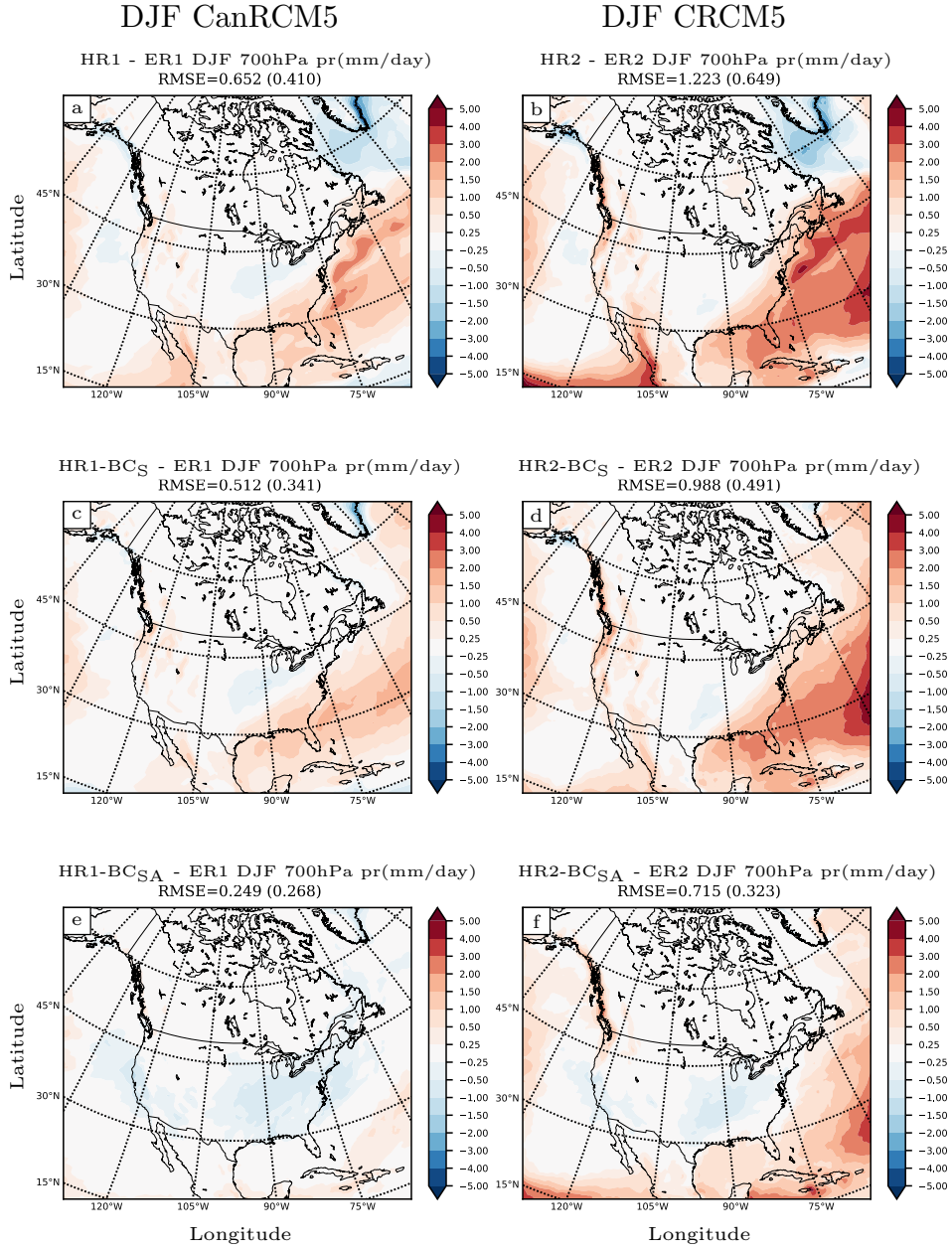


Figure S4.13: As in Fig.S4.1 except for DJF total precipitation (pr).

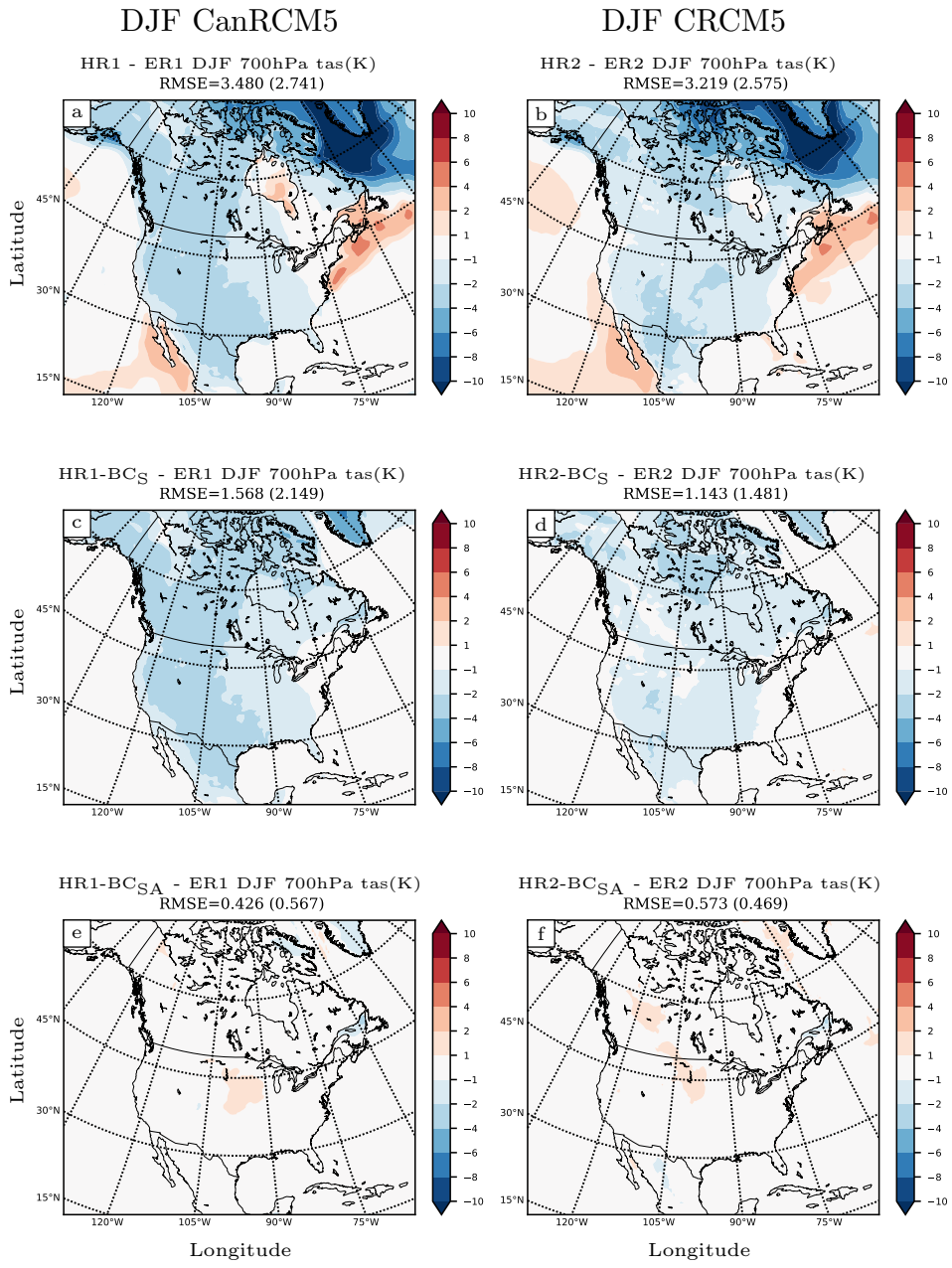


Figure S4.14: As in Fig.S4.1 except for DJF screen tenperature (tas).

S5 Impact of ERBC on Climate Change Responses

Plots similar to Figs. 8 and 9 are presented here for each variable and season summarized in Table 5.

In Figs. S5.1-S5.14, the climate-change response of mean variables represented by the climatological differences between the periods 1981-2010 and 2071-2100 (on the 700hPa for multi-level fields) is presented following the format of Fig. 8 in the paper. The responses of the global model are presented in the first columns, CanRCM5 in the second columns, and CRCM5 in the third columns. First rows, panels a-c respectively: the response in the uncorrected ensembles: FG − HG, CanRCM5 FR1 − HR1, and CRCM5 FR2 − HR2 (See Tables 1 and 2). Second rows, panels d-f respectively: the response in the ERBC ensembles: FG-BC_{SA} − HG-BC_{SA}, FR1-BC_{SA} − HR1-BC_{SA}, and FR2-BC_{SA} − HR2-BC_{SA}. Third rows, panels g-i: the difference between the ERBC response in the second row minus the uncorrected response in the first row. In the third rows, response differences that are statistically significant at the 95% level are coloured while those that are not are shaded grey. The areal percentage of statistically significant differences in the third rows is evaluated over the entire domain and displayed in each panel's title, with values in parentheses representing evaluations over land only.

In Figs. S5.15-S5.28, the climate-change response of the standard deviation of the interannual variability of variables (on the 700hPa for multi-level fields) is presented following the format of Fig. 9 in the paper. For the example of zonal wind (ua), the response is expressed as, $\mathrm{Rua_{sd}}$ resulting in, panels a-c, climate change response of standard deviation of interannual variability in the in the absence of ERBCs ($\mathrm{Rua_{sd}^{uncorrected}}$); panels d-f, climate change response of standard deviation of interannual variability with the application ERBCs ($\mathrm{Rua_{sd}^{ERBC}}$); and panels g-i, ERBC-induced change in the $\mathrm{Rua_{sd}}$ response, expressed as the deviation in the ratio of variability: $(\mathrm{Rua_{sd}^{ERBC}})/(\mathrm{Rua_{sd}^{uncorrected}}) - 1$. Positive deviations indicate increased variability, while negative deviations indicate decreased variability relative to the uncorrected models. Changes in the response that are statistically significant at the 95% level are coloured while those that are not are shaded grey. The areal percentage of the whole domain covered by statistically significant ERBC induced changes in variability are displayed in the title of each panel of the third row with the areal percentage over land displayed in parentheses.

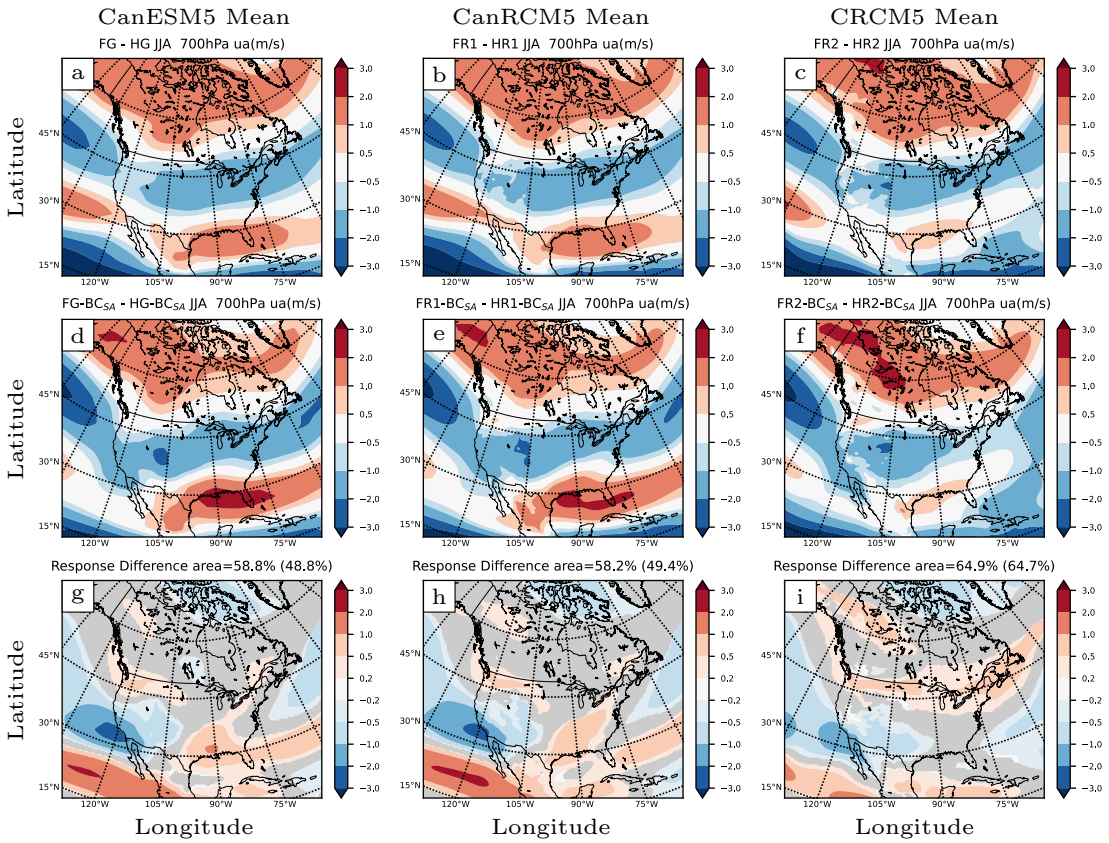


Figure S5.1: JJA zonal wind (ua) mean responses.

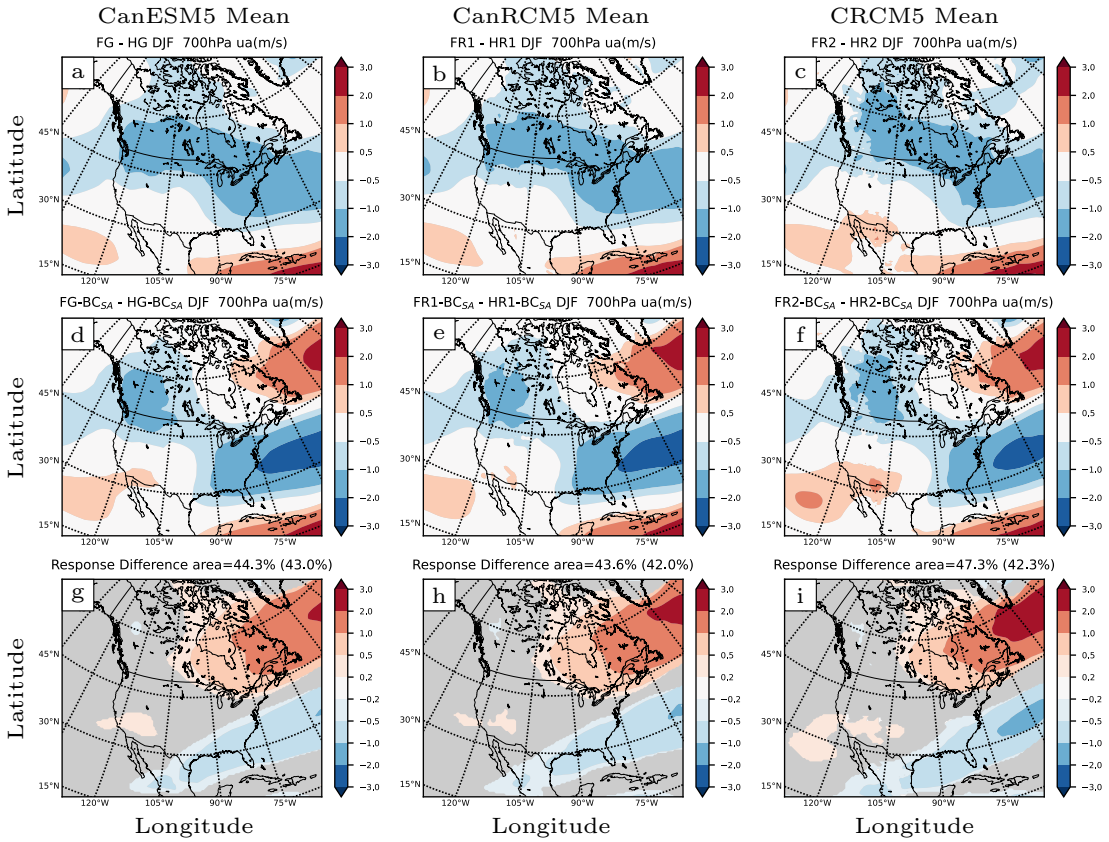


Figure S5.2: DJF zonal wind (ua) mean responses.

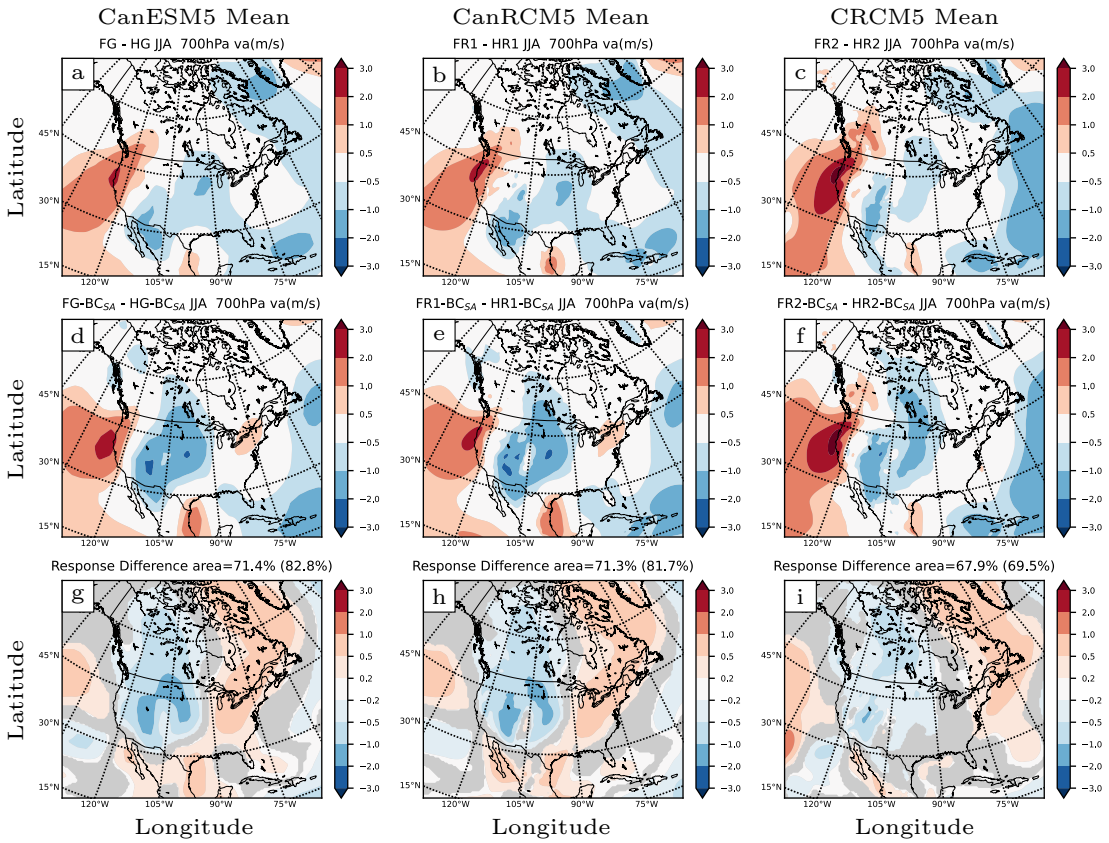


Figure S5.3: JJA meridional wind (va) mean responses.

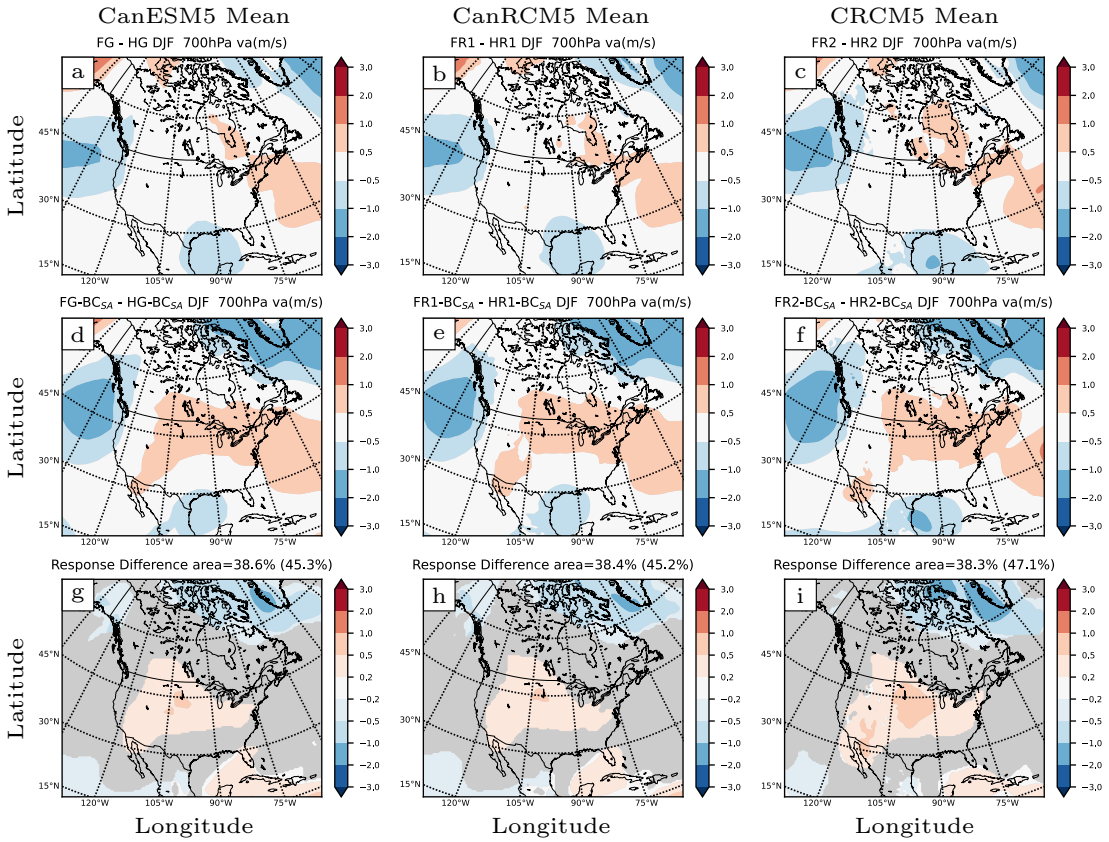


Figure S5.4: DJF meridional wind (va) mean responses.

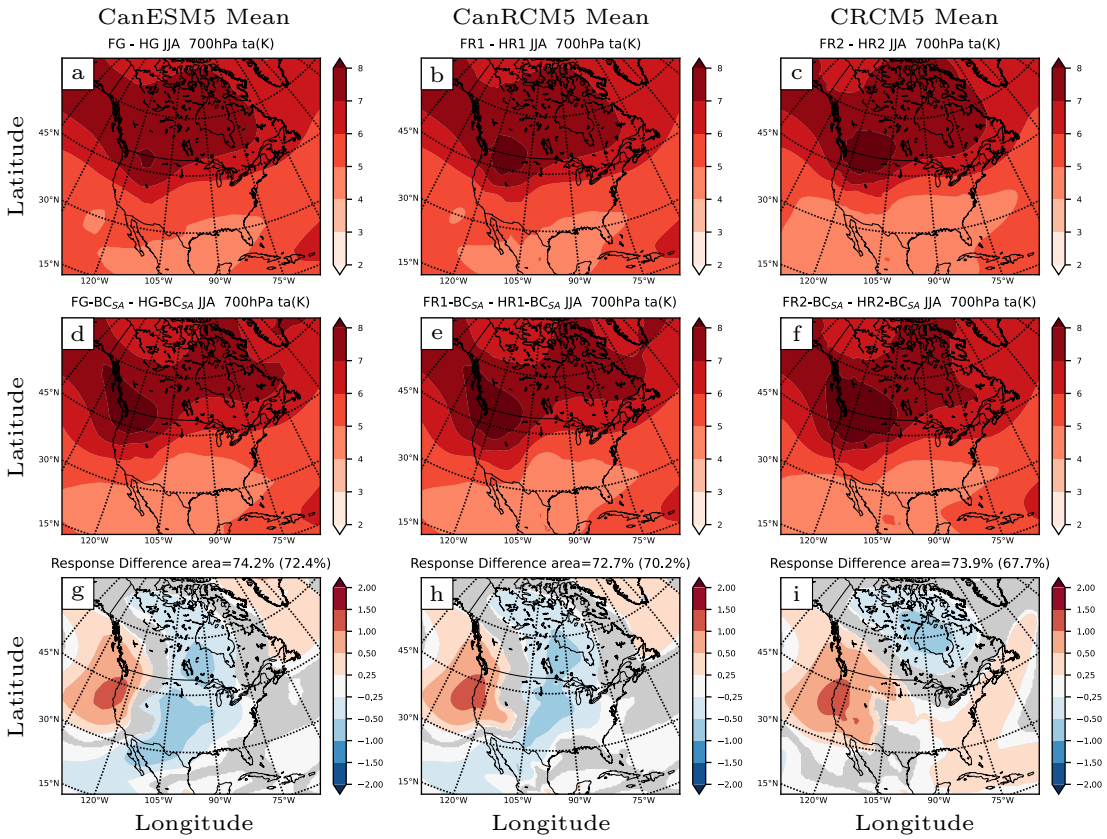


Figure S5.5: JJA air temperature (ta) mean responses.

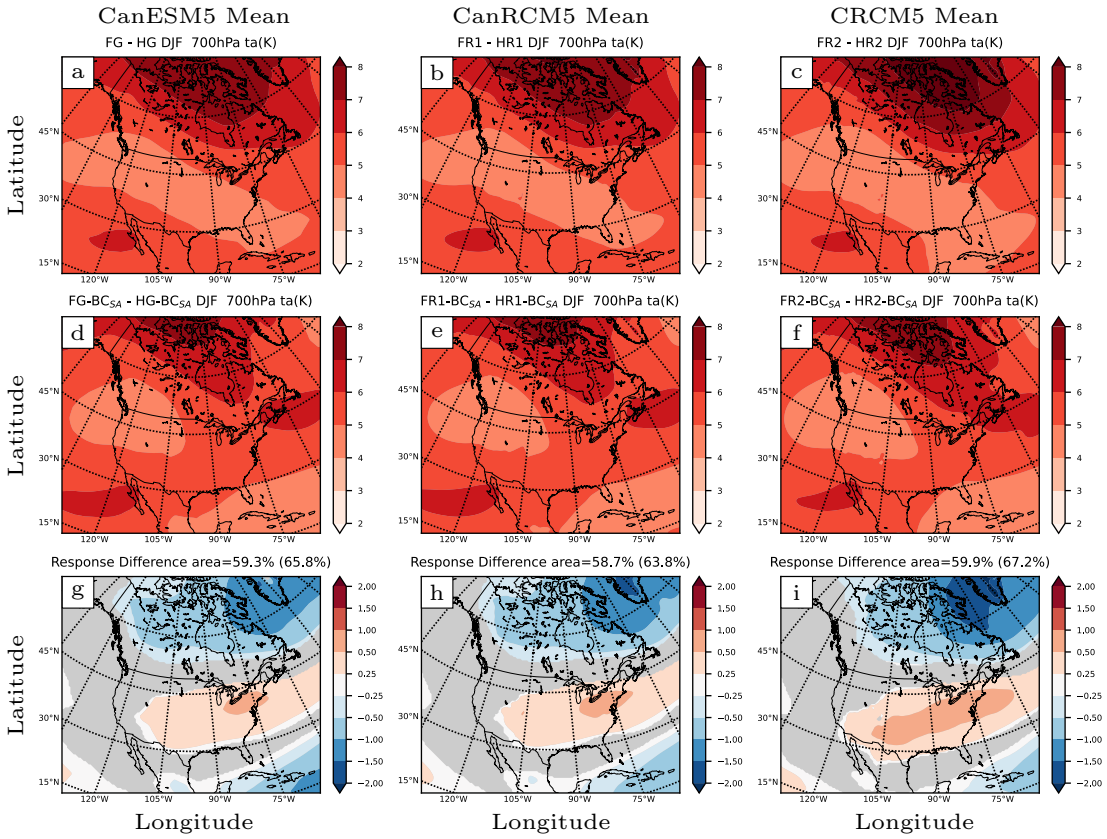


Figure S5.6: DJF air temperature (ta) mean responses.

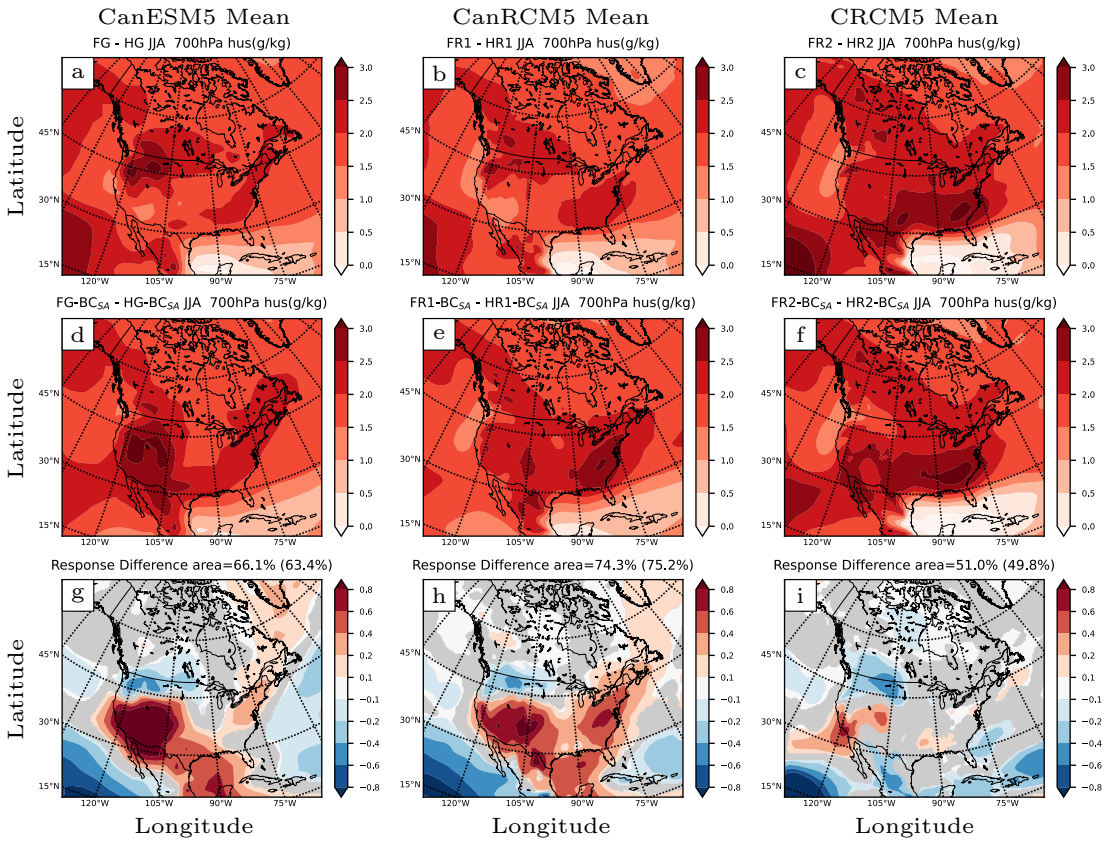


Figure S5.7: JJA specific humidity (hus) mean responses.

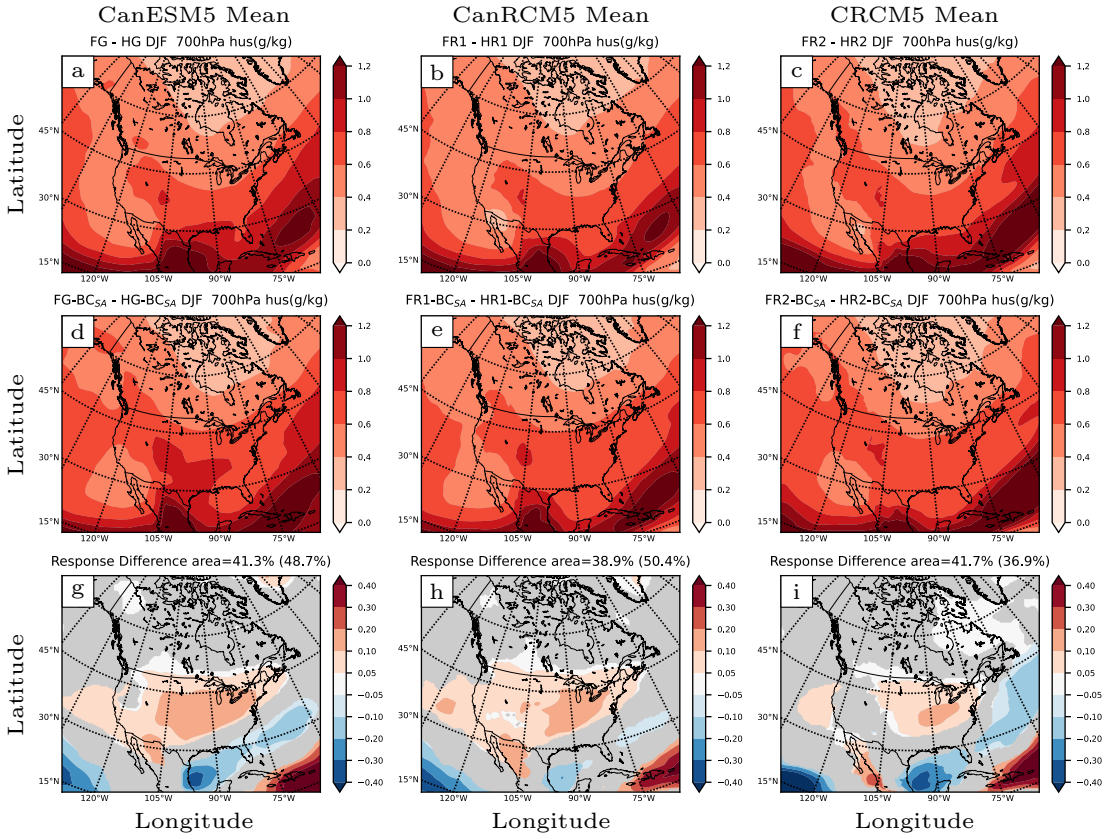


Figure S5.8: DJF specific humidity (hus) mean responses.

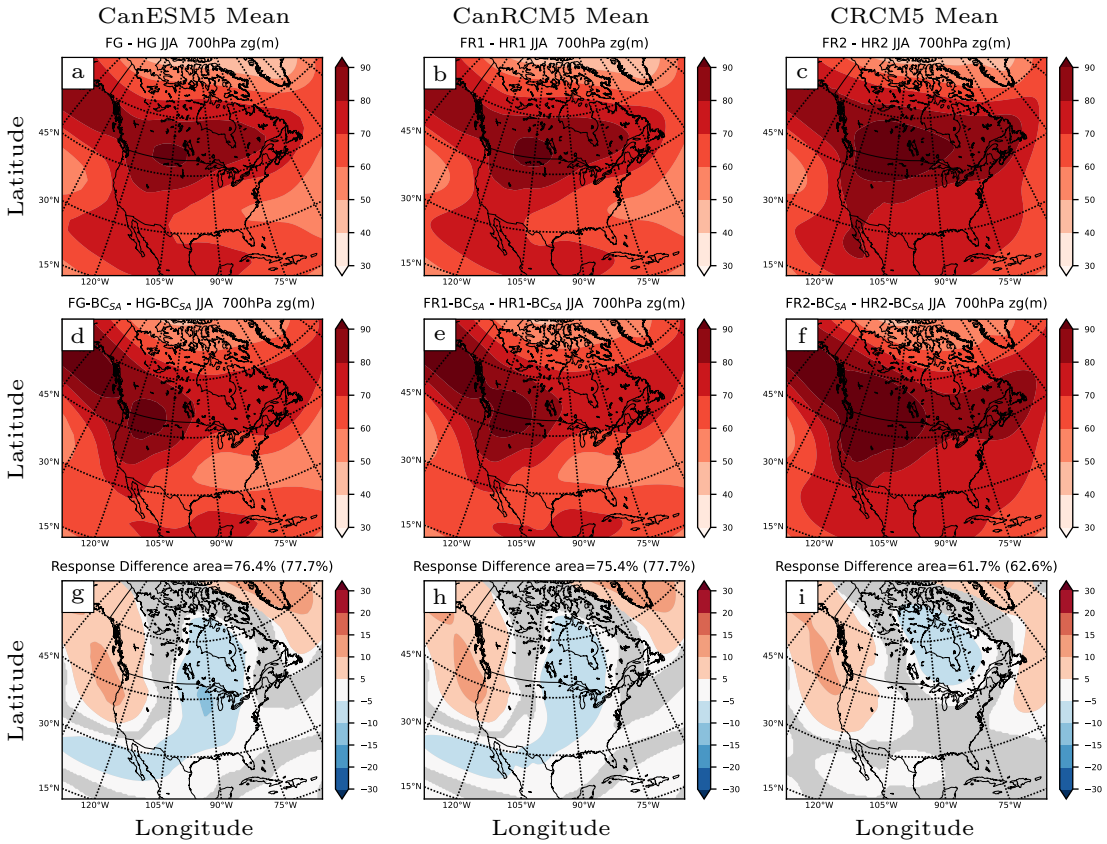


Figure S5.9: JJA geopotential height (zg) mean responses.

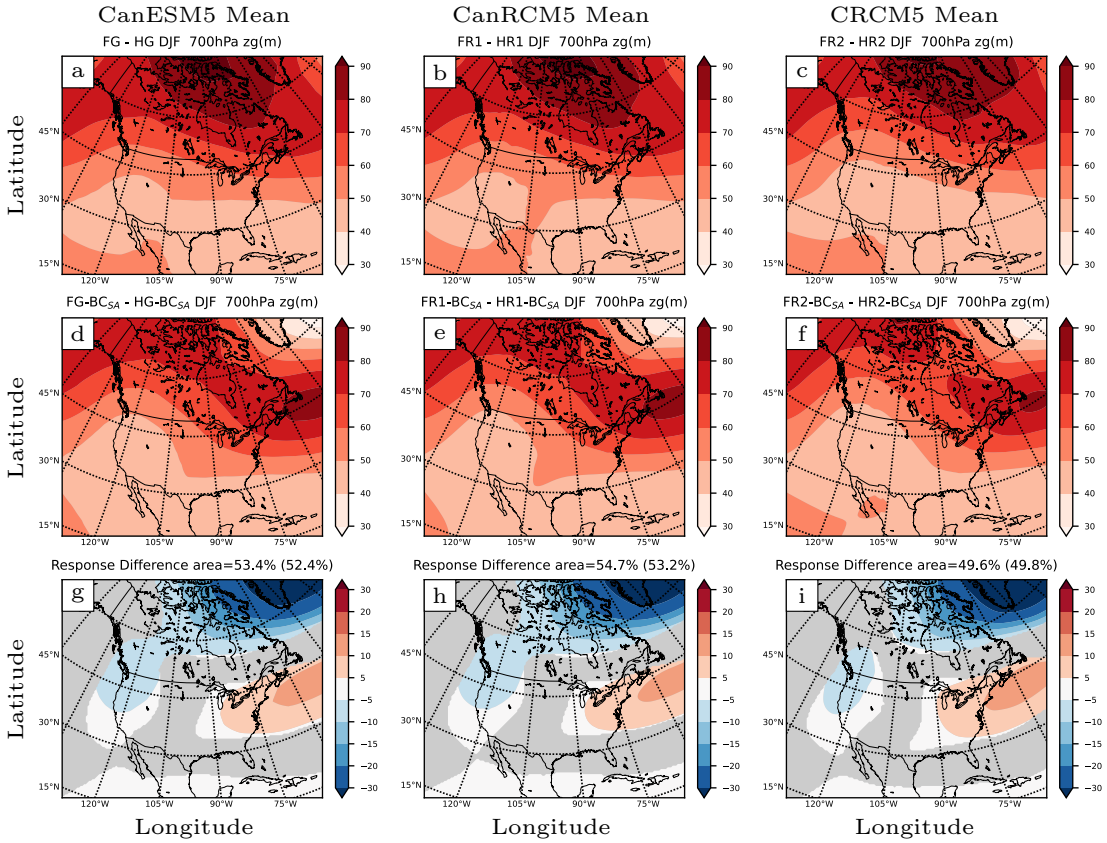


Figure S5.10: DJF geopotential height (zg) mean responses.

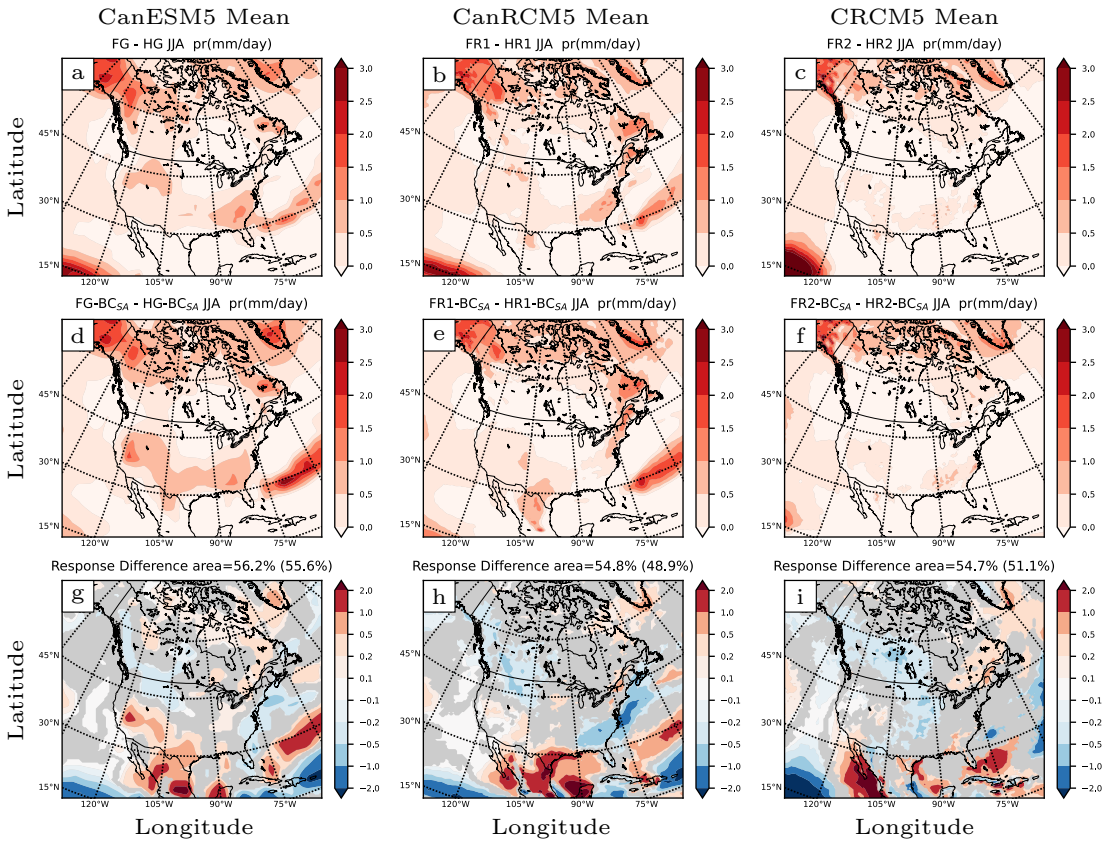


Figure S5.11: JJA total precipitation (pr) mean responses.

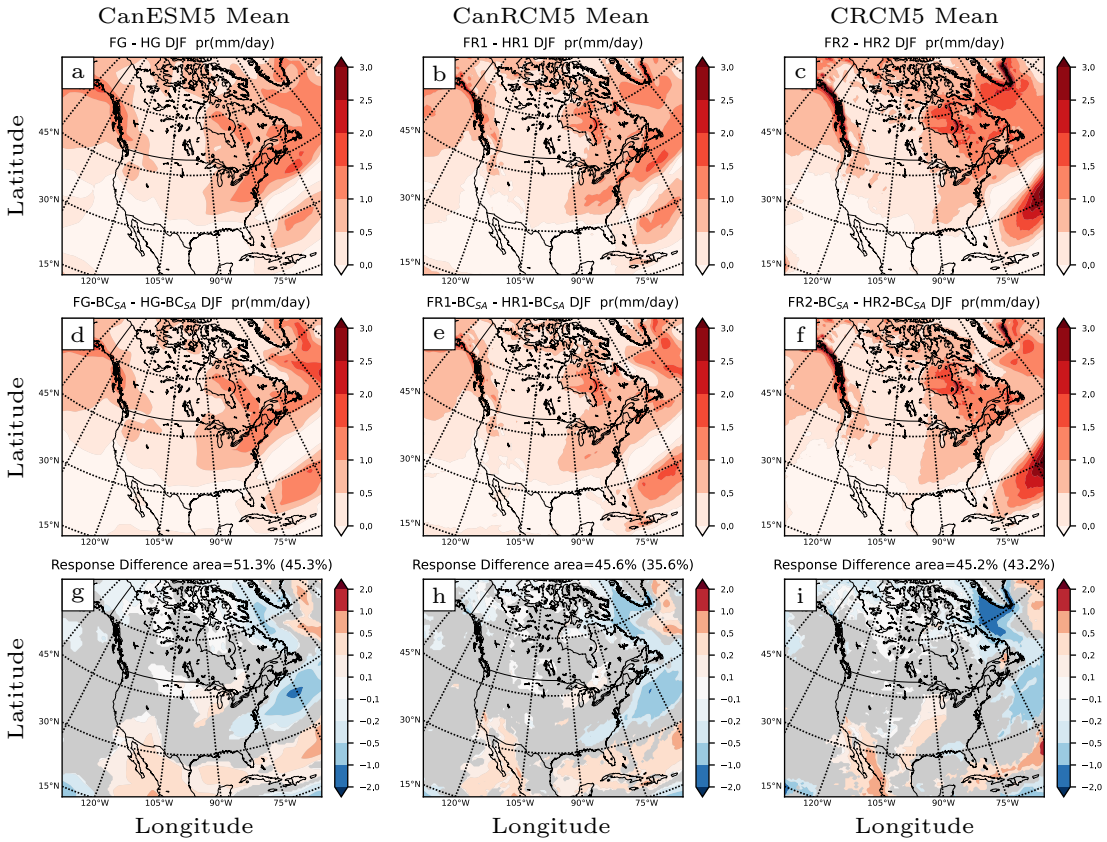


Figure S5.12: DJF total precipitation (pr) mean responses.

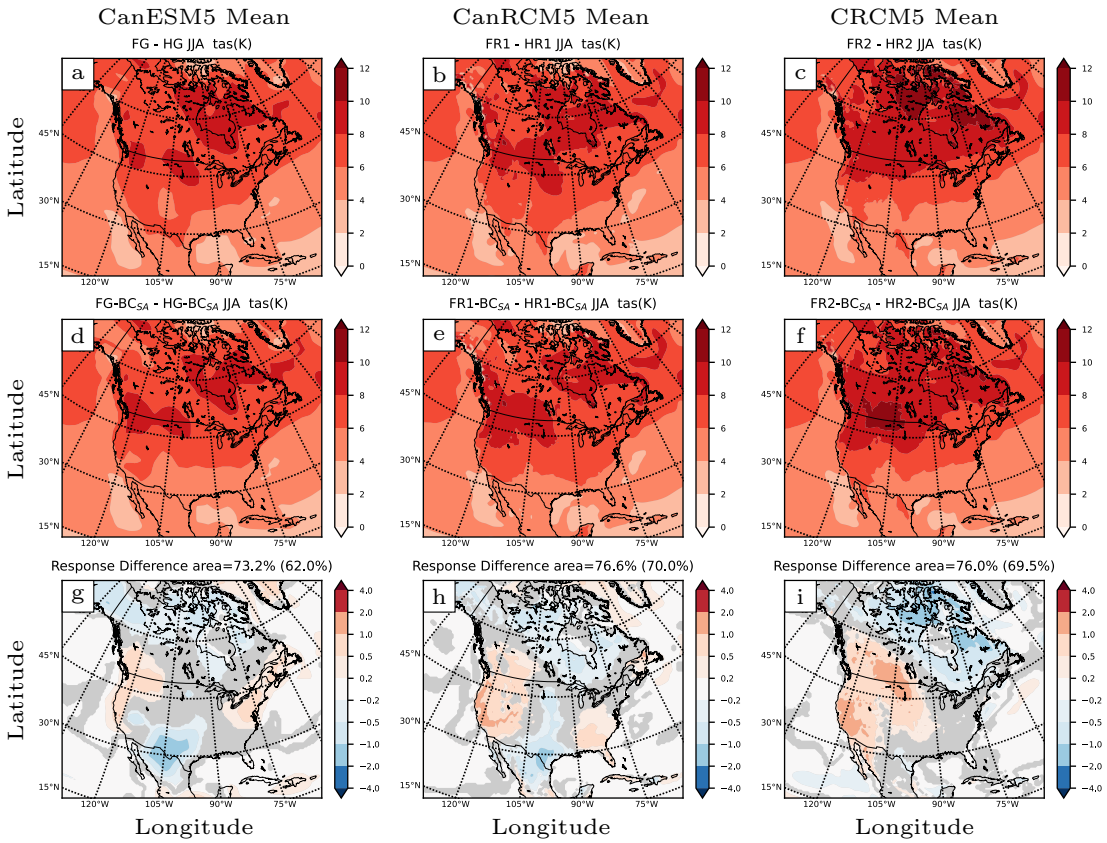


Figure S5.13: JJA screen temperature (tas) mean responses.

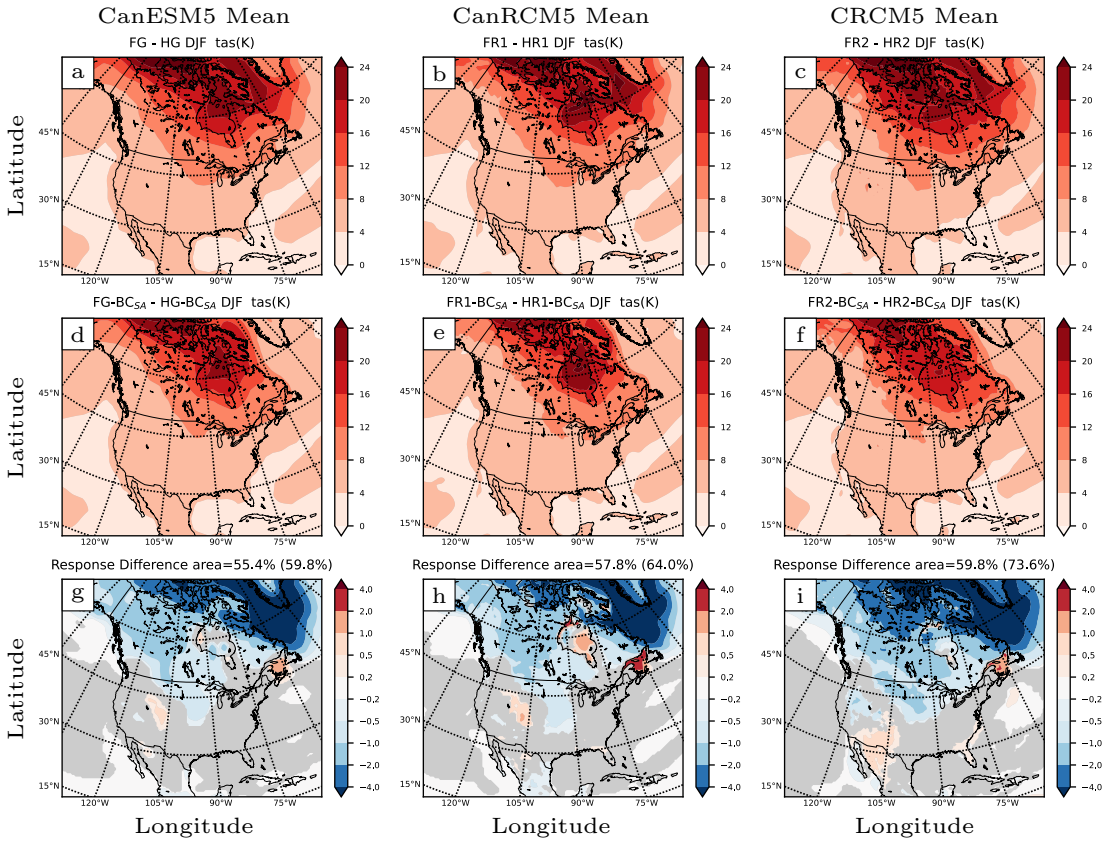


Figure S5.14: DJF screen temperature (tas) mean responses.

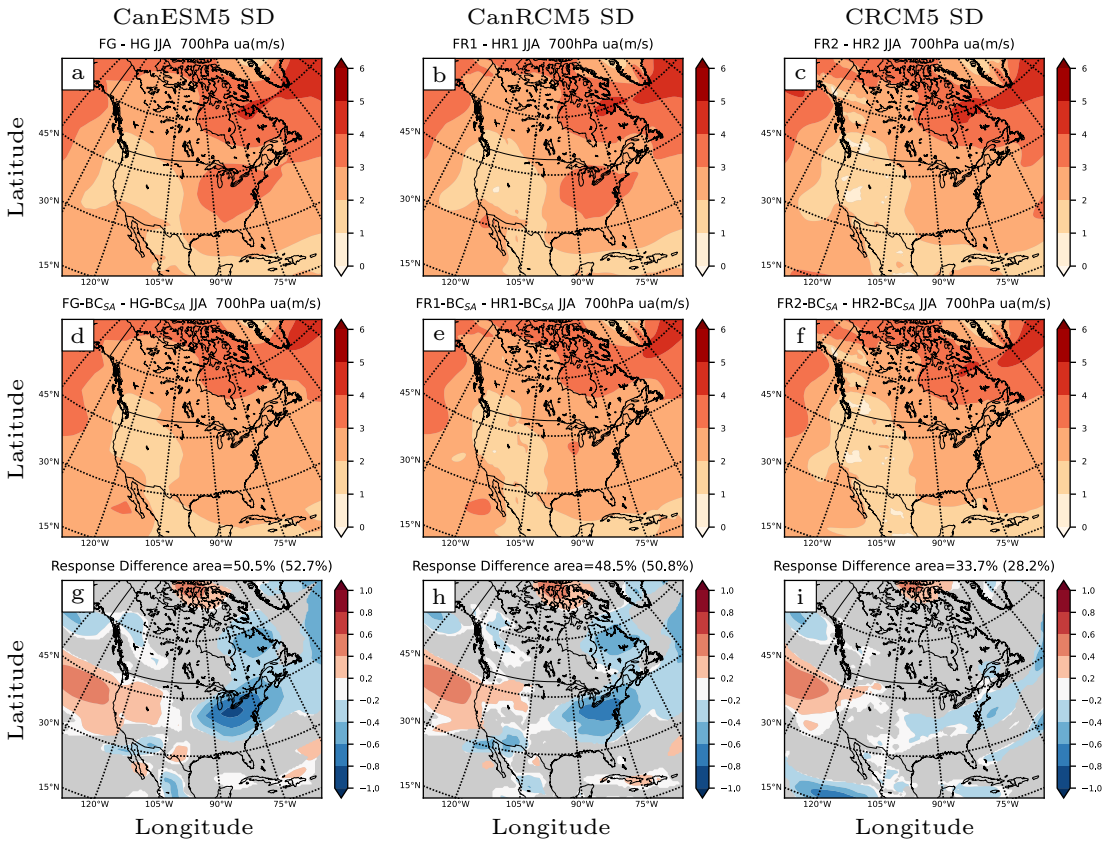


Figure S5.15: JJA zonal wind (ua) standard deviation responses.

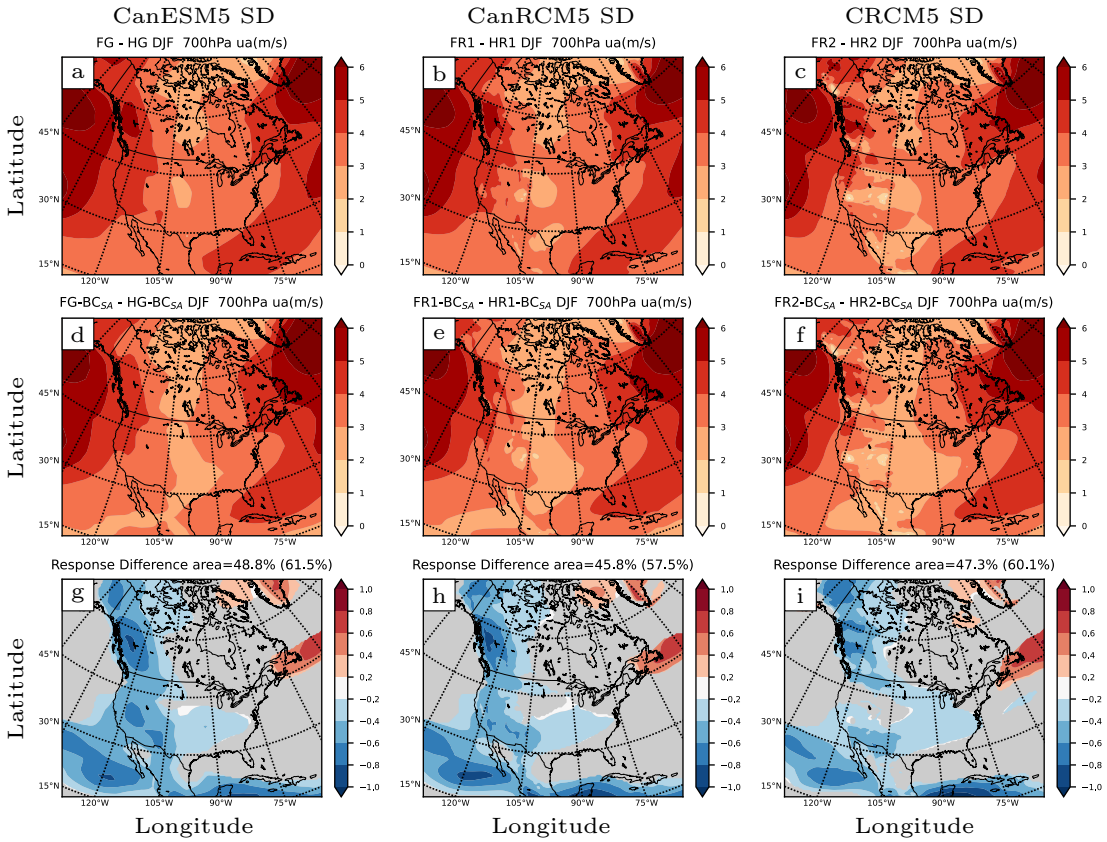


Figure S5.16: DJF zonal wind (ua) standard deviation responses.

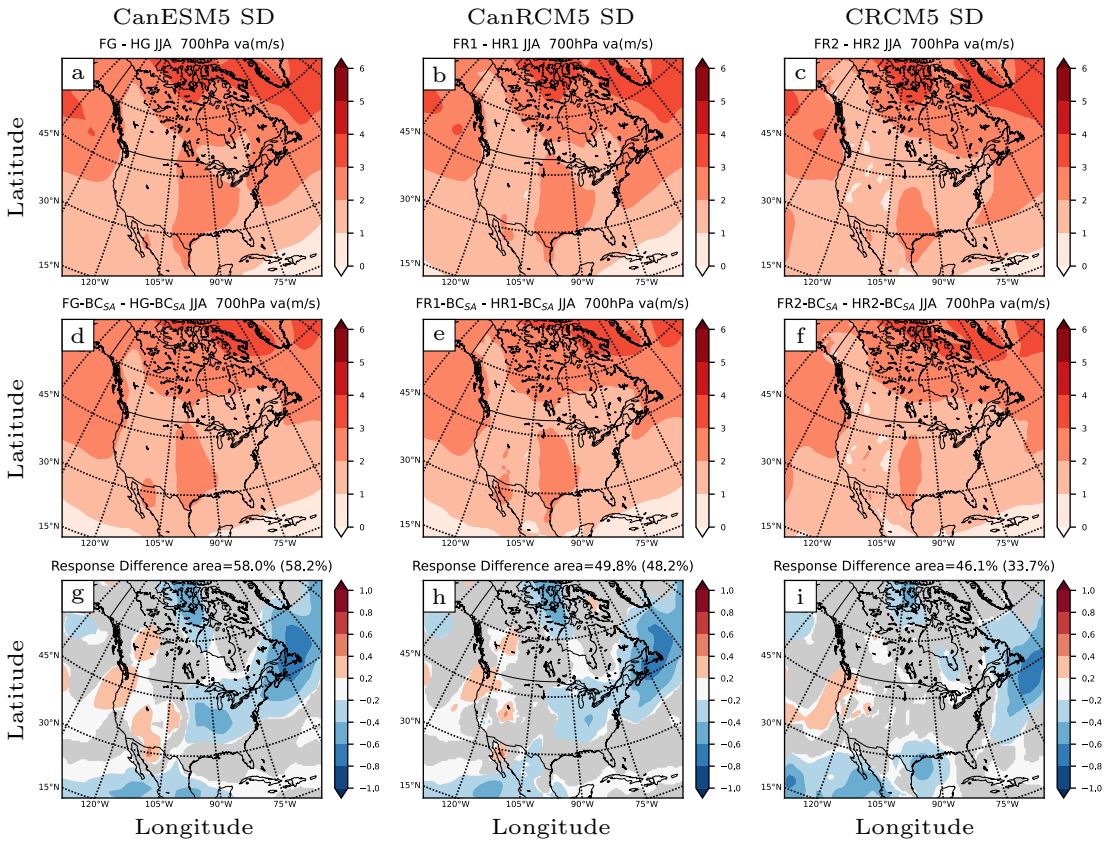


Figure S5.17: JJA meridional wind (va) standard deviation responses.

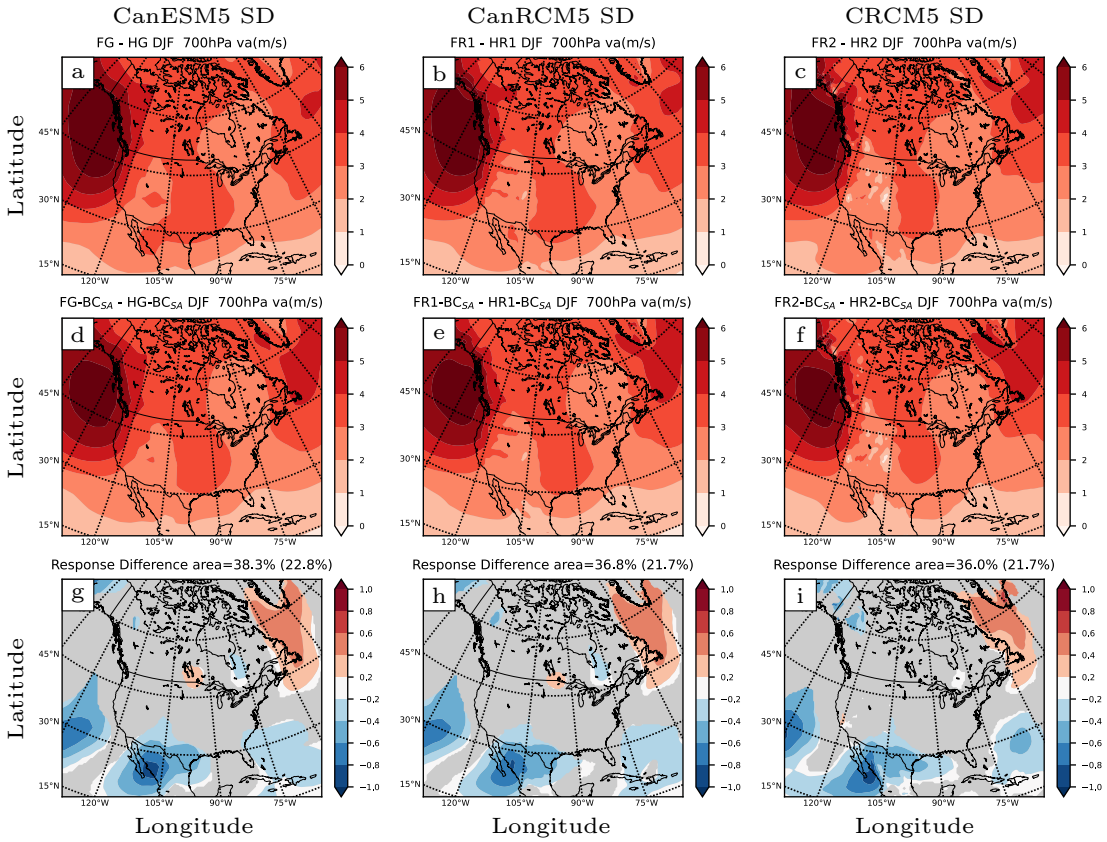


Figure S5.18: DJF meridional wind (va) standard deviation responses.

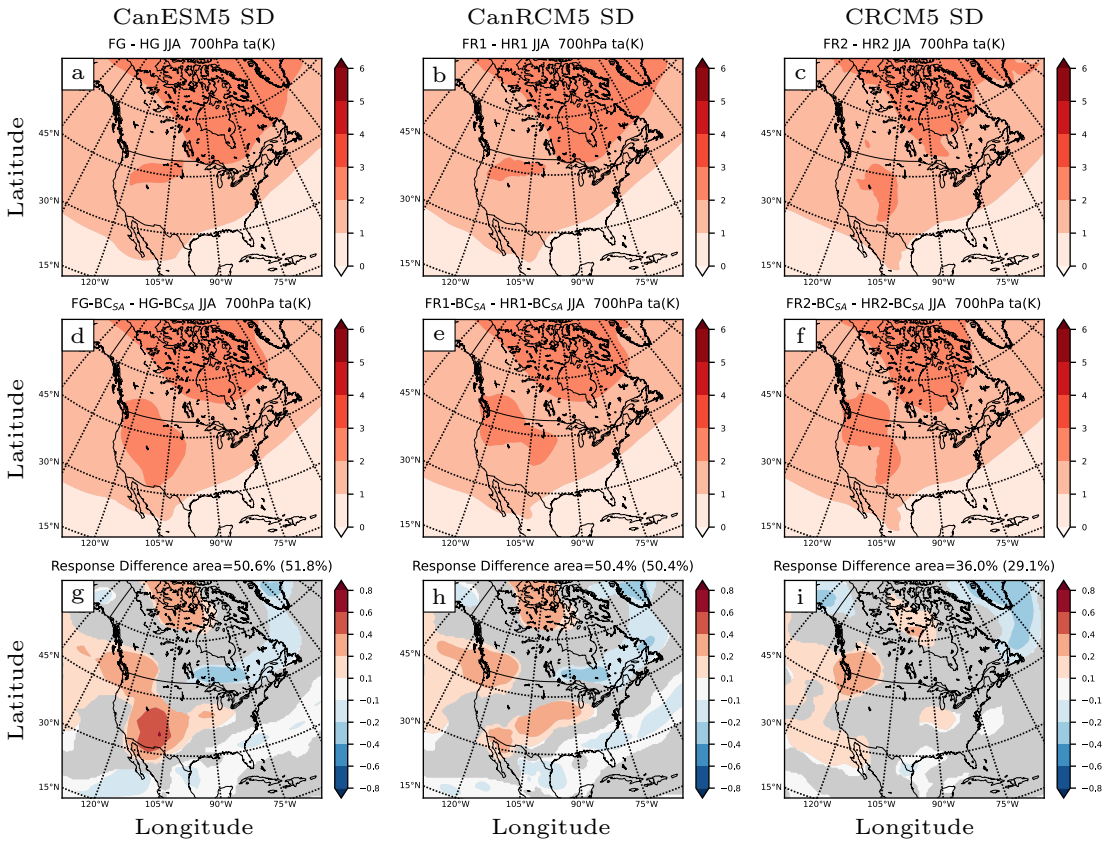


Figure S5.19: JJA air temperature (ta) standard deviation responses.

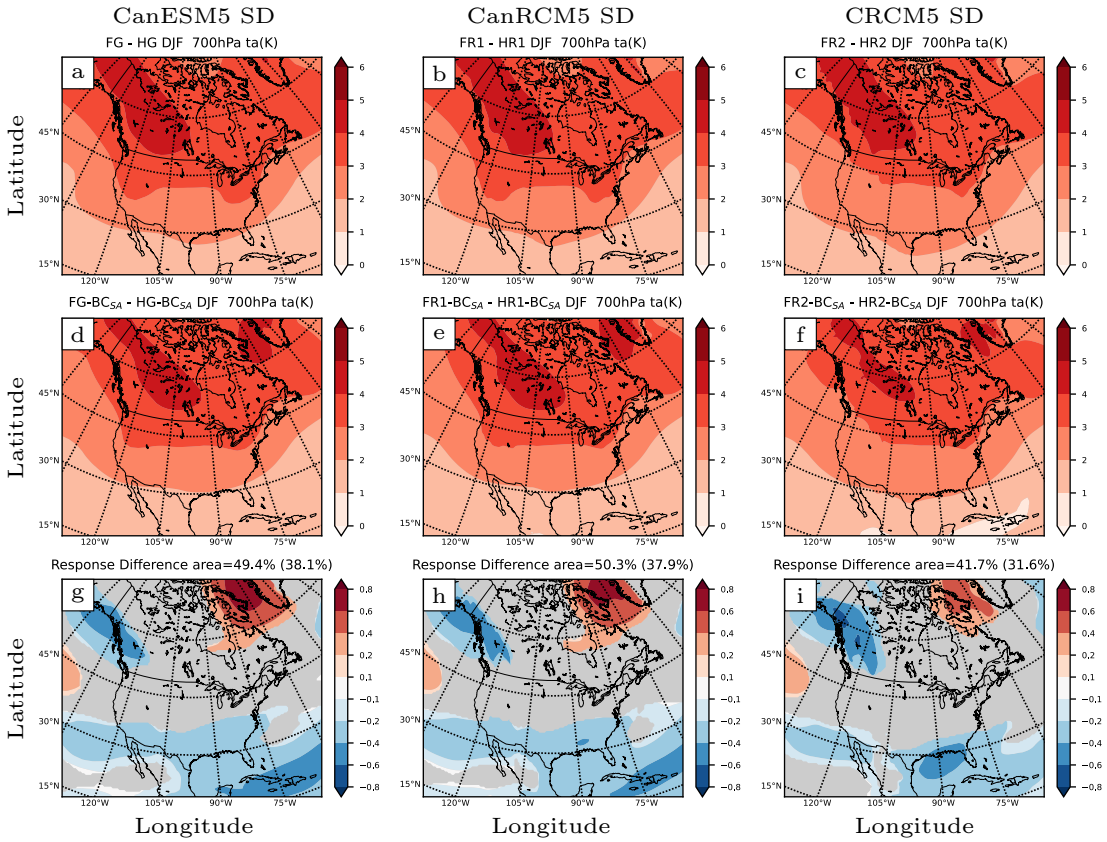


Figure S5.20: DJF air temperature (ta) standard deviation responses.

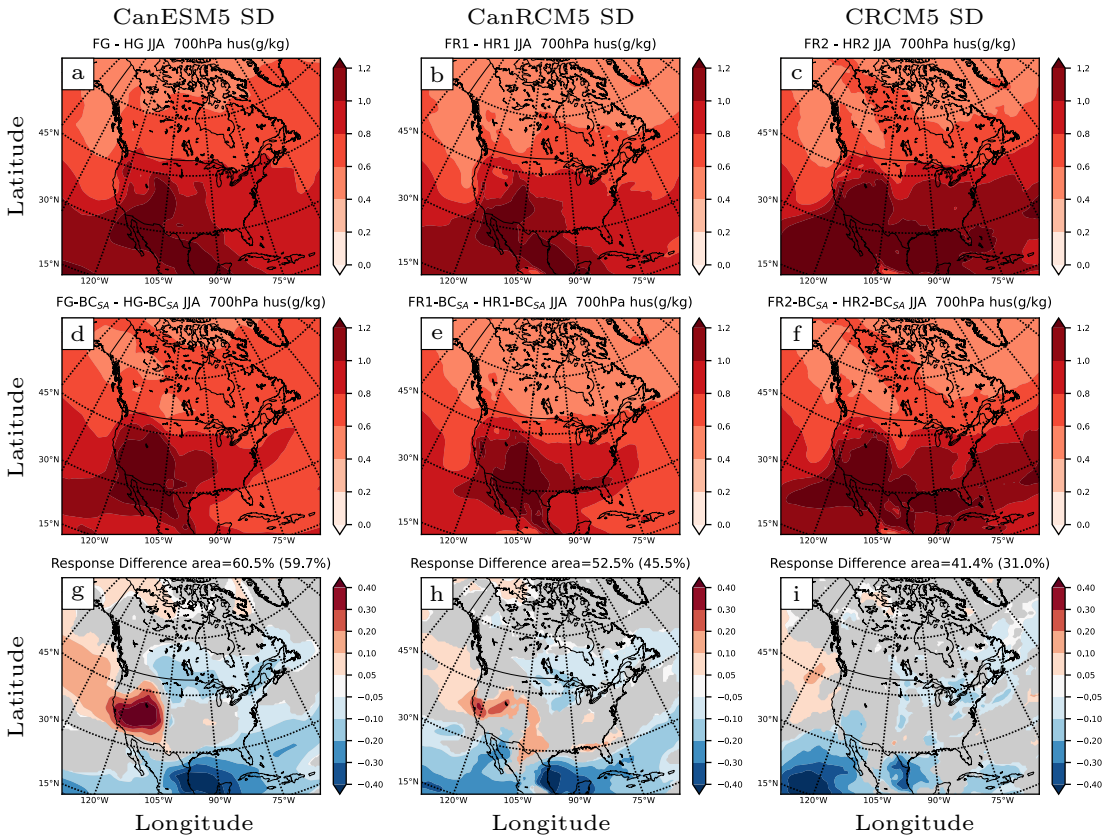


Figure S5.21: JJA specific humidity (hus) standard deviation responses.

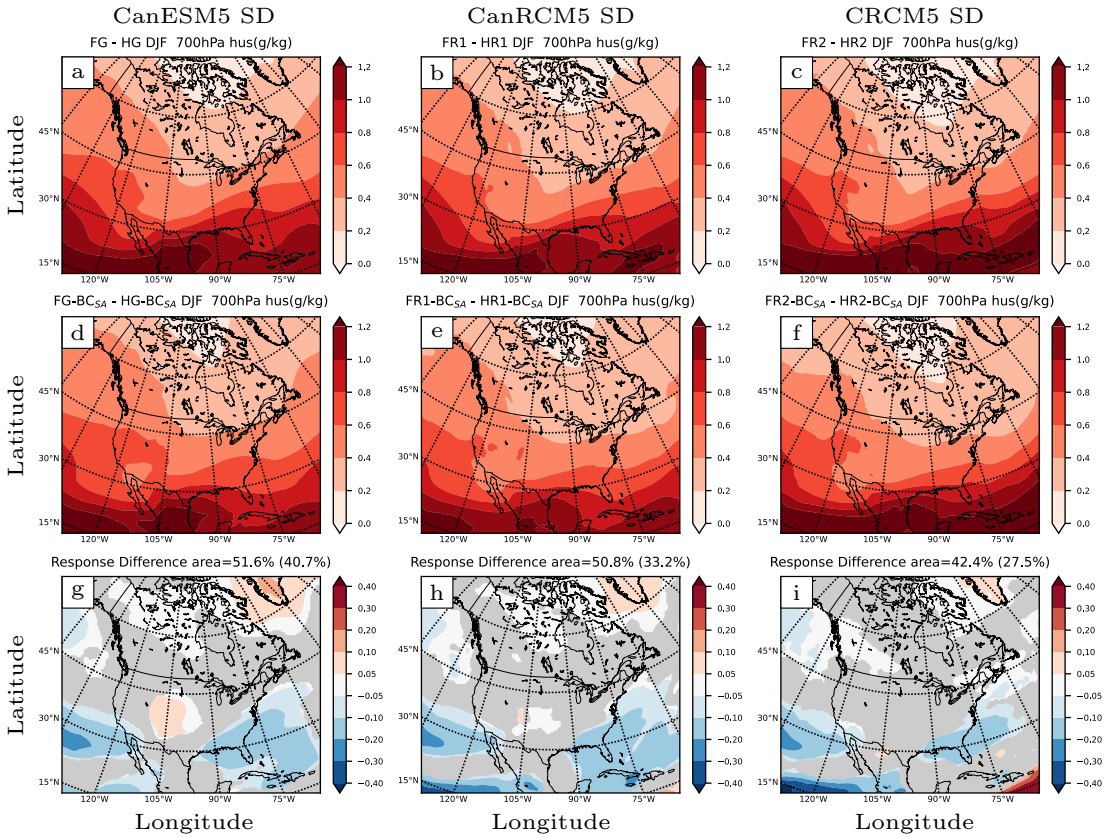


Figure S5.22: DJF specific humidity (hus) standard deviation responses.

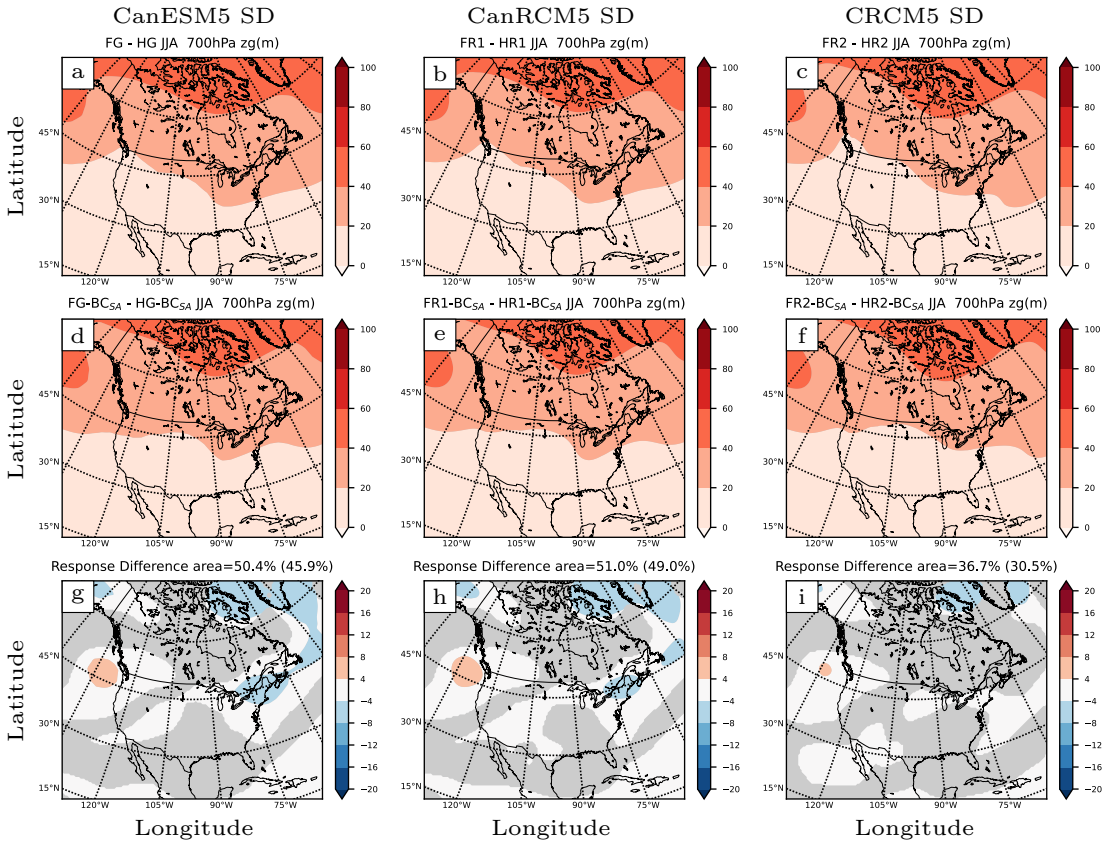


Figure S5.23: JJA geopotential height (zg) standard deviation responses.

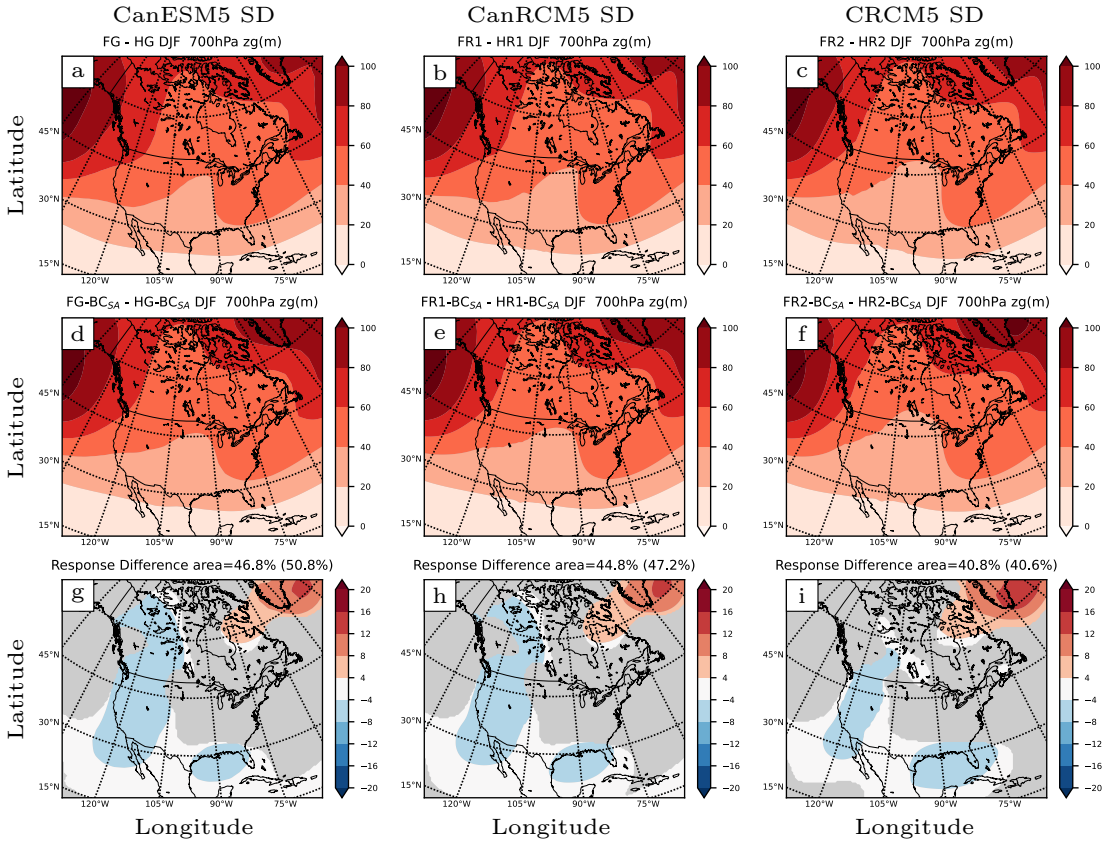


Figure S5.24: DJF geopotential height (zg) standard deviation responses.

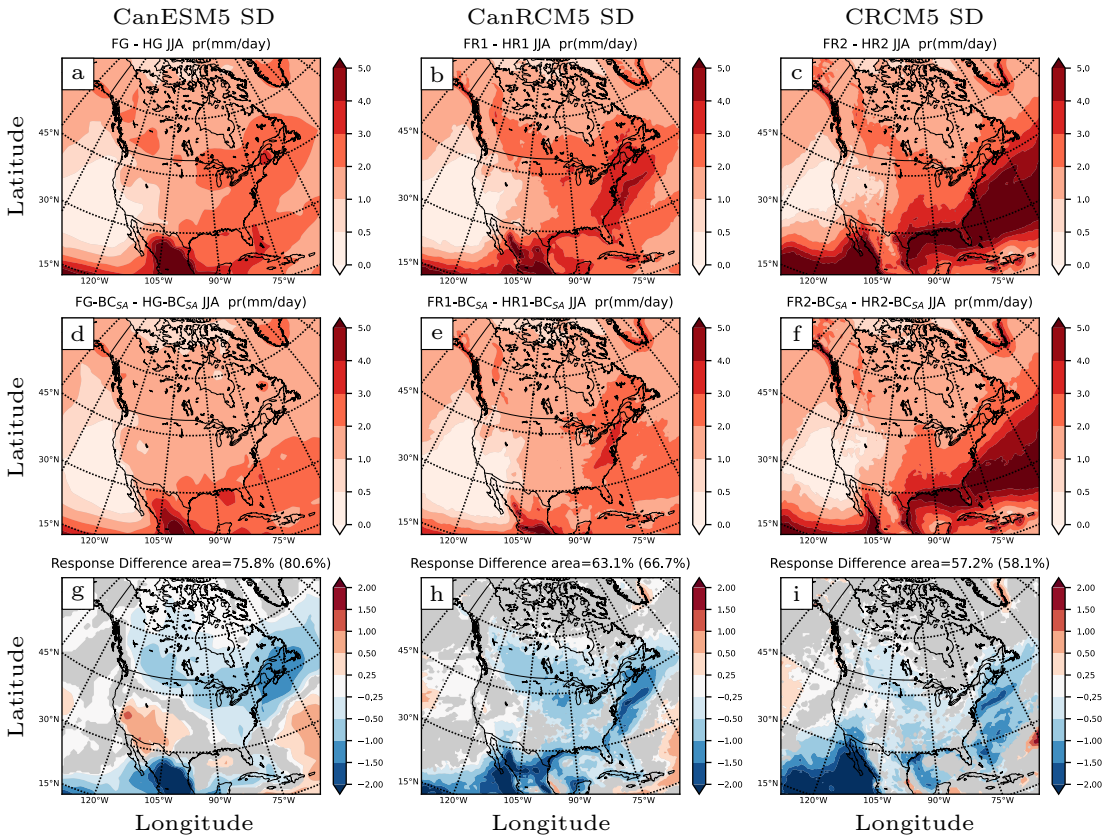


Figure S5.25: JJA total precipitation (pr) standard deviation responses.

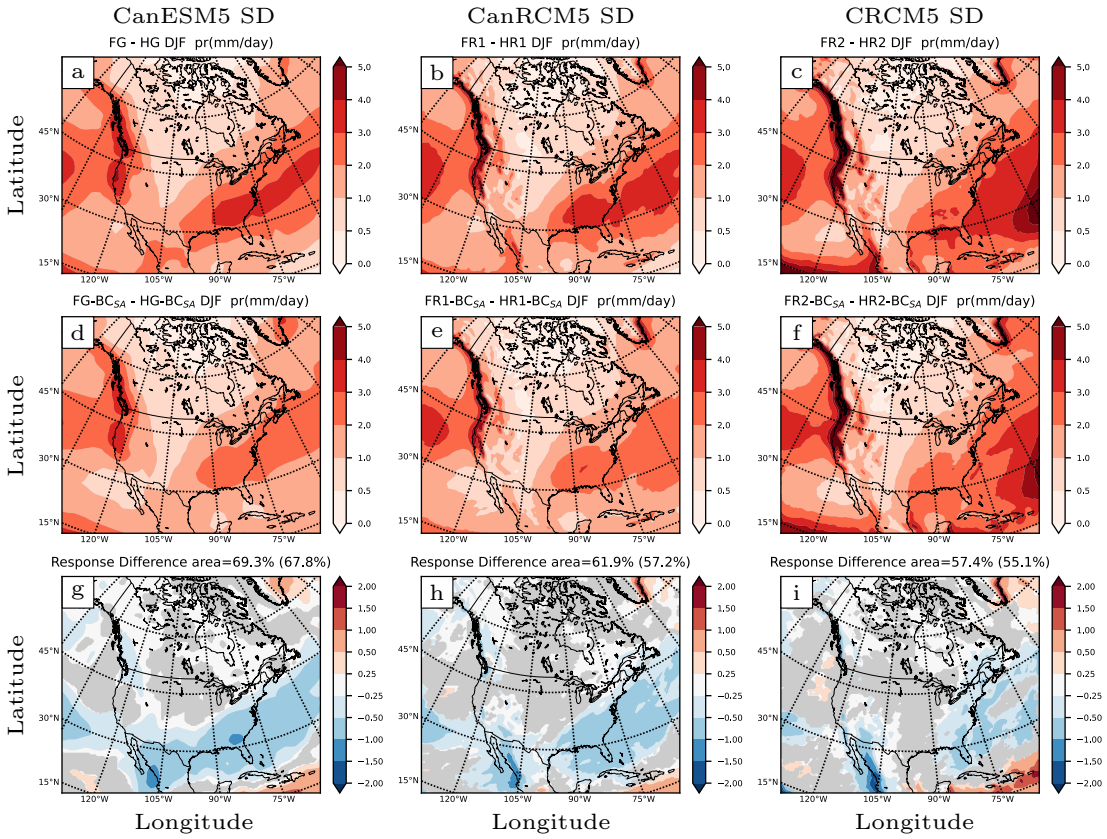


Figure S5.26: DJF total precipitation (pr) standard deviation responses.

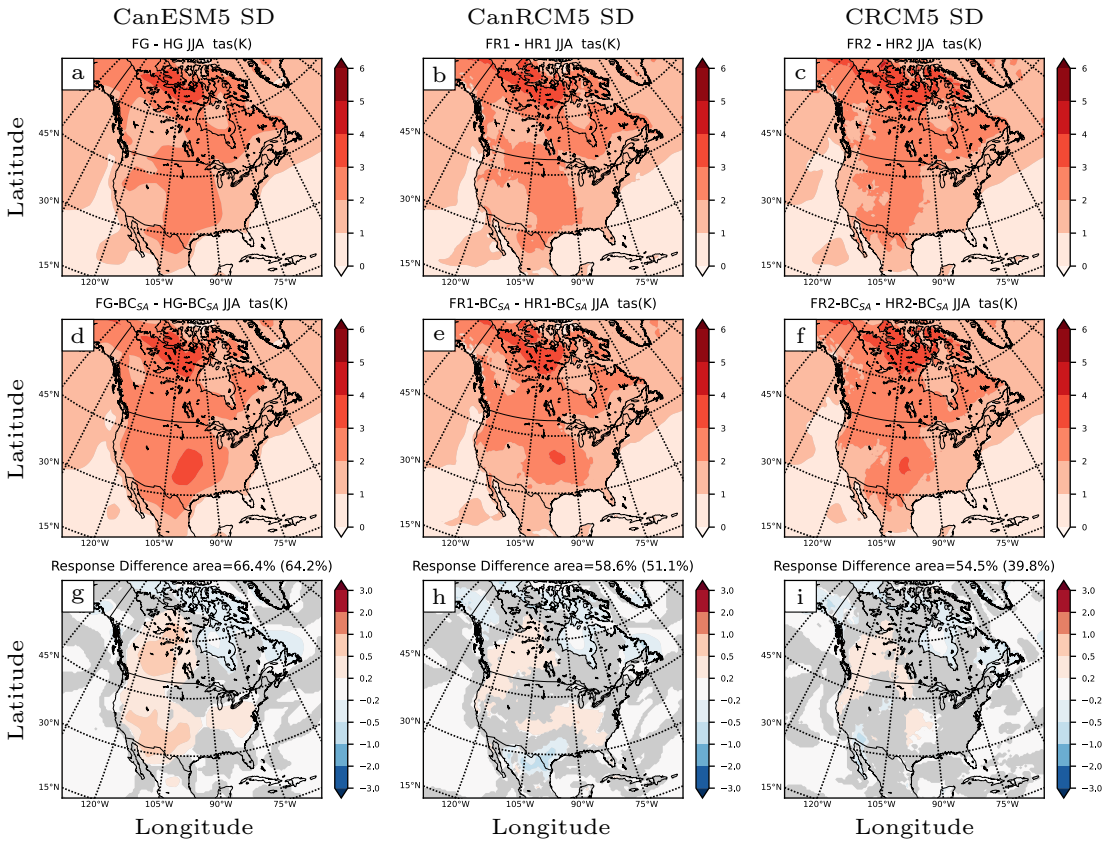


Figure S5.27: JJA screen temperature (tas) standard deviation responses.

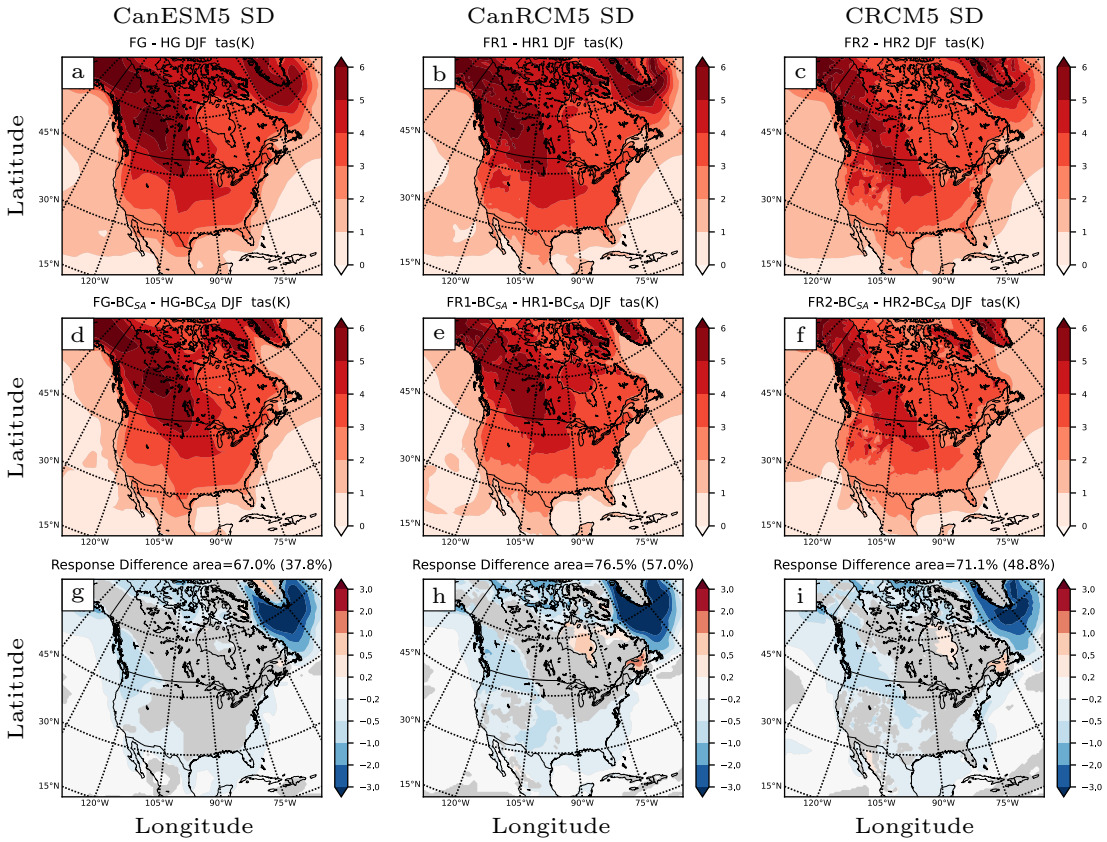


Figure S5.28: DJF screen temperature (tas) responses.